

PEOPLE'S DEMOCRATIC REPUBLIC OF ALGERIA
Ministry of Higher Education and Scientific Research



Memory

**Presented with a view to obtaining the Master's degree in Mechanical
Engineering**

University Echahid Hamma Lakhdar d'El Oued

Faculty of Technology

Department: Mechanical Engineering

Option: *Electromechanical Engineering*

Presented by:

Hamid Mohammed Elfateh – Youmbai Maroua

Title

**Enhancing Photovoltaic System
Reliability and Performance Through
Fault Detection and fault control**

Directed by:

Dr.Mahmoudi Abdelkader	MCB	Supervisor
Dr.Labioud Chouaib	MCB	Protractor
Dr.Miloudi Khaled	MCB	Examiner
Dr.Laouamer Mosbah	MCB	Examiner

College year 2023/2024

بِسْمِ اللَّهِ الرَّحْمَنِ الرَّحِيمِ

﴿وَمَا تَوْفِيقِي إِلَّا بِاللَّهِ عَلَيْهِ تَوَكَّلْتُ وَإِلَيْهِ أُنِيبُ﴾

«صَدَقَ اللَّهُ الْعَظِيمُ»

ACKNOWLEDGEMENTS

First and foremost,

We extend our gratitude to the Almighty God - Allah - for granting us the courage and patience to persevere through years of study.

*We wish to convey our sincere appreciation to **Dr. Mahmoudi Abdelkader**, a faculty member at Echahid Hamma Lakhdard 'El Oued University, for his guidance and supervision of this research endeavor.*

We are deeply grateful to the esteemed members of the jury for their participation in the evaluation of this work, an honor that we deeply cherish.

*We would also like to express heartfelt thanks to **Dr. Labiod Chouaib**, **PHd student Bebboukha Ali**, **Dr. Zenina Mohammed Laid**, who contributed to the development and completion of this dissertation.*

Finally,

We are profoundly thankful to our parents for their unwavering support throughout the extensive duration of our studies.





DEDICATION



*To the memory of my dear friend **Ihssene** ,*

I dedicate these words to your cherished memory. You were always a source of inspiration and support for me, and not a day goes by without feeling the immense void left by your absence. Your memory will forever live in my heart, and our shared moments will always be an inseparable part of my life.

You left an indelible mark on my life, and your spirit will continue to light my path despite the distance between us. I pray that God embraces you with His boundless mercy and grants you a place in His eternal paradise.

*Until we meet again in the gardens of
eternity, my dear friend.*

Youmbai Maroua



DEDICATION

We praise Allah Almighty for His grace and help in completing this research.

To the one who gave us everything he had so we could fulfill his hopes, to the one who constantly pushed us forward towards our goals, to the person who embodied humanity with all his strength, to the one who sacrificed so much for our education, revering knowledge, to the first teacher in life, our beloved fathers may Allah prolong thier life.


To the one who gave her child all the love and tenderness, to the one who endured everything, who took care of me with true care and was our support in hardships, who always prayed for our success, who followed our steps closely in our work, to the one whose smile comforted us—our mothers, the most precious angel to our heart and eyes—may Allah reward her for all her sacrifices in this life and the hereafter.

To them, we dedicate this humble work to bring a bit of happiness to their hearts.

To our brothers and sisters who shared with us the burdens of life;

*To our supervisor **Dr.MAHMOUDI ABDELKADER**,we are deeply grateful for your crucial technical support in our graduation research. Your assistance made the completion possible and has greatly inspired us. We sincerely appreciate your encouragement and unwavering support.*

*we also dedicate the fruit of my efforts to our esteemed professor, **Dr.LABIOD CHOUAIB**, who, whenever the path darkened before us, we turned to him, and he illuminated it for us. Whenever despair crept into our hearts, he instilled hope in us to move forward. Whenever we asked for knowledge, he provided it, and whenever we requested some of his precious time, he generously gave it to us despite his numerous responsibilities.*



*To Phd student **BEBBOUKHA ALI** ,we want to take this moment to express our deep gratitude for your immense and generous support in bringing this research to completion. We are extremely thankful for your help.*

*To all the professors of the Department of
Mechanical Engineering;*

And to everyone who believes that the seeds of successful change lie within ourselves before they exist in anything else.

Merciful ALLAH , be a source of support and strength for the people of Gaza. Protect them and grant them peace and security. Heal their wounded, have mercy on their martyrs, and grant them relief from their suffering.

FREE PALASTINE.

HAMID MOHAMMED ELFATEH
YOUMBAI MAROUA.



Abstract:

Photovoltaic (PV) systems hold immense potential for clean energy generation, but their performance and reliability are often hampered by hidden faults. This research explores innovative fault detection and control techniques to unlock the full potential of PV systems. We delve into: Identifying and analyzing common PV faults, including mismatched modules, shading, inverter issues, and connection failures, highlighting their impact on energy output and system lifespan. Implementing advanced detection methods, ranging from traditional data analysis to cutting-edge artificial intelligence (AI) and machine learning algorithms, for early and accurate fault diagnosis. Developing proactive control strategies, such as smart module bypass diodes and adaptive inverter control, to mitigate fault effects and maximize energy production. Evaluating the effectiveness of these techniques through simulations and real-world system deployments, quantifying improvements in reliability, performance, and energy yield.

keywords : Fault Isolation, Fault Detection , Diagnosis, PV System , MPPT control

Résumé :

Les systèmes photovoltaïques (PV) ont un immense potentiel pour la génération d'énergie propre, mais leurs performances et leur fiabilité sont souvent entravées par des défauts cachés. Cette recherche explore des techniques innovantes de détection et de contrôle des défauts pour libérer le plein potentiel des systèmes PV. Nous nous plongeons dans : L'identification et l'analyse des défauts PV courants, y compris les modules non appariés, l'ombrage, les problèmes d'onduleurs et les défaillances de connexion, en mettant en évidence leur impact sur la production d'énergie et la durée de vie du système, La mise en œuvre de méthodes de détection avancées, allant de l'analyse traditionnelle des données aux algorithmes de pointe en intelligence artificielle (IA) et en apprentissage automatique, pour un diagnostic précoce et précis des défauts, Le développement de stratégies de contrôle proactives, telles que les diodes de contournement intelligentes des modules et le contrôle adaptatif des onduleurs, pour atténuer les effets des défauts et maximiser la production d'énergie, L'évaluation de l'efficacité de ces techniques par le biais de simulations et de déploiements de systèmes réels, en quantifiant les améliorations en termes de fiabilité, de performances et de rendement énergétique.

Mots-clés : Isolation de Défaut, Détection de Défaut, Diagnostic, Système PV, Commande MPPT.

ملخص:

نظم الطاقة الشمسية (PV) تحمل إمكانيات هائلة لتوليد الطاقة النظيفة، لكن أداؤها وموثوقيتها غالبًا ما يتعرضان للتقليل بسبب الأخطاء الخفية. تستكشف هذه الأبحاث تقنيات الكشف عن الأعطال والتحكم المبتكرة لإطلاق القدرة الكاملة لنظم الطاقة الشمسية. نتعمق في: تحديد وتحليل الأعطال الشائعة في نظم PV ، بما في ذلك الوحدات غير المتطابقة، والظلال، ومشاكل المحولات، وفشل الاتصالات، مع التركيز على تأثيرها على إنتاج الطاقة وعمر النظام. تنفيذ أساليب كشف متقدمة، تتراوح من التحليل التقليدي للبيانات إلى خوارزميات الذكاء الاصطناعي وتعلم الآلة الحديثة، للتشخيص المبكر والدقيق للأعطال. تطوير استراتيجيات التحكم الاستباقية، مثل الثنائيات المنحرفة الذكية للوحدات والتحكم التكيفي في المحولات، للتخفيف من آثار الأعطال وتحقيق الحد الأقصى لإنتاج الطاقة. تقييم فعالية هذه التقنيات من خلال المحاكاة ونشر النظم العملية، وقياس التحسينات في الموثوقية والأداء وعائد الطاقة.

الكلمات المفتاحية: كشف الأعطال ، عزل الأعطال ، تشخيص ، نظام PV ، تحكم MPPT.

Contents

List of Figures

List of tables

Notations

Resume

General introduction 1

Chapter I: Potovoltaic system Generalities.

I.1. Introduction:.....	3
I.2. Photovoltaics:.....	3
I.2.1. Photovoltaics effects:	4
I.2.2. Photovoltaics technologies:.....	5
I.2.2.1. Crystalline silicon:	5
I.2.2.2. Thin films:	6
I.2.2.3. Emerging technologies:	7
I.3. Solar energy:	8
I.3.1. Solar radiation:	8
I.3.1.a. Solar spectrum:	8
I.3.1.b. Extraterrestrial radiation and the length of the day:	10
I.3.2. Operating Principles of a cell:	11
I.3.2.1. Semiconductor materials :	11
I.3.2.2. Classification of Semiconductors :	11
I.3.3. Types of Extrinsic Semiconductors:	12
I.4. Formation of Photovoltaics:.....	13
I.5. Photovoltaic systems :.....	14
I.5.1. Stand-alone (off-grid) PV systems :.....	14
I.5.1.1. Grid-connected PV systems :	15

I.5.1.2. Hybrid photovoltaic systems:	15
I.5.3. Regulator :	16
I.6. Photovoltaic module:	17
I.6.1. Composition of a photovoltaic module :	17
I.6.2. Series and Parallel Connection of a PV Module :	17
I.6.2.1. Series connection :	17
I.6.2.2. Parallel connection :	18
I.6.2.3. Safeguarding of a PV module :	19
I.7. Characteristics of a photovoltaic generator :	21
I.7.1. Current-Voltage Characteristics :	21
I.8. Impact of Irradiance and Temperature:	22
I.8.1. Impact of Irradiance:	22
I.8.2. Influence of temperature :	23
I.8.3. Orientation of solar panels :	23
I.8.4. Use of photovoltaic energy:	24
I.9. Advantages and disadvantages of PV (photovoltaic) energy:	25
I.9.1. Advantages of PV (photovoltaic) energy:	25
I.9.2. disadvantages of PV (photovoltaic) energy:	26
Conclusion:	26

Chapter II: Control and command of the converter

II. Introduction:	27
II.1. Fault detection and diagnosis methods :	27
II.1.1. Types of faults :	27
II.1.2. Diagnostic Methods :	30
II.1.3. Model-based methods:	31
II.1.4. Knowledge-Based Methods:	34

II.2. Chopper (DC-DC Boost):	35
II.2.1.Chopper boost modeling :	36
II.2.2 Command MPPT:	37
II.2.3 Classification of MPPT Controls According to the Search Type :	37
II.2.4. Command MPPT Modeling:.....	39
II.3. Photovoltaic Panel Defects:	41
II.3.1. Shading Fault:	41
II.3.1.1. Partial-Shading Fault:.....	42
II.3.2. Bypass Diode faults :	42
II.3.2.1. Module Fault :	43
II.3.2.2. Bypass diode anti-reverse fault :	43
II.3.2.3. Bypass diode connection Fault:.....	44
II.3.3. Decrease in shunt resistance (R_{sh}) :	44
II.3.4. Increase in series resistance (R_s) :	45
Conclusion:	45

Chapter III: Modeling and simulation of healthy and faulty PV systems and fault detection.

III.1. Modeling and simulation:.....	46
III.1.1. Photovoltaic module modeling:.....	46
III.1.2. Solar cell modeling:.....	47
III.1.3. PV module characteristics :	48
III.2. PV module faults :	50
III.3. Fault Diagnosis PV System :	50
III.3.1. Interpretation of results :	51
III.4. DC-DC boost Simulation :	52
III.4.1. Dimensioning and Calculation of the Components Constituting the Boost Chopper Used :	52

III.5. Fault Diagnosis PV System with MPPT control:.....	57
III.5.1 Diagnosis PV System with MPPT control healthy model:.....	57
III.5.2 Diagnosis PV System with MPPT control faulty model diode by-pass disconnected:	58
III.5.3. Diagnosis PV System with MPPT control faulty model diode by-pass short-circuited:	58
III.5.4. Diagnosis PV System with MPPT control faulty model Shading of a cell of the submodule 1 and another of the submodule 2 of the panel at 50%:.....	59
III.5.5. Diagnosis PV System with MPPT control faulty model Shading of one cell in in submodule of the panel at 50%:	59
III.5.6. Diagnosis PV System with MPPT control faulty model Shading of one cell in submodule of the panel at 100%:	59
III.5.7. Diagnosis PV System with MPPT control faulty model shading of a cell of the submodule 1 and another of the submodule 2 of the panel at 100%:.....	60
III.5.8. Diagnosis PV System with MPPT control faulty model Decrease the shunt resistors (Rsh = 5 Ω) module:.....	61
III.5.9. Diagnosis PV System with MPPT control faulty model Increase the serie resistors (Rs = 0.9 Ω) module:	61
III.5.10. Interpretation of results:.....	62
Conclusion:.....	64

Chapter IV: Experimental validation of the detection fault method

IV. Introduction :.....	65
IV.1. Tools Employed:	65
IV.1.1. Chopper components:.....	65
IV.2. The solar panel:.....	69
IV.3. Current Sensor:	69
IV.4. Voltage Sensor:	70
IV.5. Photoresistor:	70
IV.6. The Microcontroller (ARDUINOBOARD):.....	71

IV.6.1. Definition:	71
IV.6.2. Characteristics :	71
IV.6.3. Why Arduino NodeMCU (LoLin) :	72
IV.6.4. Arduino software interfaces :	72
IV.7. Results:.....	73
IV.7.1. Chopper Results :	73
IV.7.1.1. Steps of Work:	73
IV.7.1.2. Interpretation of Results :	87
IV.7.2. MPPT control:	88
Conclusion :	95

General conclusion

Bibliography

Figures list

Figure I.1: the photovoltaic effect.	4
Figure I.2: monocrystalline and polycrystalline solar cells.....	6
Figure I.3: a typical structure of GIGS solar cell.	7
Figure I.4: A typical structure of multi-junction solar cells.	7
Figure I.5: the extraterrestrial solar spectrum (ETS) at the average distance between the wavelength.	8
Figure I.6: Plot of spectral irradiance for different values of AM and zenith (latitude ¹ / ₄ 36°, longitude ¹ / ₄ 45°, and tilt angle ¹ / ₄ 36°).	9
Figure I.7 The insolation measurements for the year 2020.....	10
Figure 1.8: presents a graphical representation of extraterrestrial radiation (<i>G_o</i>) and the calculated clearness index (<i>K_t</i>).....	10
Figure I.9: p-type semiconductor:	12
Figure I.10: n-type semiconductor.	13
Figure I.11: the Structure of photovoltaic.	13

Figure I.12: Stand-alone (off-grid) PV systems.	14
Figure I.13: Schematic of Stand-alone PV system.	14
Figure I.14: Schematic representation of a grid-connected PV system.	15
Figure I.15: Hybrid photovoltaic systems.	16
Figure I.16: Basic structure of an autonomous solar energy system.	16
Figure I.17: Composition of a photovoltaic solar module.	17
Figure I.18: Charge-Solar-SolarPanelsSeriesWired.	18
Figure I.19: Resulting characteristic of a grouping of ns cells in series.	18
Figure I.20: Parallel Connection of PV Cells.	19
Figure I.21: Resulting characteristic of a grouping of n p cells in parallel.	19
Figure I.22: Series/parallel wiring of photovoltaic modules with their protection diodes.	20
Figure I.23: Influence of illumination on I(V) and P(V).	22
Figure I.24: The influence of temperature on the I (V) and P(V) characteristics.	23
Figure I.25: The influence of temperature on the P(V) and I(V) characteristics.	23
Figure I.26: Orientation of solar panels.	24
Figure I.27: An application of photovoltaic systems.	25
Figure II.1: Faults created between the panels.	27
Figure II.2: Voltage and Current of the PV Array under LL Fault.	28
Figure. II.3: LG Fault.	28
Figure II.4: Voltage and Current of the PV Array under LG Fault.	28
Figure II.5: Double line to ground (LLD) fault.	29
Figure II.6: Voltage and Current of the PV Array under LLG Fault.	29
Figure II.7: Bypass Diode Fault.	29
Figure II.8: Voltage and Current of the PV Array under Bypass Diode Fault.	29
Figure II.9: Fault Detection and Isolation (FDI) Procedure.	32
Figure II.10: Principle of residual generation through parametric estimation.	32

Figure II.11: general principle of an observer, which includes a state model of the system closed by the estimation error.....	33
Figure II.12: Parity space diagnostic.....	34
Figure II.13: Pattern Recognition-Based Diagnostic System Diagram (Fuzzy logic).	34
Figure II.14: General structure of a diagnostic expert system.	35
Figure II.15: Principle Diagram of a Chopper.	36
Figure II.16: Parallel (Boost) Chopper.....	36
Figure II.17: Modeling of Chopper(DC-DC boost),Matlab/Simulink.	36
Figure II.18: MPPT techniques.	37
Figure II.19: PV-characteristic curves of P&O MPPT technique V-I-P curve.....	38
Figure II.20: Partial Flowchart of Variable P&O Algorithm.	39
Figure II.21: Diagram of Nemuric Mppt control.	40
Figure II.22: modeling of MPPT control, Matlab/Simulink.	40
Figure II.23: P&O (Perturb and Observ) algorithm.	41
Figure II.24: Partial shading on the PV Panel.....	43
Figure II.25: Bypass Diode Fault Configuration.....	43
Figure II.26: Module Fault Configuration.....	43
Figure II.27: Installation of a PV field with a faulty reverse diode.	44
Figure II.28: Bypass diode dis-connected.	44
Figure II.29: Increasing series resistance fault	45
Figure III.1: Solar cell equivalent circuit-five-parameters model.....	48
Figure III.3: I-V Characteristic of a PV module under STC (25 Cand1000W/m2).....	49
Figure III.4: P-V Characteristic of a PV module under STC (25 Cand1000W/m2).....	49
Figure III.5: I-V Curves of different type of faults.	51
Figure III.6: Diagram of a Boost Chopper Powered by a Photovoltaic Generator.	52
Figure III.7: Generation of the Control Signal for $\alpha=0.85$ and $f_s=5000$.Matlab,Simulink.....	54
Figure III.8: Block Diagram of the Boost Chopper for $\alpha=0.85$, Matlab/Simulink.	54

Figure III.9: Generation of the Control Signal for $\alpha=0.94$ and $f_s=5000$.Matlab,Simulink.....	55
Figure III.11: Voltage Curve DC-DC boost	56
Figure III.12: Diagnosis PV system. Healthy model with MPPT controller.Matlab,Simulink.	56
Figure III.13: The Power of PV Healthy model with MPPT controller. Matlab,Simulink.....	57
Figure III.14: The Power of PV faulty model with MPPT controller F1. Matlab,Simulink...	58
Figure III.15: The Power of PV faulty model with MPPT controller F2. Matlab,Simulink...	58
Figure III.16: The Power of PV faulty model with MPPT controller F3. Matlab,Simulink...	59
Figure III.17: The Power of PV faulty model with MPPT controller F4. Matlab,Simulink...	59
Figure III.18: The Power of PV faulty model with MPPT controller F5. Matlab,Simulink...	60
Figure III.19: The Power of PV faulty model with MPPT controller F6. Matlab,Simulink...	60
Figure III.20: The Power of PV faulty model with MPPT controller F7. Matlab,Simulink...	61
Figure III.21: The Power of PV faulty model with MPPT controller F8. Matlab,Simulink...	61
Figure IV.1 : for the «50T65FSC-LB43106GE» and «SFA66UP30DN-T11A19G001 » mosfets.	65
Figure IV.2: 100mh Coil.	66
Figure IV.3: «470 μ F-400V »Capacitor.....	66
Figure IV.4 : « Schottky SBT80-10LS » diode.....	67
Figure IV.5:«A3130-1736» driver.	67
Figure IV.6: «EVISUN B0515S-1W 2048» Relay driver.....	68
Figure IV.7: Resistor.	68
Figure IV.8: Boost-DC Chopper prototype.....	69
Figure IV.9: Characteristics the PV array.	69
Figure IV.10: ACS712s current sensor.	70
Figure IV.11: Voltage sensor.	70
Figure IV.12: Photoresistor.	71
Figure IV.13: Arduino Uno Board	73
Figure IV.14: A, B: During the printing and drilling.	75

Figure IV.15: power supply of 12V, I=0.04.....	76
Figure IV.16: Testing of DC-boost converter.	77
Figure IV.17:Vs when $\alpha=0.85$	77
Figure IV.18:Vs when $\alpha=0.94$	78
Figure IV.19: Validation of results.	78
Figure IV.20: Validation of results.	79
Figure IV.21:The results with input voltage = 7.5V, A:duty cycle 10%, B:duty cycle 20%... 80	
Figure IV.22:The results with input voltage = 12.5V, A:duty cycle 10%, B:duty cycle 20%. 81	
Figure IV.23:The results with input voltage = 17V, A:duty cycle 10%, B:duty cycle 20%.... 82	
Figure IV.24:The results with input voltage = 21.8V.	82
Figure IV.25: The increasing of output Voltage with the variation of duty cycle, where input voltage = 7.5V.	83
Figure IV.26: The increasing of output Voltage with the variation of duty cycle, where input voltage = 12.5V.	84
Figure IV.27: The increasing of output Voltage with the variation of duty cycle, where input voltage = 17V.	85
Figure IV.28: The increasing of output Voltage with the variation of duty cycle, where input voltage = 21.8V.	86
Figure IV.29: Current results whith duty cycle variation.....	87
Figure IV.30:Global experimental test healthy model.....	88
Figure IV.31:Global experimental test faulty model “full-shading”.....	89
Figure IV.32: Global experimental test faulty model “paratial-shading”.	89
Figure IV.33: Serial curves results of MPPT control healthy model.	90
Figure IV.34: Serial curves results of MPPT control faulty model shading fault.....	90
Figure IV.35: Serial results of MPPT control faulty model shading fault	91
Figure IV.36: Serial curves results of MPPT control faulty model shading fault.....	91
Figure IV.37: Serial curves results of MPPT control faulty model shading fault.....	92
Figure IV.38: Serial curves results of MPPT control faulty model shading fault with	93

Figure IV.39: Final prototype.....	93
Figure IV.40: A, B, C and D, Final prototype.....	94

Tables list

Table I.1 : Advantages.	25
Table I.2 : disadvantages.....	26
Table II.1: Diagnostic Methods.....	30
Table II.2: Electrical-based FDD methods.....	30
Table II.3: Different diagnostic methods.	31
Table III.1: Electrical characteristics of the SUNTECH PV module.....	49
Table III.2: Different type of faults chosen for the diagnosis.	50
Table IV.1: The variations in Current and Voltage with changes in duty cycle when $V_{out}=7V$	82
Table IV.2: The variations in Current and Voltage with changes in duty cycle when $V_{out}=12.5V$	83
Table IV.3: The variations in Current and Voltage with changes in duty cycle when $V_{out}=17V$	84
Table IV.4: The variations in Current and Voltage with changes in duty cycle when $V_{out}=21.8V$	85

Notations

$x(t)$: Observed signal

$y(t)$: Output signal

$u(t)$: Input signal

$ym(t)$: Measured signal

$r(t)$: Residuals

$\hat{y}(t)$: Estimated signal

$f(t)$: Fault signal

$d(t)$: Disturbance signal

$e(t)$: Error signal

θ_n : Nominal parameter vector

$\hat{\theta}$: Estimated parameter vector

$A \in \mathbb{R}^{n \times n}$: State or evolution matrix

$B \in \mathbb{R}^{n \times m}$: Input matrix

$C \in \mathbb{R}^{p \times n}$: Output or observation matrix

D_x : Disturbance action matrix

F_x : Fault action matrix

F_y : Fault action matrix

L : Observer gain matrix

W : Parameter matrix

w_T : Network weight matrix

g : Nonlinear function of the networks

dk : Desired network output

F : Neuron transfer function

V_{oc} : Open-circuit voltage point

I_{sc} : Short-circuit current point

T : Temperature [$^{\circ}\text{C}$]

G : Solar irradiation [W/m^2]

I : Current supplied by the cell [A]

V : Voltage at the cell terminal [V]

I_{ph} : Current equivalent to the received solar radiation on the cell [A]

I_0 : Reverse saturation current of the diode [A]

V_t : Diode thermal voltage [V]

R_s : Cell series resistance [Ω]

R_{sh} : Cell shunt resistance [Ω]

a_1 : Diode ideality factor of D1

a_2 : Diode ideality factor of D2

α : Learning coefficient

α : Duty cycle

I_{out} : output current

V_e : Input voltage

V_s : Output voltage

L : inductor

C : capacitor

F_s : Switching frequency

GENERAL INTRODUCTION

Solar energy constitutes a significant source of sustainable and clean energy, with photovoltaic systems being the primary means of converting sunlight into electrical energy. With the increasing use of solar energy in various applications, there is a growing need to focus on enhancing the reliability and performance of photovoltaic systems through the utilization of effective fault detection and control techniques. Photovoltaic systems face numerous challenges that impact their reliability and performance, necessitating research into improving their operation and accurately identifying faults to avoid negative effects on their performance. Consequently, subsidiary questions arise to delineate the research path in this field, aiming to understand available fault detection techniques and how to enhance the performance of photovoltaic systems through effective fault control. Building upon this, the following hypotheses can be formulated as the basis of the research:

1. The reliability and performance of photovoltaic systems can be improved through the application of effective fault detection and control techniques.
2. Implementing fault detection and control techniques will contribute to reducing maintenance costs and increasing the service life of photovoltaic systems.

This topic was chosen for study due to the increasing demand for solar energy as a clean and sustainable alternative to traditional energy sources, along with the urgent need to improve the reliability and performance of photovoltaic systems to achieve maximum efficiency. This study aims to investigate and evaluate fault detection and control techniques in photovoltaic systems, as well as develop accurate predictive models for potential faults in these systems and provide recommendations to enhance their reliability and performance.

The significance of this study lies in reinforcing the reliability and performance of solar energy as a sustainable alternative to traditional energy sources and achieving reductions in maintenance costs and increased efficiency in the use of photovoltaic systems. The study's boundaries focus on presenting recommendations and results based on data and information available in scientific literature, with an emphasis on fault detection and control techniques in photovoltaic systems rather than other factors such as system design. The difficulties of this study lie in obtaining accurate and comprehensive data on faults occurring in photovoltaic systems and analyzing and interpreting the complex data related to the performance of photovoltaic systems and potential faults. The study consists of main chapters including

introduction, literature review, research methodology, data analysis, results and discussion, and conclusions and recommendations.

CHAPTER I

I.1. Introduction:

Among the various renewable energy sources, solar energy utilization, through the use of photovoltaic (PV), is one of the most important sources of electrical energy production around the world. Over the past few years, photovoltaic installations have experienced rapid growth worldwide. At the end of 2020, the cumulative installed capacity exceeded 760.4GW. [1] With reference to IRENA, [2] photovoltaics (PV) is the leading energy technology in terms of annual growth rate (over 35% in 2010–19). [3]

In recent years, there has been an exponential growth in photovoltaics across the world. This brings many problems associated with the quality of the systems due to several factors. The most crucial component in PV systems is the photovoltaic module whose diagnostics can be sometimes relatively difficult. The main problem is that all the modules look very similar although their quality is totally different. Defects on the modules are usually not visible by the naked eyes and also their causes should be found by the special methods. As a result, there are many installations that necessarily requires the regular monitoring. The Present-day statistics depicts the rate of degradation for power ratings in crystalline silicon photovoltaic modules by 0.8%/y. By observing the challenges involved with the PV modules and their operation, work can be carried toward the improvement in reliability and the service life of PV modules.

I.2. Photovoltaics:

Photovoltaics (PV) is a technology that converts light into electricity using semiconducting materials that exhibit the photovoltaic effect. These materials, typically silicon, generate an electric current when exposed to sunlight, making them a key component in solar panels used for renewable energy generation. The photovoltaic effect is the phenomenon of converting light into electricity. PV systems employ solar modules, each comprising a number of solar cells, which generate electrical power. PV installations may be ground-mounted, rooftop-mounted, wall-mounted, or floating. PV systems range from small, roof-top mounted or building-integrated systems with capacities from a few to several tens of kilowatts, to large utility-scale power stations of hundreds of megawatts. PV cells are used in photovoltaic systems and include a large variety of electrical devices. PV systems can supply electricity in locations where electricity distribution systems do not exist, and they can also supply electricity to an

electric power grid. [3] PV arrays can be installed quickly and can be any size. The environmental effects of PV systems located on buildings are minimal. The first practical application of photovoltaics was to power orbiting satellites and other spacecraft ,but today the majority of photovoltaic modules are used for grid-connected systems for power generation.

I.2.1. Photovoltaics effects:

The photovoltaic effect, first discovered by A. Becquerel in 1839,[5] involves converting light into electricity, known as the photovoltaic effect. This process uses photons from light to release electrons, generating a direct electric current. Solar electricity emerged in the 1930s, with silicon photovoltaic cells being developed in 1954, [6] enabling the use of solar energy. Initially employed for space vehicles in the 1960s, solar power expanded to electrify remote areas by the 1970s. Advancements in the 1980s led to megawatt-scale power plants and solar-powered consumer products in the 1990s. Prices dropped significantly in the 1990s due to improved production techniques and increased manufacturing volumes. Global photovoltaic module production surged from 5 MWp in 1982 to over 18 GWp in 2013. Algeria's Condor Electronics began producing photovoltaic panels in varying power outputs from 70 W to 285 W at competitive prices in July 2013. [7]

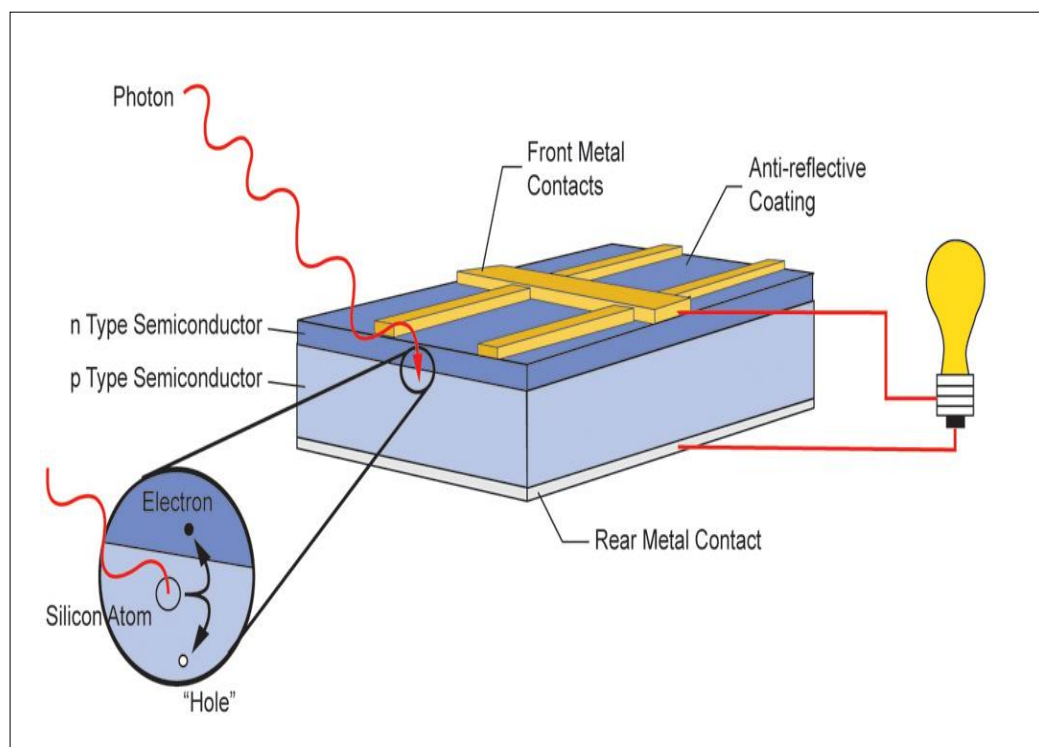


Figure I.1: the photovoltaic effect.

I.2.2. Photovoltaics technologies:

Photovoltaic (PV) technology converts sunlight into electricity using semiconductor materials exhibiting the photovoltaic effect. [8]

PV cells, or solar cells, are the fundamental units of PV systems, typically producing 1 to 2 watts of power each and made from materials like silicon, gallium arsenide, or cadmium telluride. These cells are grouped into modules or panels, which can be used individually or linked to form arrays for applications ranging from small-scale devices like calculators to large-scale utility electricity generation. [8] PV systems can be mounted on various surfaces and can either be fixed or use solar trackers to follow the sun's path. Primary PV technologies include first-generation crystalline silicon cells, second-generation thin films, and third-generation cells with emerging materials. [9]

I.2.2.1. Crystalline silicon:

Crystalline silicon is a type of photovoltaic technology used in solar cells. It is the most common type of solar cell used in commercially available solar panels, representing more than 85% of the world PV cell market sales in 2011. Crystalline silicon solar cells are made from monocrystalline (single-crystal) silicon or multicrystalline silicon. [10][11]

The first-generation involves wafer-based cells constructed from crystalline silicon (Si), incorporating materials as monocrystalline Si and polycrystalline Si. Notably, [12] the highest efficiency for Si-based wafer cells reached 26.7%. [12] Significant advancements have also been made in PV modules, reaching 24.4% efficiency. In 2019, Si-wafer-based PV technologies constituted approximately 95% of total production. [13]

The figures below show the structures of Crystalline silicon types.

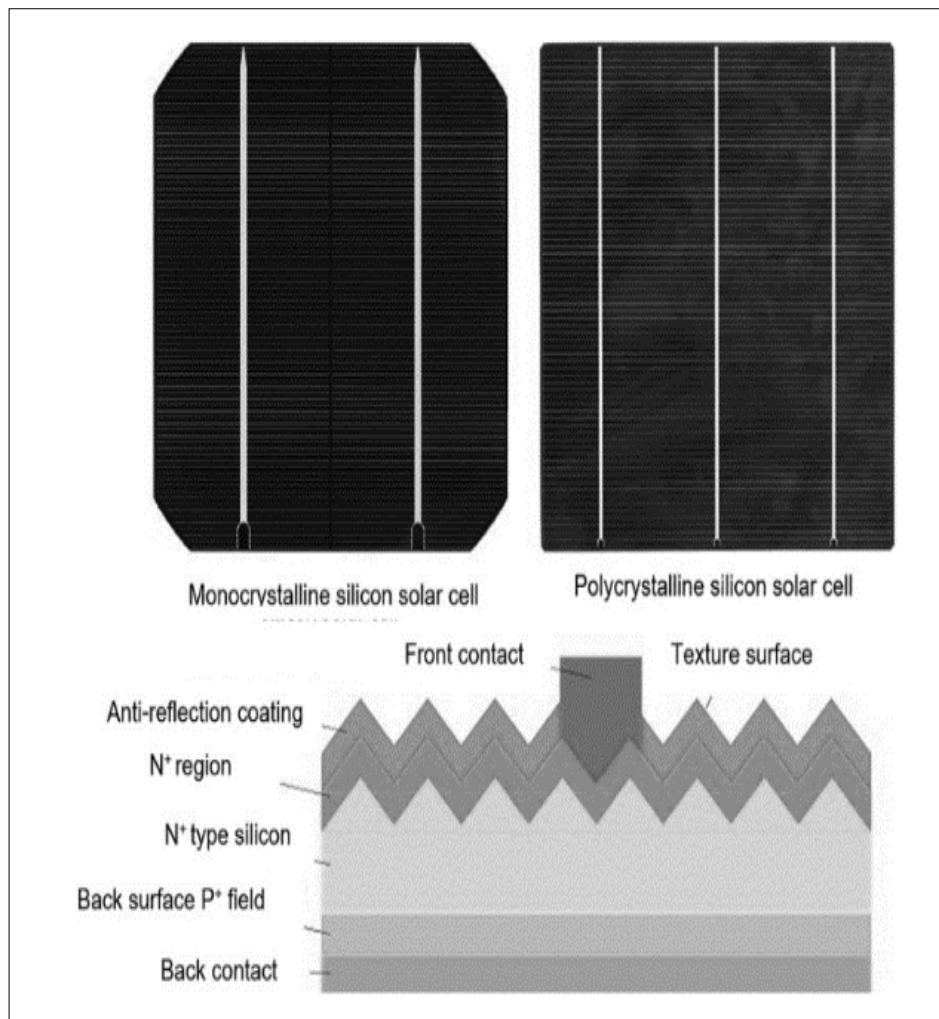


Figure I.2: monocrystalline and polycrystalline solar cells.

I.2.2.2. Thin films:

Thin-film solar cells, which are the second-generation of solar cells, consist of copper indium gallium selenide (CIGS), cadmium telluride (CdTe), amorphous silicon (a-Si), and amorphous silicon: hydrogenated (a-Si:H) cells. [12] This technology is easy to implement due to its simpler fabrication process compared to wafer-based silicon (Si) solar cells. However, their efficiency is still lower than that of the first-generation cells. The most efficient thin-film solar cells have achieved a record of 23.35% efficiency, specifically in the case of CIGS cells. Thin-film solar cell technology is the second most widely used technology in the world after wafer-based Si, contributing to about 7% of the photovoltaic (PV) market. CdTe and a-Si:H solar cells are easier to produce than CIGS, while the stability of CIGS- and CdTe-based cells is higher than that of a-Si:H cells. [11]

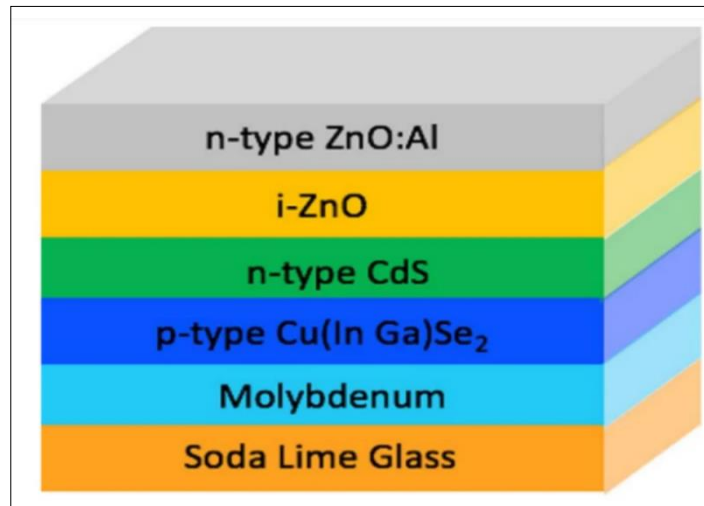


Figure I.3: a typical structure of CIGS solar cell.

I.2.2.3. Emerging technologies:

The third generation of photovoltaic technology comprises emerging technologies such as organic, dye-sensitized solar cells (DSSC), quantum dot (QD), perovskite, and multi-junction cells. These emerging technologies are known for their affordability. Among the different types of third-generation PV technology, perovskites in the form of thin films have the highest efficiency rate of 25.2%. [13]

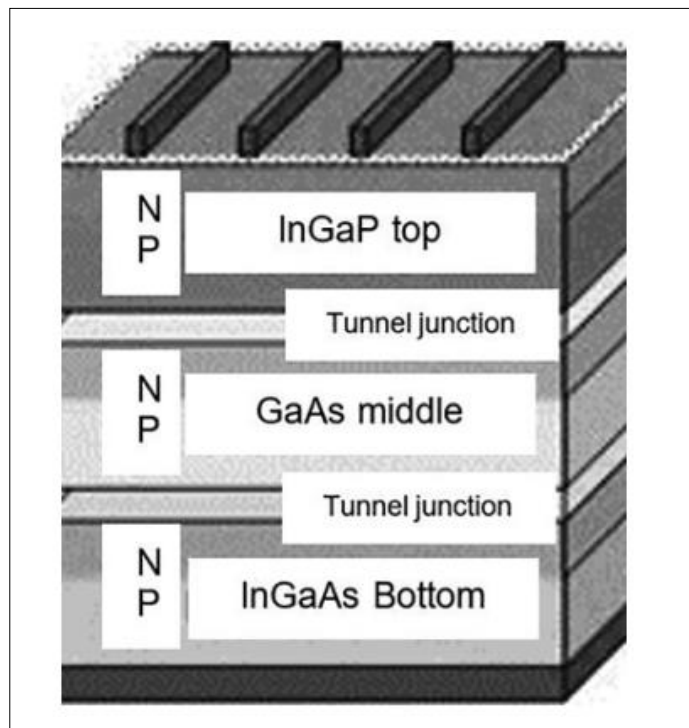


Figure I.4: A typical structure of multi-junction solar cells.

I.3. Solar energy:

Solar energy received on Earth's surface in one hour equals the energy needs for one year. With the sun emitting energy at 1367 W/m^2 , understanding its spectral factor is crucial for designing photovoltaic (PV) systems. Solar cells should absorb energy in the visible range, which contains the highest energy density. Sunlight consists of direct, diffuse, and albedo radiation, collectively termed global radiation. [6]

The atmosphere may absorb, scatter, or leave light unaffected, influenced by factors like the ozone layer, CO_2 , water vapor, and atmospheric particulate matter. [1]

The air mass affects energy absorption on the ground, with the AM0 irradiance level dropping to 1000 W/m^2 due to atmospheric conditions. AM1.5 serves as the standard test condition in solar cell design. [14]

I.3.1. Solar radiation:

Solar radiation refers to the energy emitted by the Sun as electromagnetic waves, encompassing visible and ultraviolet light as well as infrared radiation. [5]

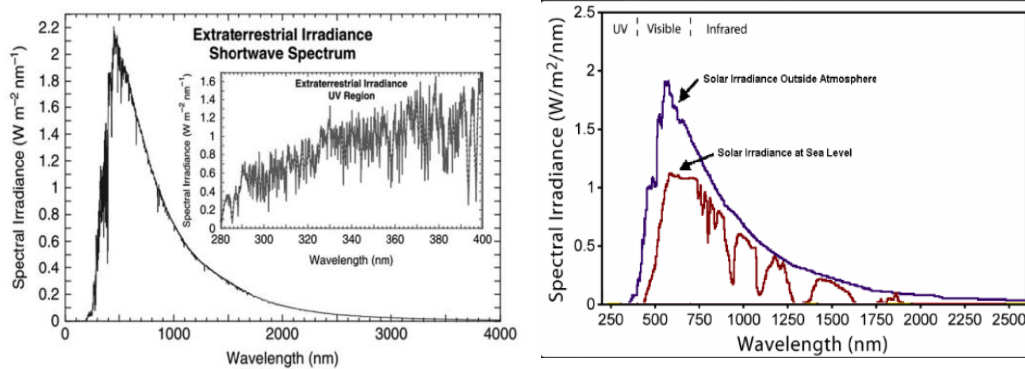


Figure I.5: the extraterrestrial solar spectrum (ETS) at the average distance between the wavelength.

I.3.1.a. Solar spectrum:

The graph (figure I.6) illustrates the modeled spectral irradiance for various air mass (AM) and zenith values: Plot of spectral irradiance for different values of AM and zenith (latitude 436° , longitude 45° , and tilt angle 436°):

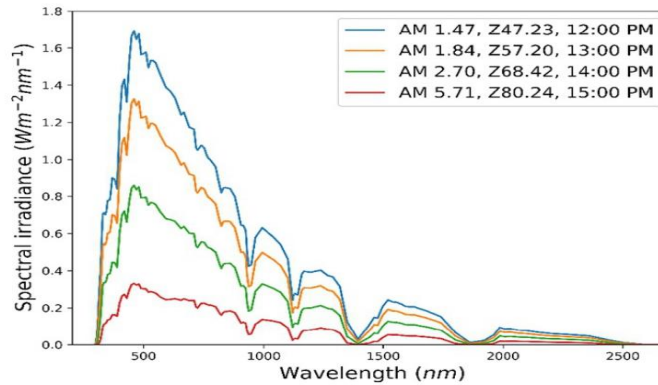


Figure I.6: Plot of spectral irradiance for different values of AM and zenith (latitude 436° , longitude 45° , and tilt angle 436°).

Renewable energy applications that harness solar radiation for terrestrial purposes primarily utilize photons, also known as "optical radiation," which fall within the spectral range of approximately 300-4000nm. [5] Solar irradiance refers to the intensity of solar energy that impacts a hypothetical unit surface and is measured in W/m². It represents an instantaneous value of energy and does not account for accumulated energy over time. Meteorologists typically use pyranometers as the primary instrument for measuring solar irradiance.

Reference solar cells are also used for measuring global solar irradiance denoted by G. [8]

The following figure I.3.3 provides a sample of the insolation recorded over the duration of 2020.[9] The daily extraterrestrial radiation on a horizontal surface (G_o) is expressed as follows:

$$G_o = \frac{24}{\pi} \left[1 + 0.033 \cos\left(\frac{2\pi d}{365}\right) \right] (\cos(\varphi) \cos(\delta) \sin(\omega_s) + \omega_s \sin(\varphi) \sin(\delta)) \quad (1.1)$$

Where d , φ , and δ are the day of the year, the latitude, and the declination, respectively. ω_s , the sunset hour angle for the horizontal surface ω_s , is given by

$$\omega_s = \cos^{-1}(-\tan(\varphi) \tan(\delta)) \quad (1.2)$$

The duration of daylight, S_o , is the time span between sunrise and sunset, and it is one of the extraterrestrial variables in the classical Angstrom (1924) equation, which can be estimated from various sources. [15][16]

$$\cos(S_o) = -\tan(\varphi) \tan(\delta) \quad (1.3)$$

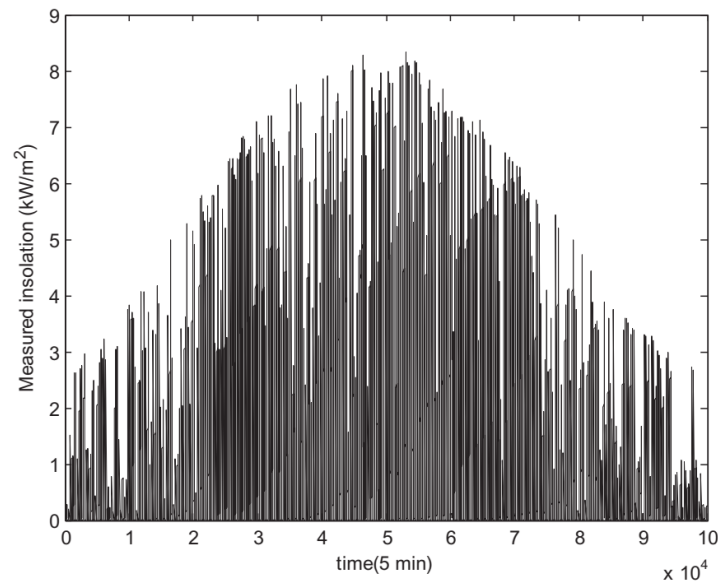


Figure I.7: The insolation measurements for the year 2020.

I.3.1.b. Extraterrestrial radiation and the length of the day:

The daily clearness index K_t is the ratio of the daily global radiation on a horizontal surface to the daily extraterrestrial radiation on a horizontal surface:

$$K_t = \frac{G}{G_o} \quad (1.4)$$

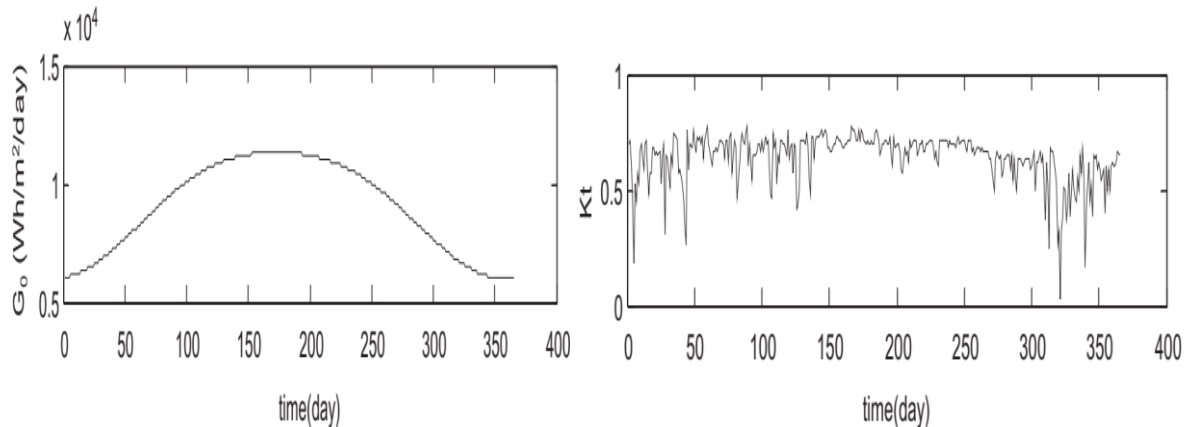


Figure 1.8: presents a graphical representation of extraterrestrial radiation (G_o) and the calculated clearness index (K_t).

I.3.2. Operating Principles of a cell:

I.3.2.1. Semiconductor materials :

Solar photovoltaics utilize semiconductors, materials with resistivity values between conductors and insulators (typically ranging from 10^{-4} to 0.5 ohmmeter). [18]

Examples include silicon, germanium, and selenium. Unlike conductors, semiconductors aren't good conductors of electricity but exhibit decreased resistance with increasing temperature, known as a negative temperature coefficient. In semiconductors, the valence band is mostly filled with electrons, while the conduction band is nearly empty, with a small energy gap between them (around 1 eV), termed the forbidden energy gap. This small gap allows for the movement of valence electrons into the conduction band with minimal energy input. [7]

I.3.2.2. Classification of Semiconductors :

Semiconductor materials can be categorized into two primary types which is: Intrinsic semiconductor (pure) and Extrinsic semiconductor (impure):

a) Intrinsic semiconductor :

An intrinsic semiconductor, also known as a pure semiconductor, is a semiconductor material that does not contain any significant dopant species. At room temperature, electron-hole pairs are created in an intrinsic semiconductor. When a potential is applied across it, conduction commences through free electrons and holes caused due to the breaking of covalent bonds through thermal energy. Therefore, the current flow in the intrinsic semiconductor is a combination of electron and hole. The number of free electrons in the conduction band is equal to the number of holes in the valence band in an intrinsic semiconductor. The current caused by electrons and holes is equal in magnitude, and the total current in an intrinsic semiconductor is the sum of hole and electron current.[18]

b) Extrinsic semiconductor :

At room temperature, intrinsic semiconductors exhibit low conductivity due to the limited number of free charge carriers (electrons and holes). To enhance the conductivity of intrinsic semiconductors, a small amount of impurity, known as a dopant, is intentionally added. This doped semiconductor is then classified as an extrinsic semiconductor. The dopants can be

electron donors (n-type dopants) or electron acceptors (p-type dopants), which increase the number of free charge carriers in the semiconductor, thereby improving its conductivity. [19]

The process of the addition of impurities to the intrinsic semiconductor is called doping. In this process, either the number of electrons increases or the number of holes increases depending on the type of impurity added. Two types of impurities are added: (1) pentavalent and (2) trivalent. Addition of pentavalent impurity produces free electrons, while in case of trivalent impurity, additional holes are generated. [18]

I.3.3. Types of Extrinsic Semiconductors:

a) P-type semiconductor:

- In p-type semiconductors, holes are the majority carriers, and electrons are the minority carriers.
- Common dopants for p-type semiconductors include boron or gallium.
- Doping with electron acceptor atoms transforms an extrinsic semiconductor into a p-type semiconductor.

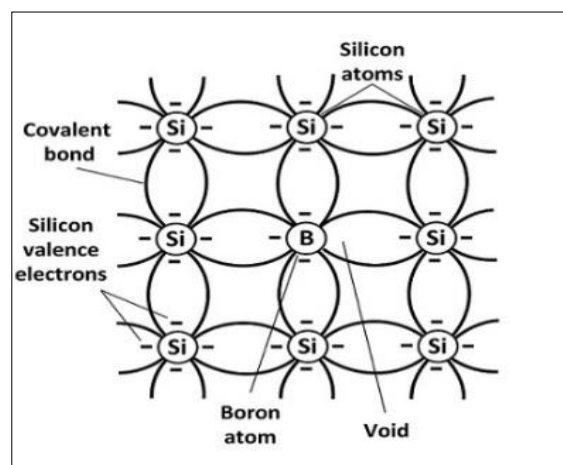


Figure I.9: p-type semiconductor:

b) N-type semiconductor:

- In n-type semiconductors, electrons are the majority carriers, and holes are the minority carriers.
- Common dopants for n-type semiconductors include phosphorus or arsenic.

-When doped with electron donor atoms, an extrinsic semiconductor becomes an n-type semiconductor.

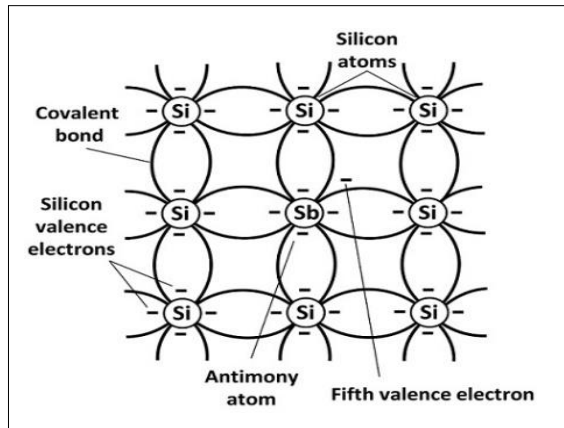


Figure I.10: n-type semiconductor.

I.4. Formation of Photovoltaics:

Photovoltaics involves converting light into electricity using semiconducting materials that demonstrate the photovoltaic effect, generating voltage or electric current when exposed to light. A photovoltaic cell comprises p-type and n-type semiconductors forming a junction. When light hits the cell, it transfers energy to electrons, allowing them to flow as an electric current. Manufacturing involves processing polysilicon, adding boron to create a p-type semiconductor. PV cells include crystalline silicon, thin-film, and organic types, each with distinct pros and cons. [8][9][14]

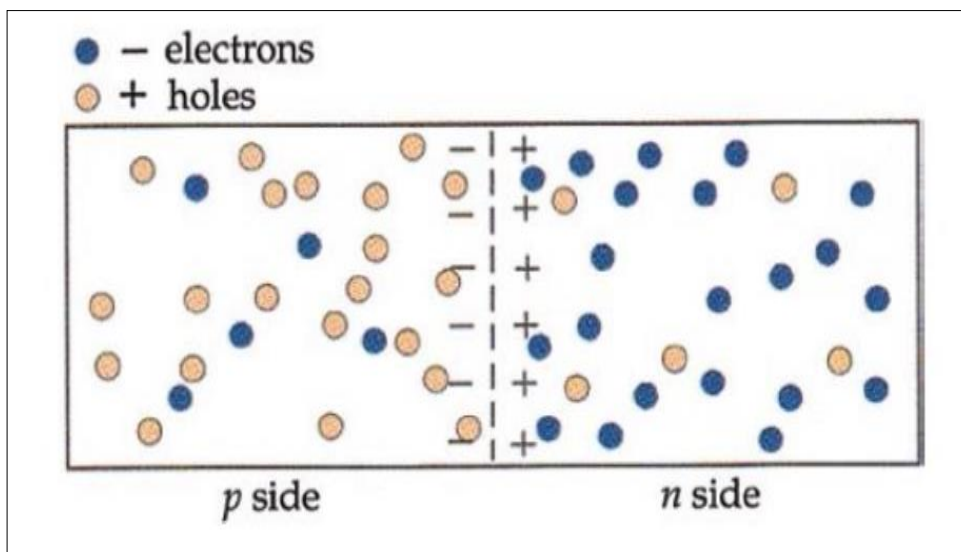


Figure I.11: the Structure of photovoltaic.

I.5. Photovoltaic systems :

I.5.1. Stand-alone (off-grid) PV systems :

Stand-alone photovoltaic (PV) systems, also known as off-grid systems, are electrical systems that consist of an array of one or more PV modules, conductors, electrical components, and loads, and are not connected to the power grid. [15] These systems are used in remote areas, where extending the power line to the grid is impractical or uneconomical, and in situations where users wish to be independent from the power provider. Stand-alone PV systems typically include solar panels, charge controllers, batteries, inverters, and other balance-of-system components. These systems are designed to provide reliable power for various applications, such as residential, commercial, and industrial uses. As it shown in the figure below (figure I.4.2)

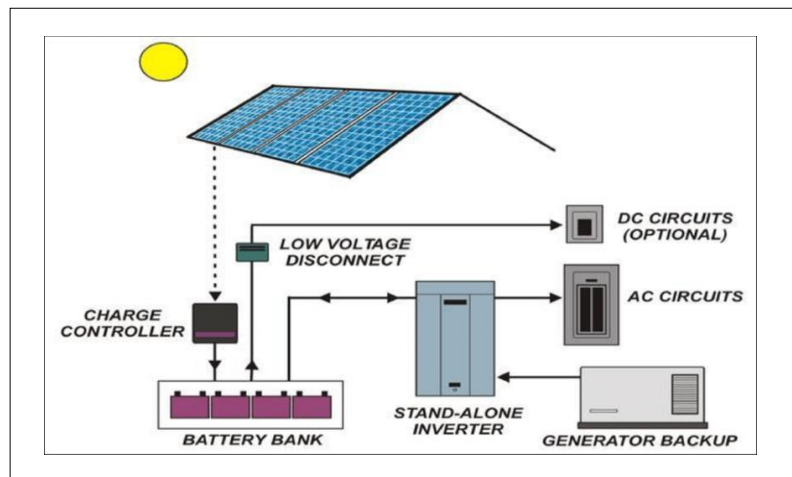


Figure I.12: Stand-alone (off-grid) PV systems.

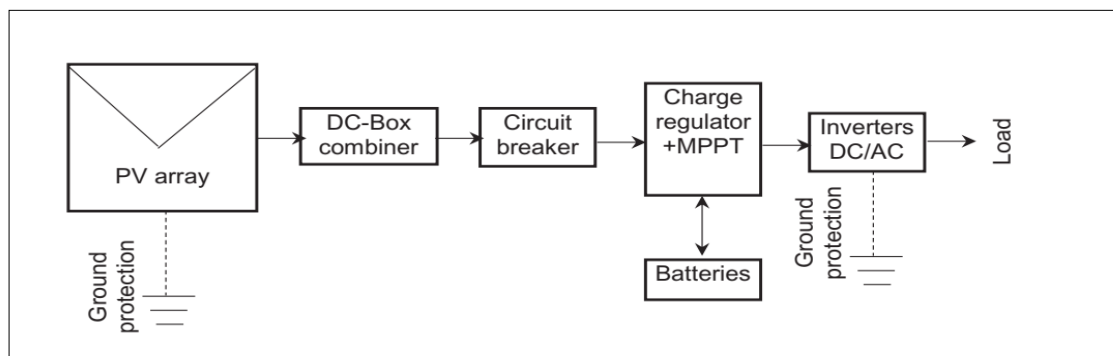


Figure I.13:Schematic of Stand-alone PV system.

I.5.1.1. Grid-connected PV systems :

Grid-connected photovoltaic (PV) systems are electricity-generating solar systems that are connected to the utility grid. These systems consist of solar panels, one or several inverters, a power conditioning unit, and grid connection equipment. They range from small residential and commercial rooftop systems to large utility-scale solar power stations. When conditions are right, the grid-connected PV system supplies excess power to the utility grid, which can be consumed by other users .A grid-connected PV system does not require a battery system, making it simpler and more cost-effective than stand-alone systems. However, it does require a connection to the utility grid, which means that the system will not function during power outages unless it has a battery backup system.[15]

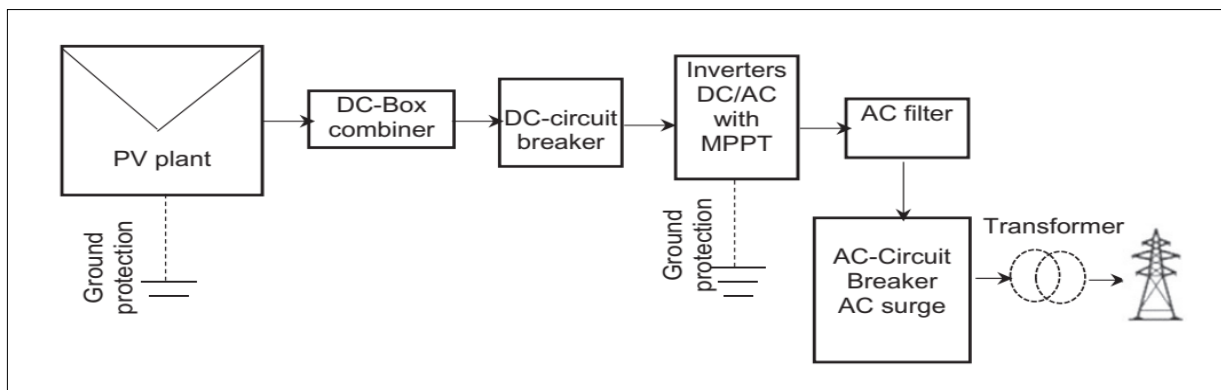


Figure I.14: Schematic representation of a grid-connected PV system.

I.5.1.2. Hybrid photovoltaic systems:

Hybrid photovoltaic (PV) systems are versatile renewable energy systems that can connect to the grid like traditional solar arrays or operate independently during power outages. These systems typically incorporate solar panels, a hybrid inverter, and a battery bank, allowing them to intelligently switch between using solar power, battery storage, and grid power. This flexibility enables homeowners to manage their energy usage, avoid peak electricity prices, and even provide backup power during grid outages. Hybrid PV systems can be a cost-effective and environmentally sustainable option, offering the benefits of both grid-tied and off-grid systems. They are designed to comply with relevant standards and can be tailored to meet specific energy needs, making them a practical choice for various applications, including residential, commercial, and industrial use.[19]

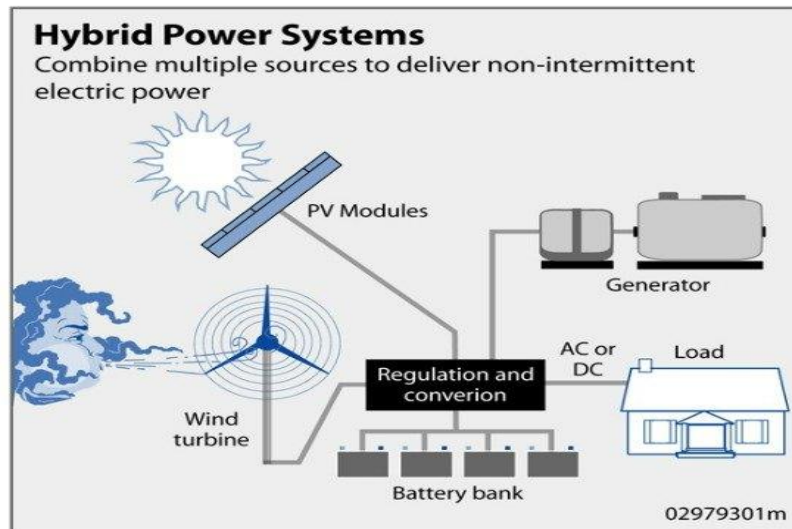


Figure I.15: Hybrid photovoltaic systems.

I.5.3. Regulator :

Charge regulators are integral components of a photovoltaic system, aiming to manage battery charging and discharging for optimal longevity. Their primary function involves curtailing current as the battery nears full charge, preventing the formation of small bubbles on the positive electrodes. [17] The charge regulator serves two primary purposes:

- Battery Protection:** By controlling the charging process, the charge regulator prevents overcharging, which can damage the battery and shorten its lifespan.
- Optimization:** The charge regulator ensures that the battery is charged efficiently, maximizing its capacity and performance.

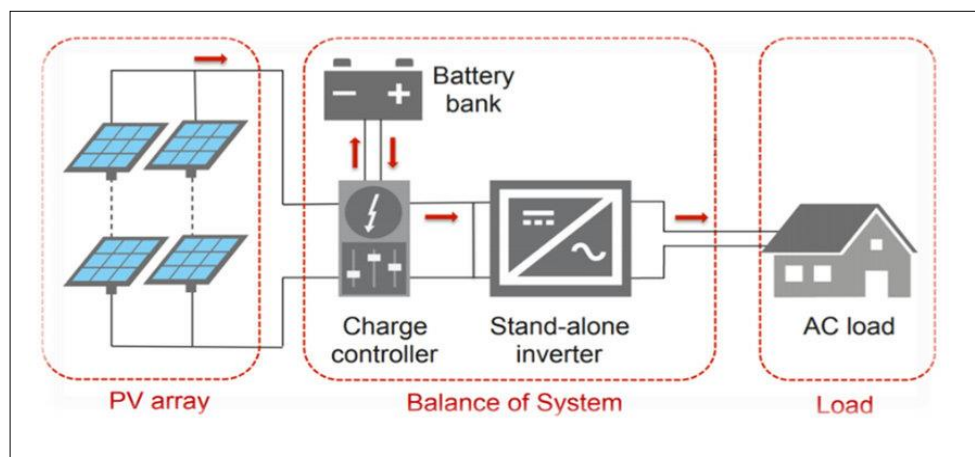


Figure I.16: Basic structure of an autonomous solar energy system.

I.6. Photovoltaic module:

I.6.1. Composition of a photovoltaic module :

A photovoltaic (PV) solar module typically consists of six primary components, as depicted in figure I.6.1:

- Aluminum frame: Provides structural support and rigidity to the module.
- Sealant: Used to fix the module and ensure watertightness.
- Glass: Offers protection to the PV cells and module.
- Ethylene-vinyl acetate (EVA) layer: Resists weather and moisture, encapsulating the PV cells.
- Photovoltaic cells: The semiconductor devices that convert sunlight into electricity.
- White Tedlar sheet: Enhances the mechanical strength of large modules, particularly in terms of durability and resistance to environmental factors. [19]

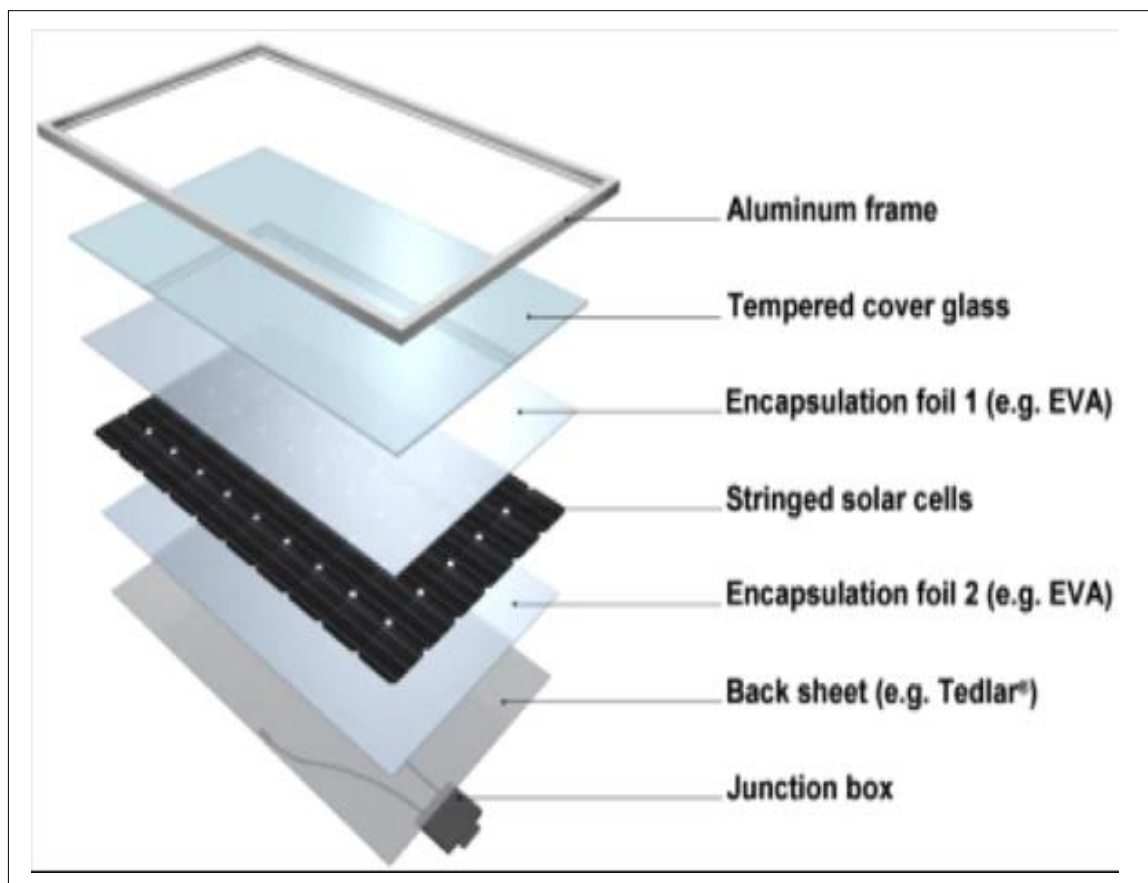


Figure I.17: Composition of a photovoltaic solar module.

I.6.2. Series and Parallel Connection of a PV Module :

I.6.2.1. Series connection :

When identical cells or modules are connected in series, the current of the branch remains constant, while the voltage increases proportionally to the number of cells or modules connected in the series configuration. This means that the voltage of the entire series branch is the sum of the voltages of each individual cell or module, resulting in a higher overall voltage output.

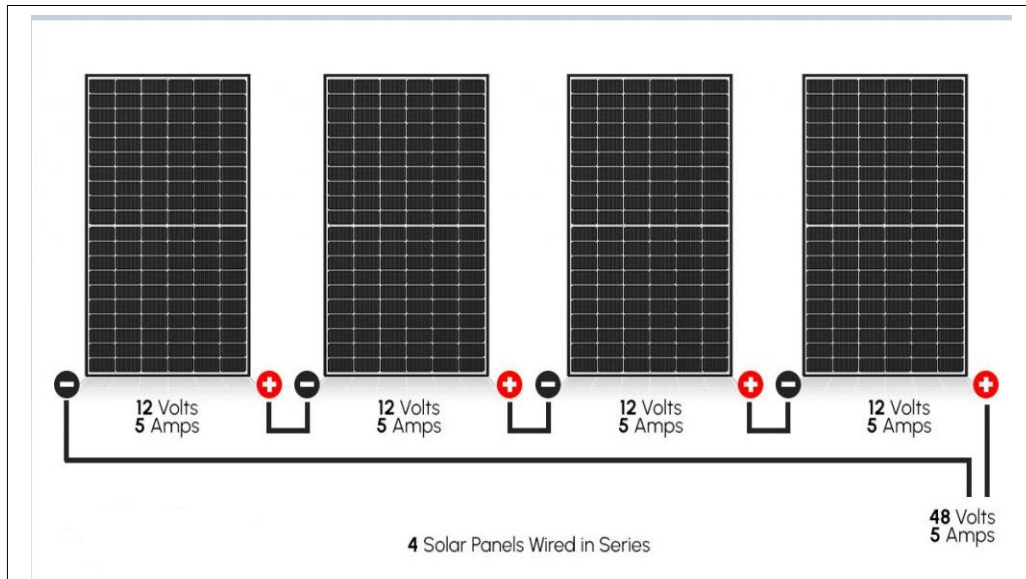


Figure I.18: Charge-Solar-SolarPanelsSeriesWired.

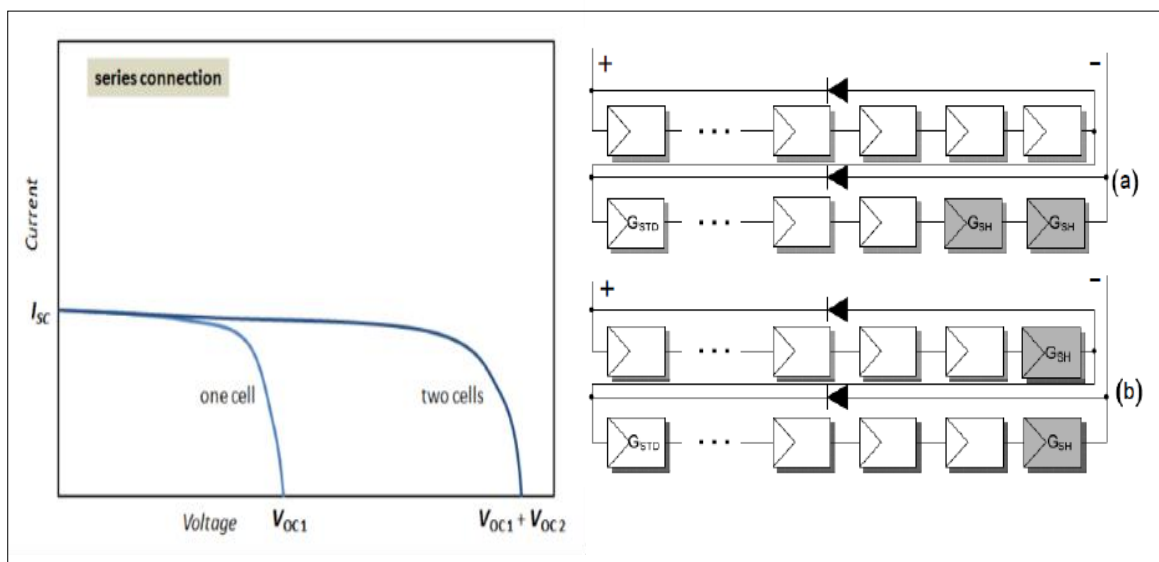


Figure I.19: Resulting characteristic of a grouping of ns cells in series.

I.6.2.2. Parallel connection :

In a parallel connection of photovoltaic (PV) modules, the voltage remains the same, while the current increases proportionally to the number of modules connected in parallel. This configuration is used to increase the current output of the system. [40]

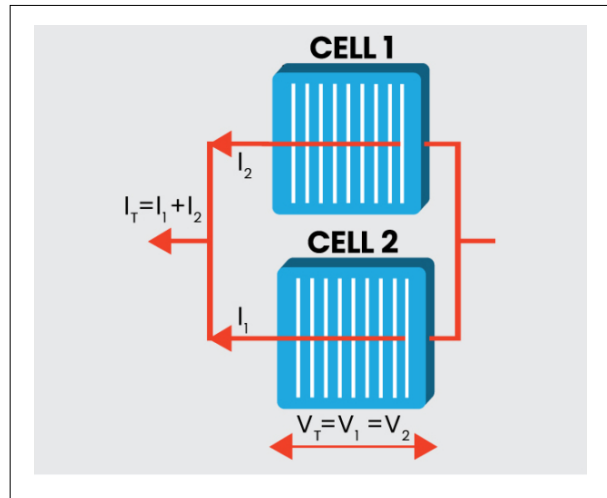


Figure I.20: Parallel Connection of PV Cells.

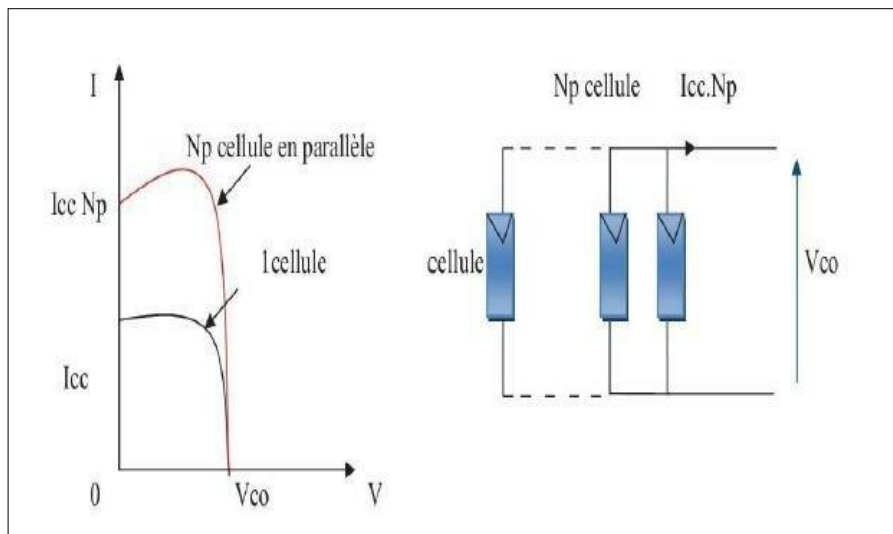


Figure I.21: Resulting characteristic of a grouping of n p cells in parallel.

I.6.2.3. Safeguarding of a PV module :

Protection of a photovoltaic (PV) module involves several measures to ensure safety and prevent damage to the system and its components. Some key aspects of PV module protection include:

- Current protection: Fuses or circuit breakers are used to protect against overcurrent, which can cause thermal effects and damage to cables and other components. These devices should be listed for DC use and have the appropriate voltage and interrupt ratings.
- Insulation monitoring: Insulation monitoring devices are used to detect any loss of insulation resistance, which can be critical for PV systems that do not require either conductor to be earthed.
- Fire protection: Since PV modules are installed outdoors and can be installed on roofs, fire protection is critical. This includes the use of double or reinforced insulation to prevent the appearance of dangerous voltage on accessible parts.
- Array protection: At the array level, fuse-links or other overcurrent protection devices are used to protect DC cable systems against overloads and short-circuit currents.
- Environmental protection: PV systems are exposed to the elements, so ambient temperature and other outdoor conditions should be considered when designing protection systems.

Here's a visual representation of a PV module with protection devices :PV Module Protection This image shows a PV module with a fuse, a bypass diode, and a junction box for protection against reverse current, overcurrent, and environmental factors. The specific protection devices and their ratings will depend on the system's design and local electrical codes. [19]

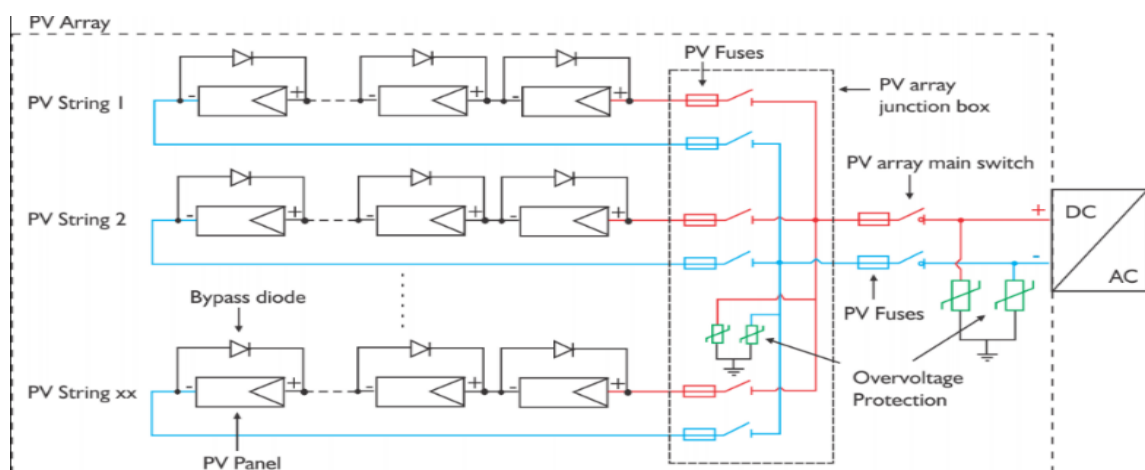


Figure I.22: Series/parallel wiring of photovoltaic modules with their protection diodes.

I.7. Characteristics of a photovoltaic generator :

I.7.1. Current-Voltage Characteristics :

The current-voltage (I-V) characteristics of a photovoltaic (PV) generator describe the relationship between the output current and voltage of a PV cell, module, or array. These characteristics are influenced by factors such as solar irradiance, temperature, and the PV device's design. Here are some key aspects of PV I-V characteristics:

- Short-circuit current (I_{sc}): The maximum current generated when the PV device's terminals are short-circuited, with zero voltage. [2]
- Open-circuit voltage (V_{oc}): The maximum voltage generated when the PV device's terminals are open-circuited, with zero current.
- Maximum power point (MPP): The operating point on the I-V curve where the product of voltage and current is maximized, representing the highest power output.
- I-V curve shape: The I-V curve is nonlinear, with a characteristic "knee" shape, and the MPP is typically located near the bend in the curve
- Effect of solar irradiance: The amount of solar radiation hitting the PV device controls the output current (I). [2]
- Effect of temperature: Increasing temperature reduces the voltage (V) of the PV device.
- I-V curve scaling: When PV devices are connected in series, the voltage increases, and when connected in parallel, the current increases. [2]

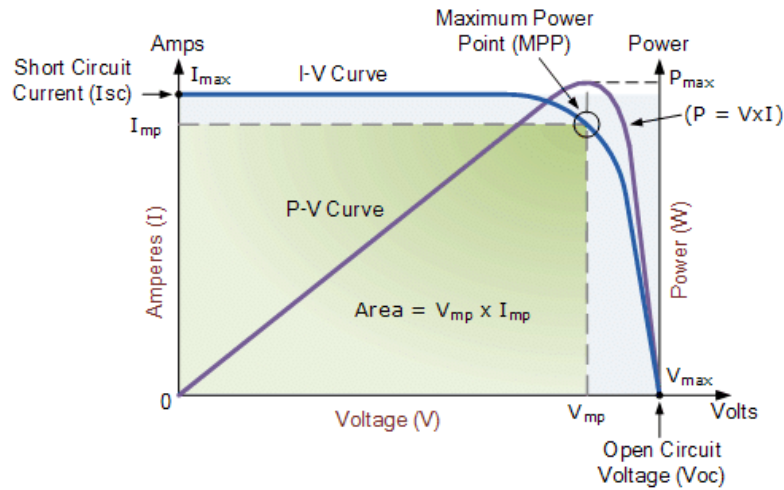


Figure I.23: Influence of illumination on I(V) and P(V).

I.8. Impact of Irradiance and Temperature:

I.8.1. Impact of Irradiance:

The influence of irradiance on photovoltaic (PV) performance is significant, as it directly affects the output current and power generated by solar cells. When all other parameters are constant, higher irradiance leads to greater output current, which in turn increases the power produced by the PV module. This relationship can be expressed mathematically, where an increase in irradiance results in higher current and power output.

Irradiance affects PV performance in the following ways:

- **Current and Power Output:** As irradiance increases, the PV module generates higher current and power, as illustrated by the I-V and P-V curves.
- **Temperature Effects:** While irradiance increases power output, higher temperatures can reduce the open-circuit voltage (Voc) of a PV module, which in turn reduces the power output. The PV module's temperature coefficient must be considered when designing a solar PV system.
- **Landscape and Obstructions:** The characteristics of the landscape, such as elevation and obstructions like trees or hills, can affect irradiance levels, which in turn influence PV performance.

- **Inverter Output:** Variations in irradiance and temperature can impact the inverter output, which is a critical component of a PV system.

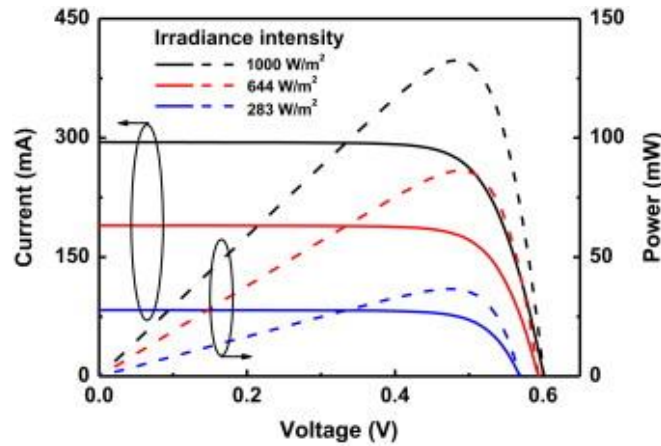


Figure I.24: The influence of temperature on the I (V) and P(V) characteristics.

I.8.2. Influence of temperature :

The temperature exerts a substantial influence on the performance of photovoltaic cells, as evidenced by experimental observations. The short-circuit current experiences a minimal change with temperature, while the open-circuit voltage is markedly affected, with a decrease of approximately -0.4% per Kelvin (K) . Consequently, temperature has a considerable impact on the efficiency of photovoltaic cells, leading to power losses ranging from 9% to 15% for a temperature increase of 30°C. [3]

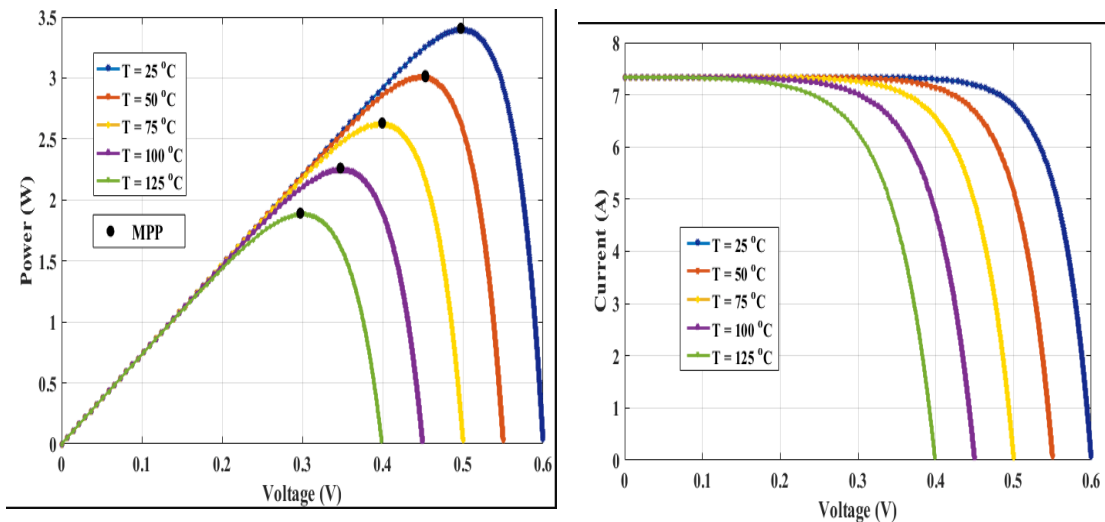


Figure I.25:The influence of temperature on the P(V) and I(V) characteristics.

I.8.3. Orientation of solar panels :

When choosing the orientation of solar panels, consider the following:

a- Direction: In the northern hemisphere, panels ideally face south, and in the southern hemisphere, they face north to capture the most sunlight throughout the day. [5]

b- Angle: The panel tilt angle typically approximates the location's latitude to maximize annual energy production, with adjustments for seasonal variations. [2]

c- Shading: Avoid shading from nearby objects or structures, as it can significantly reduce energy production. [6]

d-Tracking Systems: For increased efficiency, consider advanced tracking systems that adjust panel orientation to follow the sun's path throughout the day. [6]

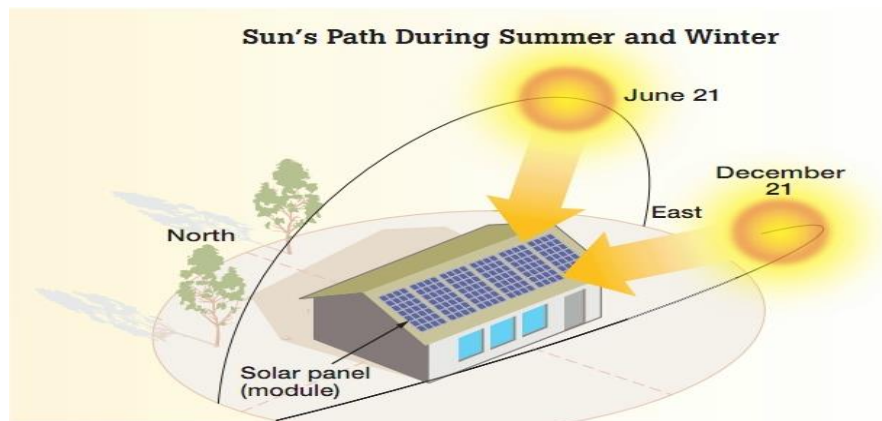


Figure I.26: Orientation of solar panels.

I.8.4. Use of photovoltaic energy:

Photovoltaic systems find application in agricultural irrigation by powering solar pumps, drawing water from wells or other sources. This provides a cost-effective and reliable solution in areas lacking grid power or where installation is expensive. Particularly useful in remote locations, solar pumps can fill livestock watering tanks or refill drinking water storage tanks in self-sufficient homes, meeting water needs beyond power line reach. [15][18]

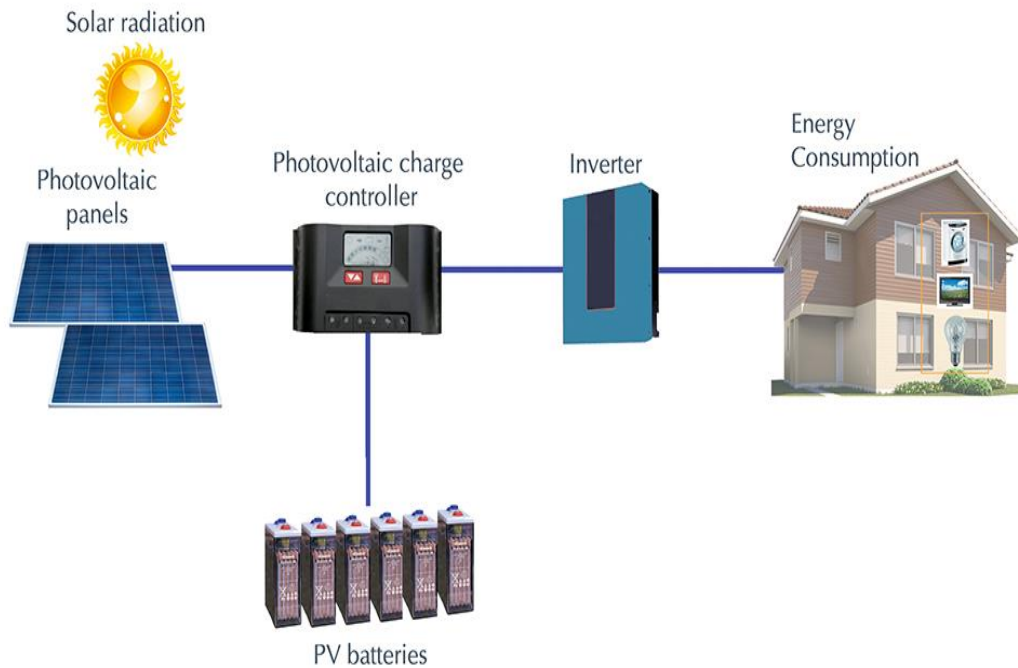


Figure I.27: An application of photovoltaic systems.

I.9. Advantages and disadvantages of PV (photovoltaic) energy:

I.9.1. Advantages of PV (photovoltaic) energy:

Table I.1 : Advantages.

Clean energy	PV systems do not emit greenhouse gases, pollute groundwater, or deplete natural resources.
Lower energy bills	Generating your own electricity can significantly reduce your energy bills.
Low maintenance	PV systems require minimal maintenance, with no moving parts and long-lasting components.
Quiet operation	PV systems are unobtrusive and operate quietly.
Renewable energy source	Solar energy is available every day and will be accessible as long as the sun exists.

I.9.2. disadvantages of PV (photovoltaic) energy:

Table I.2 : disdvantages.

High startup cost	The initial investment for PV systems can be relatively high, although it is decreasing as the industry expands.
Weather dependency	Solar energy output can be affected by weather changes, such as cloudy days, which can temporarily reduce electricity production.
Energy storage requirements	Some PV systems use batteries for energy storage, which increases the footprint, cost, and complexity of the system.
Efficiency needs improvement	PV systems need to be used with efficient appliances to reflect cost-effectiveness.
Lack of knowledge and skills	Photovoltaic technology is an emerging field, and the lack of relevant information can limit its development.

Conclusion:

While photovoltaic (PV) energy offers numerous benefits, including renewability, environmental friendliness, low operational expenses, and a lengthy lifespan, it also presents drawbacks such as initial high costs, dependency on weather conditions, space prerequisites, energy storage demands, and potential environmental impacts. Nevertheless, PV energy remains a promising and expanding energy source, capable of curbing greenhouse gas emissions and addressing climate change. As technology advances and expenses decline, PV energy is expected to become increasingly accessible and prevalent in the future.

CHAPTER II

II. Introduction:

Photovoltaic systems can experience various types of malfunctions affecting all components such as modules, cabling, protections, converters, and inverters. These issues are primarily due to external operating conditions.[63] Failures in photovoltaic systems can be attributed to shading effects, module soiling, inverter failure, [64] and mismatch caused by manufacturing discrepancies or aging of PV modules. [65] The most significant catastrophic failures in PV arrays include line-to-line (LLF), ground (GF), and arc (AF) faults. [7]

In this chapter we We will discuss that the advanced monitoring techniques have been developed for photovoltaic systems, aiming to predict failures and optimize system performance. Some fault detection algorithms rely on simulating the electrical circuit of PV generators, while others utilize electrical signal methods like time domain reflectometry or maximum power point tracking analysis. Predictive models for power production compare measured and modeled outputs, with various monitoring systems incorporating statistical analysis and artificial intelligence methods. [4] [58]

II.1. Fault detection and diagnosis methods :

II.1.1. Types of faults :

a- LL Fault: a defect in the PV array that develops between two sites with different potentials. The points could be on separate strings or on the same string, as it shown in figure II.1. [59]

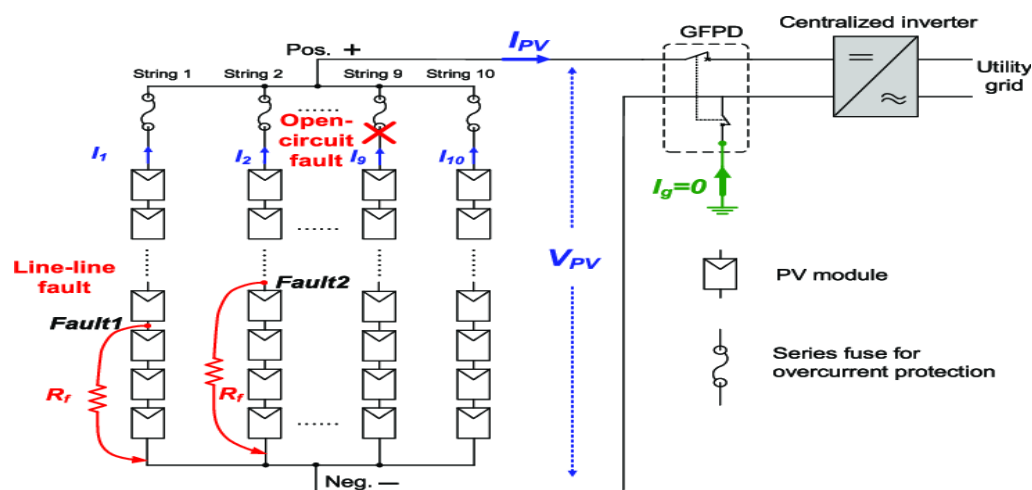


Figure II.1: Faults created between the panels.

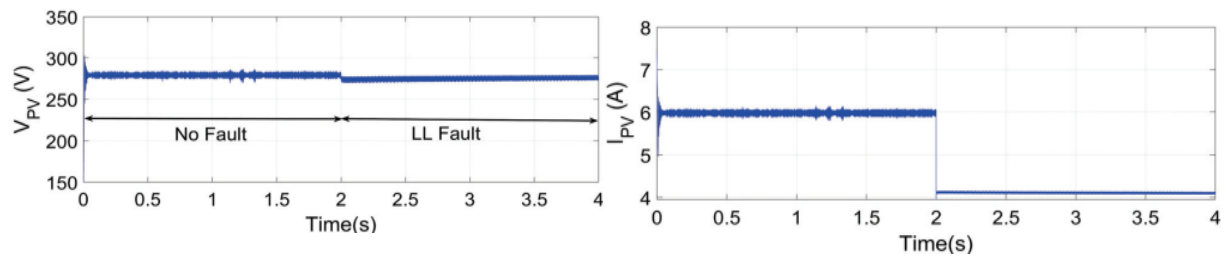
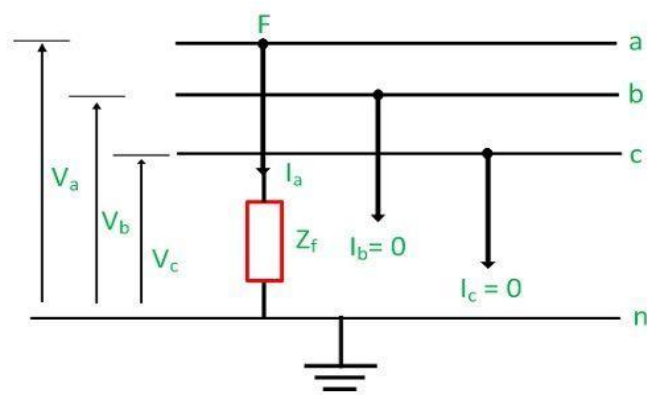


Figure II.2: Voltage and Current of the PV Array under LL Fault.

b-LG Fault : Between a location in the first string and the earth, [59] an LG fault is produced. As its illustrated in figure II.3 and figure II.4.



Single line-to-ground fault

Circuit Globe

Figure. II.3: LG Fault.

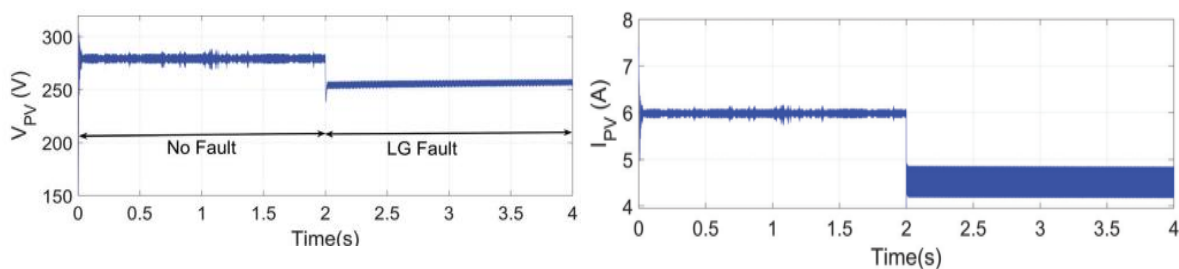


Figure II.4: Voltage and Current of the PV Array under LG Fault.

c-LLG Fault : Between two places in the first two strings and the ground, an LLG fault is formed. [59][58]

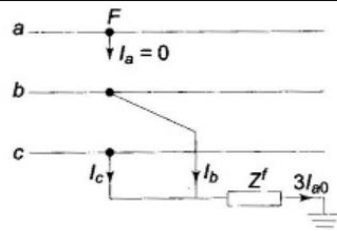


Figure II.5: Double line to ground (LLD) fault.

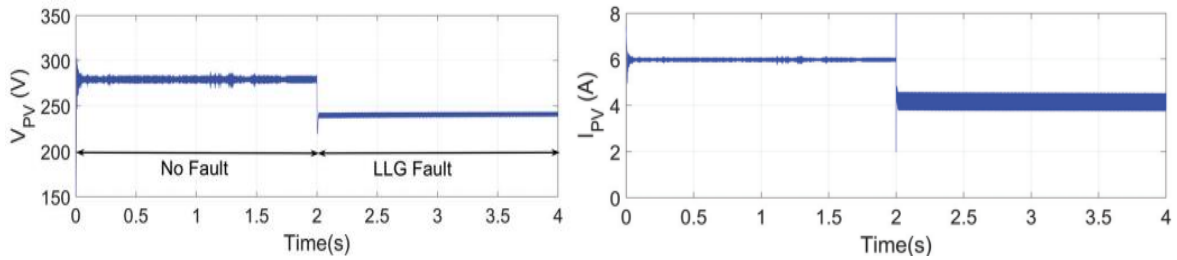


Figure II.6: Voltage and Current of the PV Array under LLD Fault.

d-Bypass Diode Fault : One of the panels in the first string has a short-circuited bypass diode.

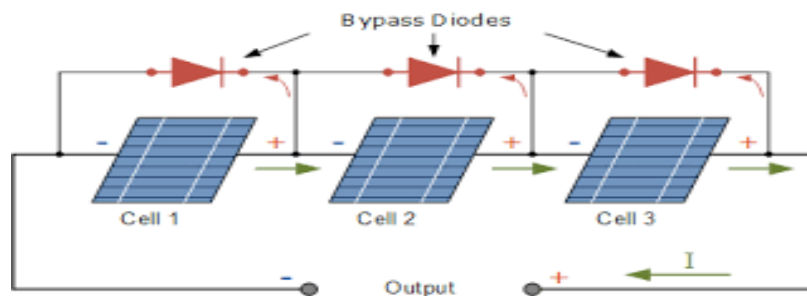


Figure II.7: Bypass Diode Fault.

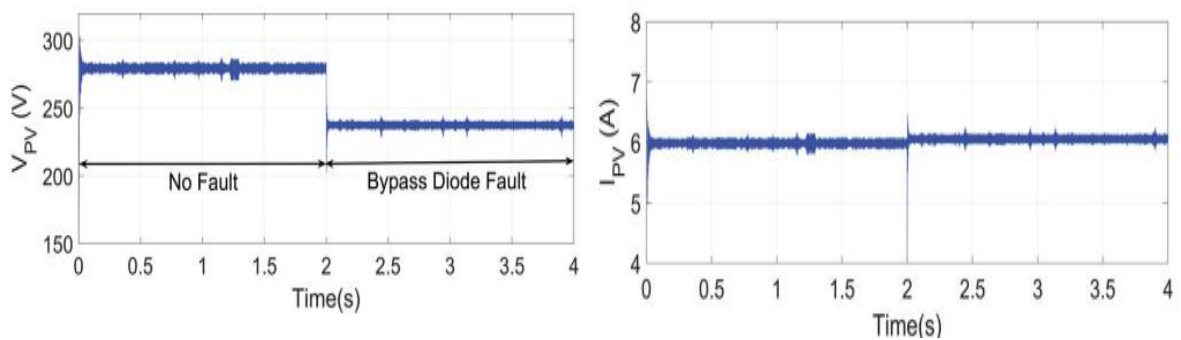


Figure II.8: Voltage and Current of the PV Array under Bypass Diode Fault.

II.1.2. Diagnostic Methods :

Numerous fault diagnosis techniques (FDD) approaches have been presented in the literature. These techniques can be characterized by three key features: selectivity (i.e., the capacity to discriminate between distinct defects), the ability to promptly discover malfunctions, and the required input data (climatic and electrical data). [20]

Table II.1: Diagnostic Methods.

Method for detection	description
Visual & Thermal Methods	Used for detecting discoloration, browning, surface soiling, hot spots, breaking, and delamination
Electrical Methods	Utilized for detecting and diagnosing faulty photovoltaic modules (PVM), strings, and arrays including arc faults, grounding faults, diode faults. [22]

The majority of electrical-based FDD techniques use a PVS model of some kind to identify different kinds of failures. Only electrical methods will be examined and discussed in this section. Electrical techniques can also be categorized into five groups. [23]

Table II.2: Electrical-based FDD methods.

Electrical-based FDD methods				
Statistical and signal processing approaches (SSPA)	I-V characteristics analysis (IVCA)	Power losses analysis (PLA)	voltage and current measurement (VCM)	artificial intelligence techniques (AIT)

Once the necessary knowledge is enumerated, the diagnostic procedures for a particular industrial system are classified. Numerous methods have been created to aid in the diagnosis of faults. These many techniques will be shown, [24] by being divided into three classes: reasoning mode-based functional and hardware modeling diagnostic techniques, physical modeling diagnostic techniques, and external signature analysis diagnostic techniques.

Model-based techniques rely on basic physical concepts and quantitative or qualitative models that take into account the interactions and structure of the system's components. [25]

Expert knowledge and reasoning are the foundation of knowledge-based techniques. [9][10][11]

System characteristics are extracted from stored data using database-based methodologies. [26][27]

Instead than creating a model to represent the behavior of the system being studied, the study concentrates on the direct creation of residues. [28]

Table II.3: Different diagnostic methods.

Decision model	Analytically-Based	Parametric estimation
		State watcher
		Parity space
	Knowledge-based	System expert
		Qualitative (fuzzy)
	Has data-based	Fuzzy logic
		Neural network
		Neuro-fuzzy

II.1.3. Model-based methods:

Diagnostic techniques based on models are prevalent in the literature. Their use has grown significantly, especially when it comes to important sectors like heavy industry, transportation, and energy systems. [8][10][13][14] This FDI (Fault Detection and Isolation) strategy includes methods for fault localization, fault detection, and residual generation, as was previously addressed. The strategy is shown in Figure (II.9). [26]

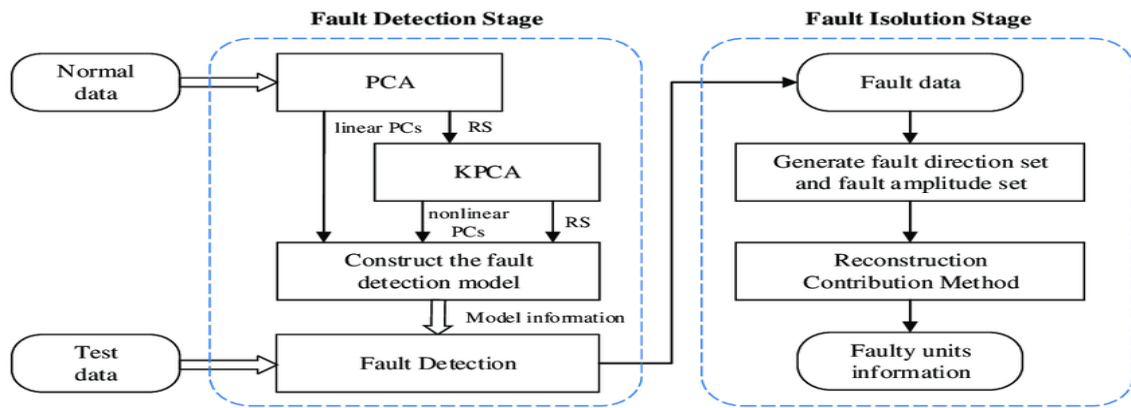


Figure II.9: Fault Detection and Isolation (FDI) Procedure.

• **Parametric estimation :**

Whether it is based on knowledge or representation, a mathematical model of a system comprises a collection of parameters, the numerical values of which are typically unknown. Techniques for parametric estimating enable defining the parameter vector that the model employed, derived from a collection of system measurements.

The physical properties of the system are altered when a failure arises, which causes the parameters to significantly deviate from their nominal values. Stated differently, any discernible departure of the parameters from their stated values points to a problem. For this reason, it's fascinating to look for a parametric estimator to diagnose industrial systems. As a result, it is possible to compare the estimated and actual system parameters. [27][28]

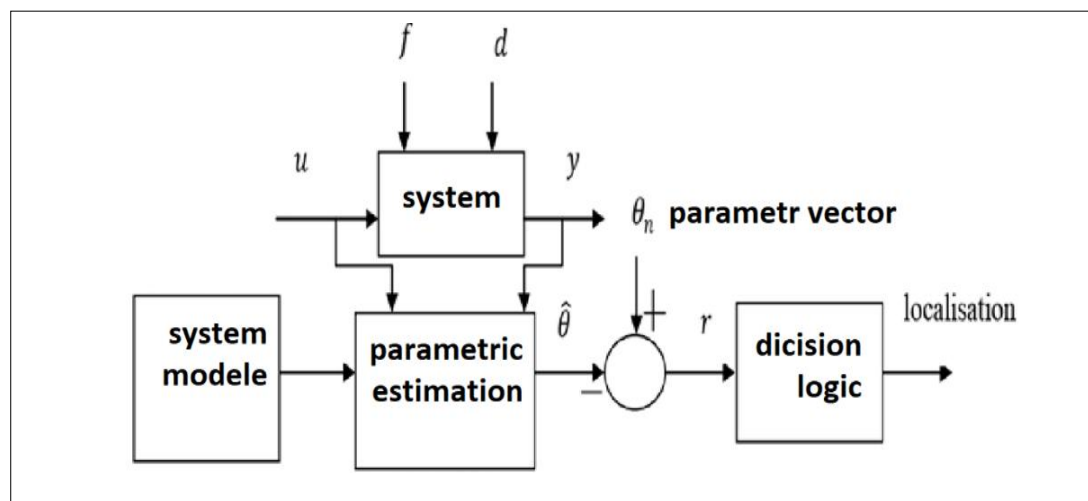


Figure II.10: Principle of residual generation through parametric estimation.

• State observation:

Whether a control law is being implemented or a system needs to be diagnosed, the problem of state estimation is important. Observers who gauge the system's outputs using quantifiable variables—that is, the inputs and outputs—are the foundation of residual generation. The discrepancy between the measured and estimated outputs is known as the residual. [29][30]

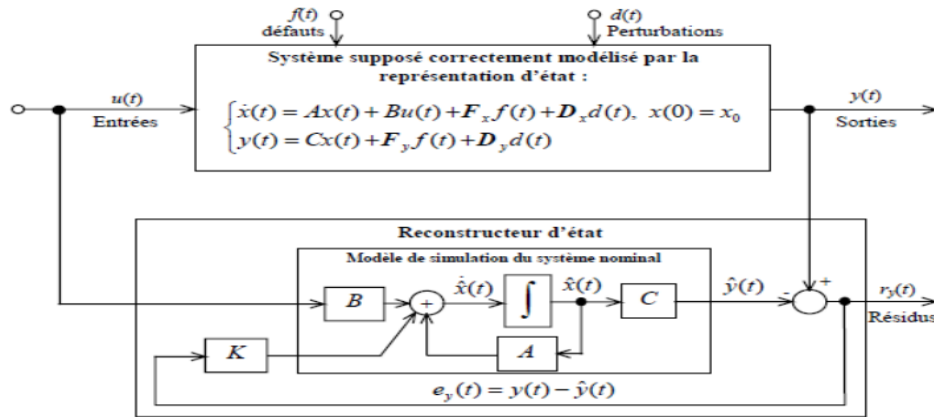


Figure II.11: general principle of an observer, which includes a state model of the system closed by the estimation error.

Where:

$A \in R^{n \times n}$: The state or evolution matrix, $B \in R^{n \times m}$ is the input vector.

$C \in R^{p \times n}$:The output or observation vector.

Dx :Represents the action of perturbations $d(t)$.

F_x and F_y :The fault action matrices $f(t)$ to be detected.

L :The observer gain matrix.[30][31]

• Parity space :

The Parity Space method is a valuable technique used in fault diagnosis, particularly in dynamic systems. It involves creating residuals that are insensitive to structured disturbances, aiding in fault detection and isolation. This method utilizes geometric procedures to determine null subspaces efficiently, enhancing fault diagnosis robustness. The Parity Space approach is

widely studied and applied in various fields, such as control engineering and aerospace systems, showcasing its effectiveness in recognizing faults and avoiding accidents. [27][32]

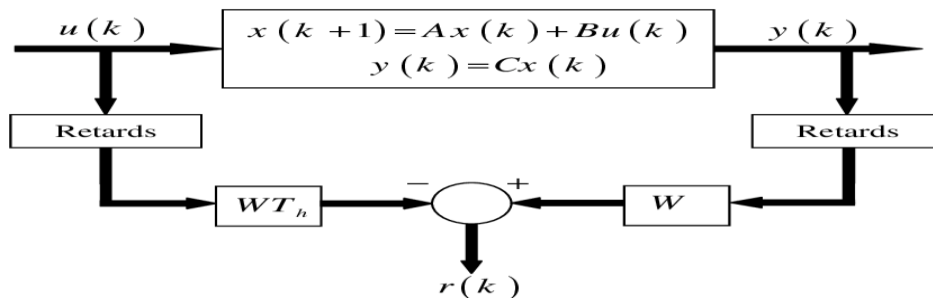


Figure II.12: Parity space diagnostic.

II.1.4. Knowledge-Based Methods:

When it is not physically possible to simulate the devices that connect the problems' causes, several techniques are used. They are predicated on test results. Neural networks, fuzzy logic, pattern recognition, and expert or knowledge-based systems are a few of these techniques. [33][34]

• Pattern Recognition :

This method combines techniques that enable a shape to be automatically classified according to how similar it is to a reference shape. Put otherwise, it is imperative to determine which category of recognized objects—that is, shapes—the observed object—also called a shape—belongs to. Using q parameters, or features, which stand for the elements of a feature vector, a shape is determined. [35][36]

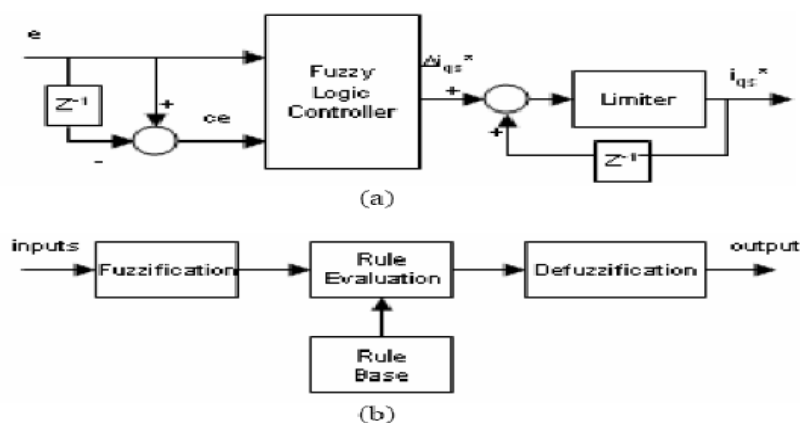


Figure II.13: Pattern Recognition-Based Diagnostic System Diagram (Fuzzy logic).

There are three main steps involved in developing a pattern recognition-based diagnostic method:

- Creation of a training database.
- Selection and parameterization of a classifier.
- Effective utilization of the classifier during the operational phase.

• **Expert system :**

Even though the investigated area is complex and prevents all feasible elements of the conditions, an expert system is needed to supply responses connected to a particular state. As a result, a repair professional bases their diagnosis on only a portion of the whole picture. They deepen their diagnosis by offering pertinent extra information about the system to be diagnosed, show all potential conclusions, and develop new assumptions based on the set of accessible signs. [37]

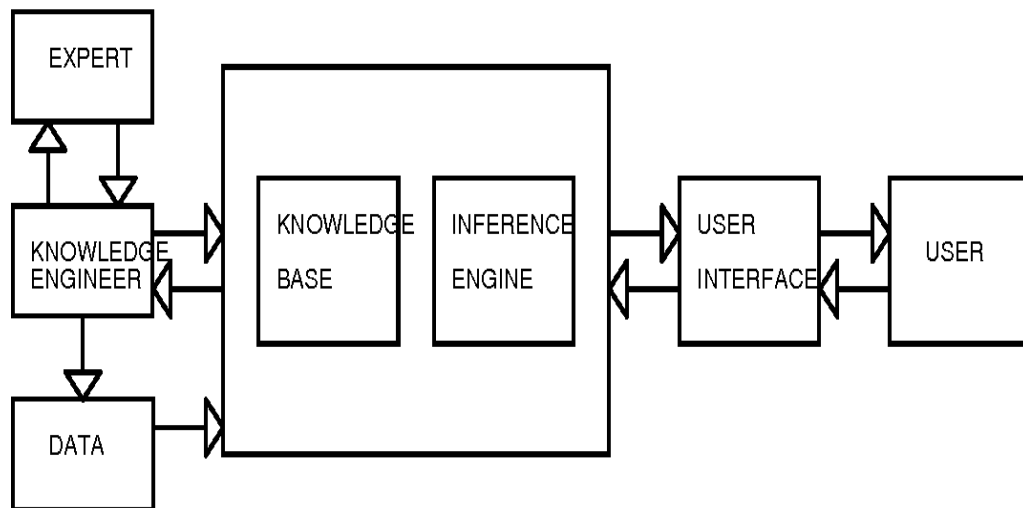


Figure II.14: General structure of a diagnostic expert system.

II.2. Chopper (DC-DC Boost):

A DC-DC converter that boosts the input DC voltage to a predetermined output voltage is called a boost chopper, sometimes referred to as a step-up chopper. It functions by changing a constant voltage into a greater magnitude voltage. The components of the boost converter are an inductor, a diode, a capacitor, and a solid-state switch (similar to a transistor) coupled in a certain way. Pulse width modulation (PWM) is used to control the switch in order to adjust the output voltage. When the switch is on and conducting, as well as when the switch is off and the diode is on, are the two primary modes of operation for the boost converter. In practical boost converters, it is crucial to keep the duty cycle within a specific range in order to avoid instability.

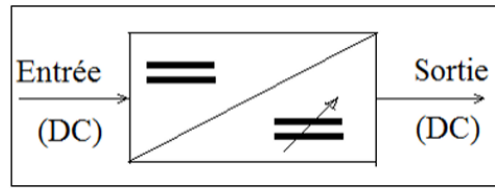


Figure II.15: Principle Diagram of a Chopper.

II.2.1.Chopper boost modeling :

- 1• A study on the modeling and control of a boost chopper linked to an AC drive system, focusing on digital control aspects within a hybrid electric system.
- 2• Research detailing the modeling and controller design for a non-inverting buck-boost chopper, presenting a successful switching strategy and a state-space model for decision-making.

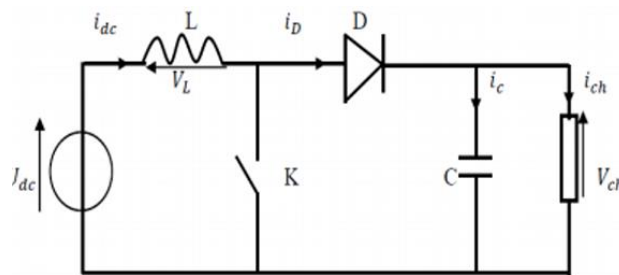


Figure II.16: Parallel (Boost) Chopper.

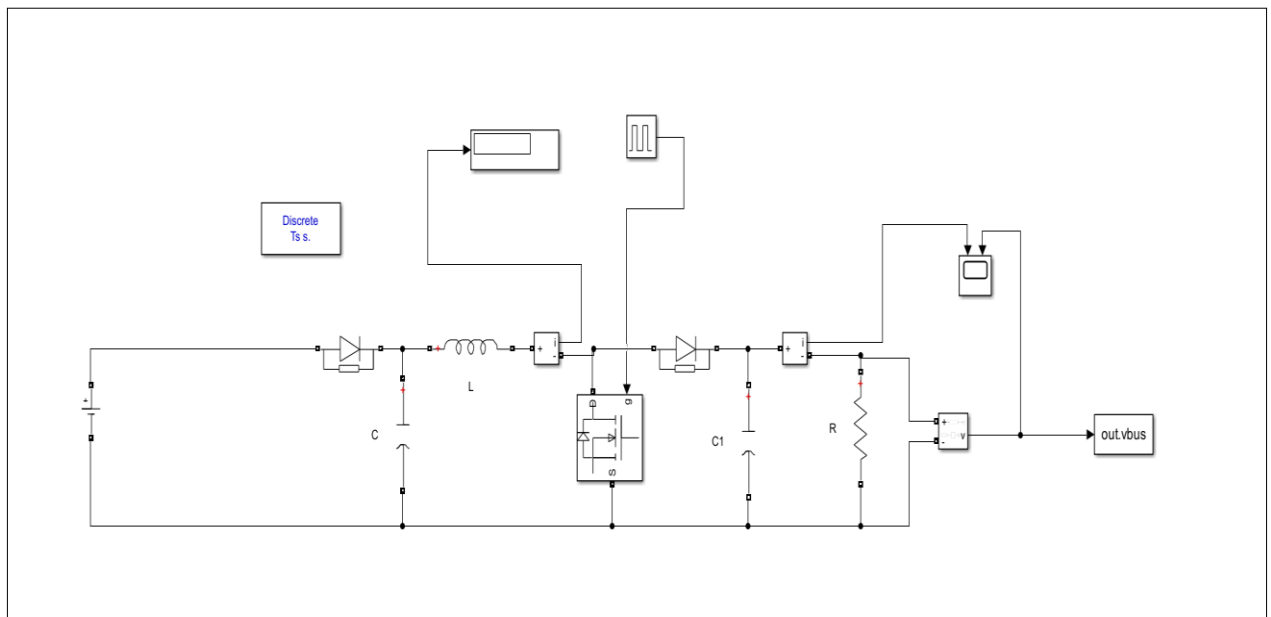


Figure II.17: Modeling of Chopper(DC-DC boost),Matlab/Simulink.

II.2.2 Command MPPT:

The MPPT (Maximum Power Point Tracking) control is a method that allows the PV generator to operate at its maximum power regardless of the weather conditions of irradiation and temperature. The principle of this control is based on the automatic variation of the duty cycle α of a DC-DC converter to the appropriate value in order to continuously maximize the power output of the PV panel.

Choppers are employed as power interfaces, with the MPPT regulator controlling them to adapt the chopper's output voltage to the voltage needed by the load. One may think of a number of approaches to get the most power out of a solar panel based on this rule and the kind of controller being used. [21]

Measuring the effectiveness of the control responsible for controlling the power converter is possible thanks to the efficiency of the operational point (η_{MPPT}).

$$\eta_{MPPT} = \frac{P_{pv}}{P_{mpp}} \quad (2.1).$$

II.2.3 Classification of MPPT Controls According to the Search Type :

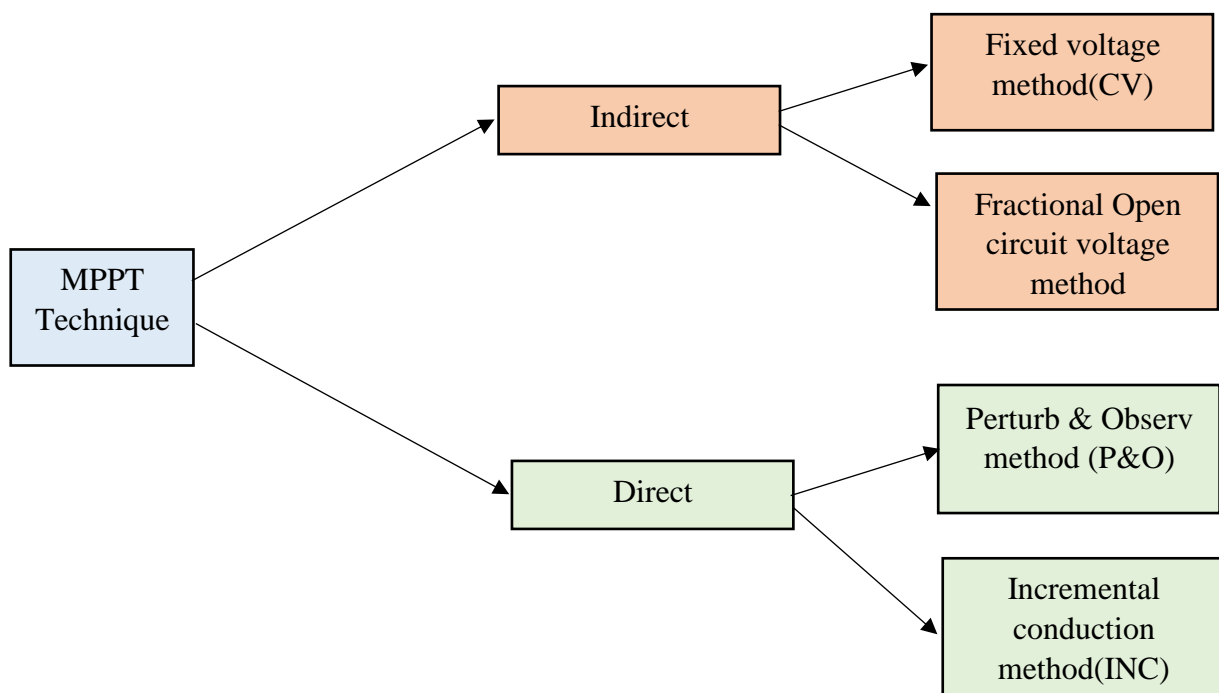


Figure II.18: MPPT techniques.

In our project we used P&O (Perturb and observ) method.

1-P&O (Perturb and observ) method:

The P&O technique is commonly preferred for its simplicity and straightforward implementation. This method involves taking the voltage V_{pv} and current I_{pv} as inputs and determining the duty cycle value α as output. The core concept of this approach, as indicated by its name and depicted in Figure II.19, is to disturb the V_{pv} voltage while adjusting the duty cycle α . Subsequently, the algorithm calculates the power generated by the panel $P(n)$ and compares it to the previous power $P(n-1)$. If the power increases, it signifies proximity to the Maximum Power Point (MPP), maintaining the duty cycle variation in the same direction. Conversely, a decrease in power indicates moving away from the MPP, prompting a reversal in the duty cycle variation direction, as demonstrated in Figure II.20. [39]

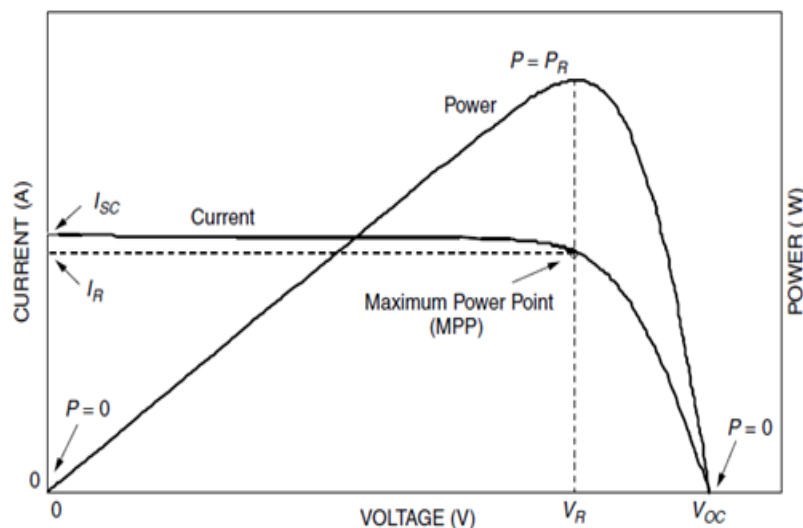


Figure II.19: PV-characteristic curves of P&O MPPT technique V-I-P curve.

2-Pertutber and Observer (P&O) Algorithms with Variable Step Size :

The P&O algorithm's step size ($d\alpha$) selection affects both the algorithm's convergence time to the maximum power point and the oscillation that occurs around it. To obtain an appropriate balance between precision and speed, P&O algorithms with configurable step sizes between two or more variables exist. The algorithm suggested by is one of these. This algorithm compares the absolute amount of power variation with a threshold, and then adjusts the step size between two values, C1 and C2. [40]

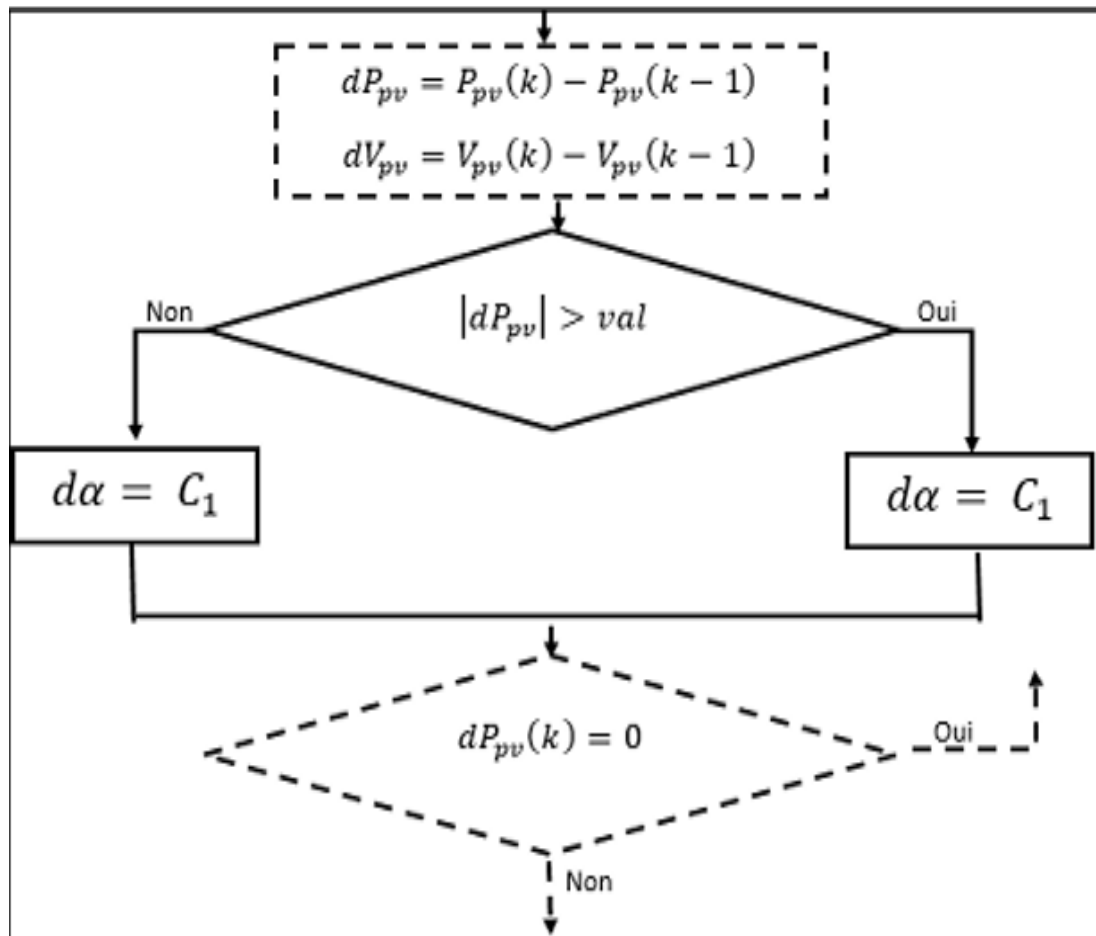


Figure II.20: Partial Flowchart of Variable P&O Algorithm.

II.2.4. Command MPPT Modeling:

The modeling of Maximum Power Point Tracking (MPPT) techniques involves simulating and optimizing the performance of photovoltaic systems under varying conditions. Several studies focus on enhancing the efficiency of MPPT algorithms through modeling:

- A study presents a step-by-step modeling of a photovoltaic system with different MPPT techniques, emphasizing the algorithm's role in finding the maximum power output.
- Modified MPPT techniques and their impact on improving both steady-state and dynamic performance of PV systems under changing climatic conditions. [40]
- Research on MPPT algorithms based modeling and control for photovoltaic systems under variable climatic conditions highlights the importance of efficient control strategies. [40][41]

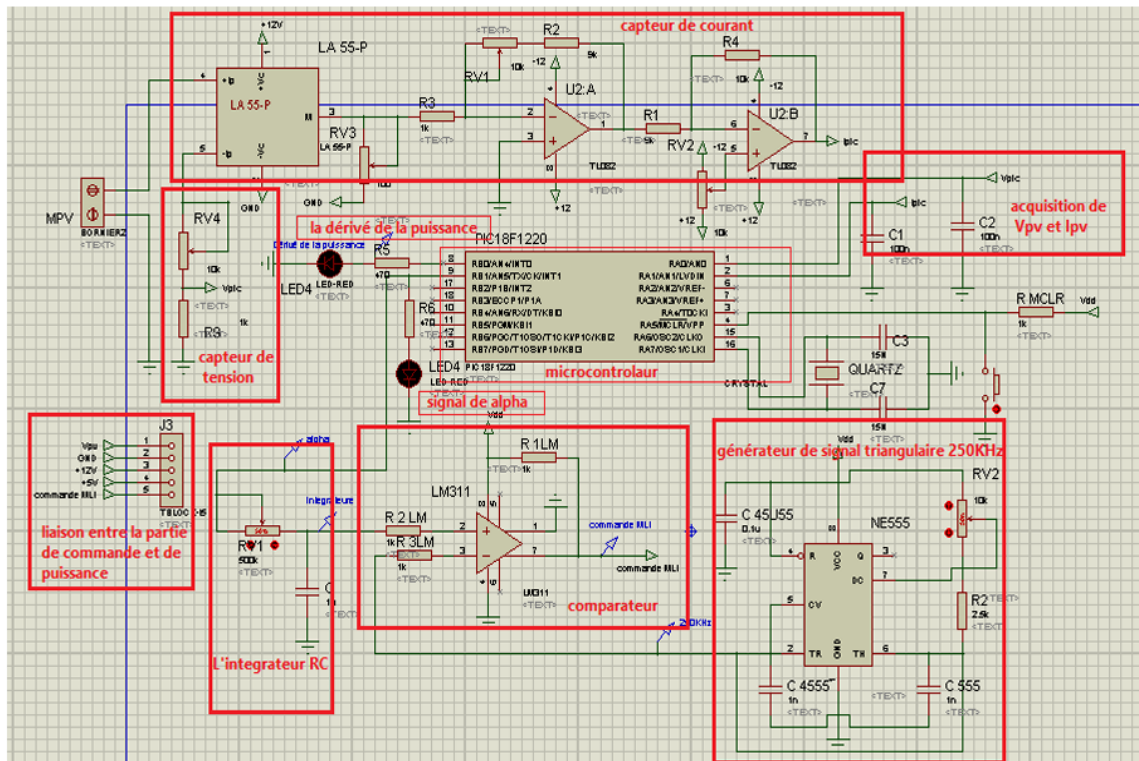


Figure II.21: Diagram of Nemuric Mppt control.[66]

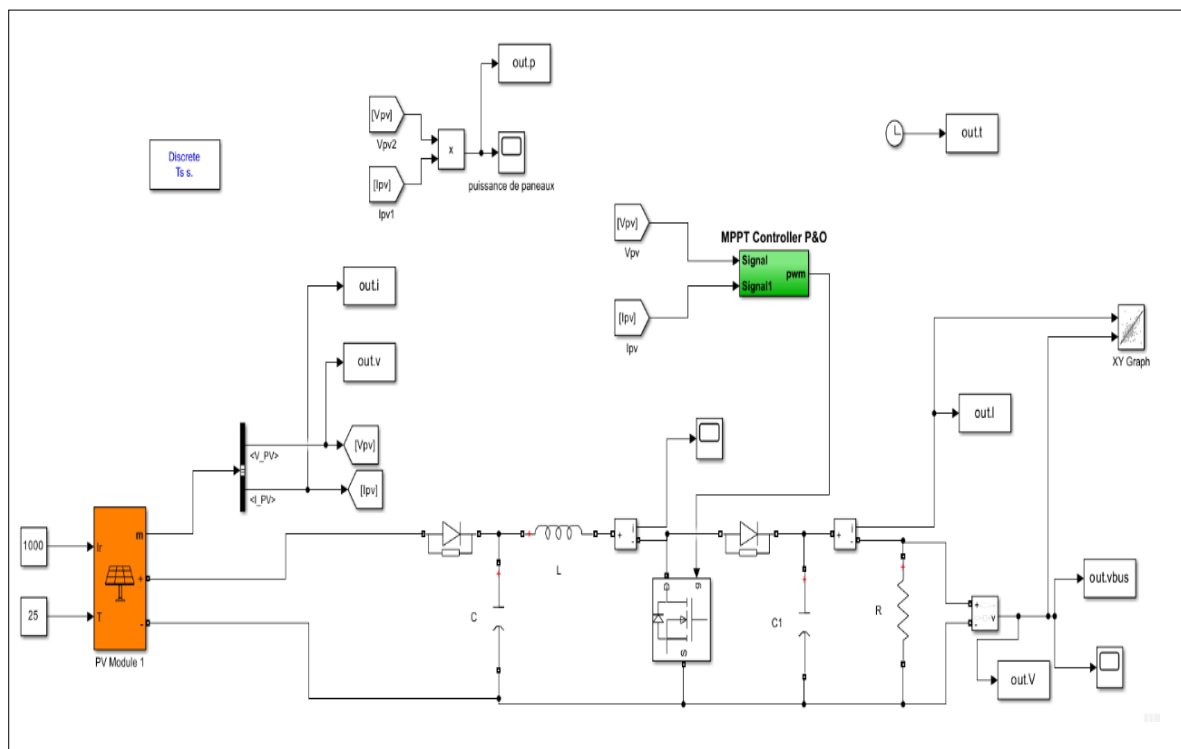


Figure II.22: modeling of MPPT control, Matlab/Simulink.

The figure below represents the algorithm we followed in our research

```

function D_k = fun (D_k1,V_k,V_k1,I_k,I_k1,ds)
P_k1=I_k1*V_k1;
P_k=I_k*V_k;
dP=P_k1-P_k;
dV=V_k-V_k1;
if dP>0
    if dV>0
        D_k=D_k1+ds;
    else
        D_k=D_k1-ds;
    end
else
    if dV>0
        D_k=D_k1-ds;
    else
        D_k=D_k1+ds;
    end
end
end

```

Figure II.23: P&O (Perturb and Observ) algorithm.

II.3. Photovoltaic Panel Defects:

In a photovoltaic system, there exist four distinct sorts of loss. [35]

- Long-term, inefficient defects: These happen when there is a physical malfunction and the system is not linked for an extended period of time. [29]
- Short flaws that have zero efficiency: These happen when the inverter briefly disconnects, briefly cutting off the system. [29]
- Defects in shading: These happen when a shadow crosses across something, such as cables, buildings, trees, clouds, etc.
- Flaws causing efficiency loss when there is no shading: occurs as a result of various defects and errors in maximum power point tracking (MPPT). [32]

II.3.1. Shading Fault:

Shading faults in photovoltaic (PV) systems can significantly impact their performance leading to power losses and hotspots across shaded cells, [1] faults are not always visible and can be caused by various factors, including localized shading, dirt, or manufacturing defects detecting and mitigating shading faults is essential for maintaining optimal performance and

preventing potential electrical faults and decreased energy generation capacity. Various detection methods have been developed to identify and mitigate the effects of shading on solar panels, including EL images, infrared (IR) technology, and the new ultraviolet (UV) fluorescence technique. The impact of shading on PV systems is significant, with studies showing that shading can compromise the output of a PV system by up to 20%. Therefore, effective fault detection and management strategies are crucial to ensure the reliability and efficiency of solar power generation. [42]

II.3.1.1. Partial-Shading Fault:

The impact of partial shading on the performance of the system. Partial shading can lead to power losses and the creation of hotspots across shaded cells, significantly affecting the efficiency of the PV system. [44]

Partial shading occurs when a portion of the photovoltaic (PV) array experiences some degree of shading, a phenomenon that naturally arises due to transient clouds. Additionally, nearby obstructions can cast shadows, leading to diminished power output. Consequently, shading conditions are a critical consideration in PV system design and planning. The resultant power reduction necessitates classifying power output scenarios into either partial shading conditions or malfunctioning panels.

Certain studies, such as [60], treat partial shading as a failure mode. This simplified perspective obviates the need to distinguish between partial shading and faulty solar panels. Conversely, partial shading has been examined in isolation [61], revealing the impact of bypass diodes activated under shading conditions, which result in non-linear I-V curves with distinctive features. However, this study does not specify appropriate classification criteria nor does it relate shading to fault conditions. The findings are significantly influenced by the panel configuration and the placement of bypass diodes.

A study conducted in the UK [62] explores fault classification under partial shading conditions. This method involves measuring the error frequency in specific segments of the solar plane, defined by solar elevation on the y-axis and solar azimuth on the x-axis, based on the sun's position. Small, five-minute intervals of this plane are analyzed in isolation. A fault is classified as partial shading if the error frequency in the segment surpasses an empirically

determined threshold. The frequency is calculated by comparing the number of fault-free instances within a segment to the number of faults occurring within that segment.



Figure II.24: Partial shading on the PV Panel.

II.3.2. Bypass Diode faults :

A bypass diode is a crucial component in photovoltaic (PV) systems that protects partially shaded PV cells from fully operating cells in full sun within the same array. [45] It is used to ensure that the shaded PV cells do not consume power and instead divert the current flow of the two good cells through itself, maintaining the operation of the other two PV cells by creating a parallel path. This ensures that when a cell or panel becomes shaded or faulty, the bypass diodes provide an alternate current, preventing hot spots and power loss. The bypass diode prevents hot spots by regulating the current from the sunlight, and when used with an MPPT charge controller, it can increase power production under shady conditions in certain situations. [46]

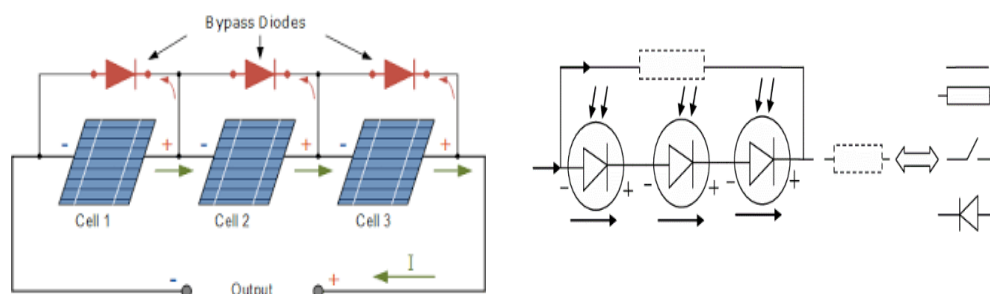


Figure II.25: Bypass Diode Fault Configuration.

II.3.2.1. Module Fault :

Il electrical problems connected to a module's connection within a PV string are included in the module fault category. These electrical malfunctions consist of a shorted-

circuiting module, a parallel-connected module, and an impedance as well as the module's polarity being reversed. [47]

II.3.2.2. Bypass diode anti-reverse fault :

It can lead to significant issues, such as power loss and potential safety hazards. When an anti-reverse diode breaks down or malfunctions, it can create a path for current flow, causing faults in the serial circuit and affecting the overall performance of the system . The anti-reverse diode is linked to four other fault types in addition to the bypass diode: reversed polarity, open circuit, arbitrary impedance, and short circuit. The figure below (figure II.26) describe the module fault configuration. [46][48]

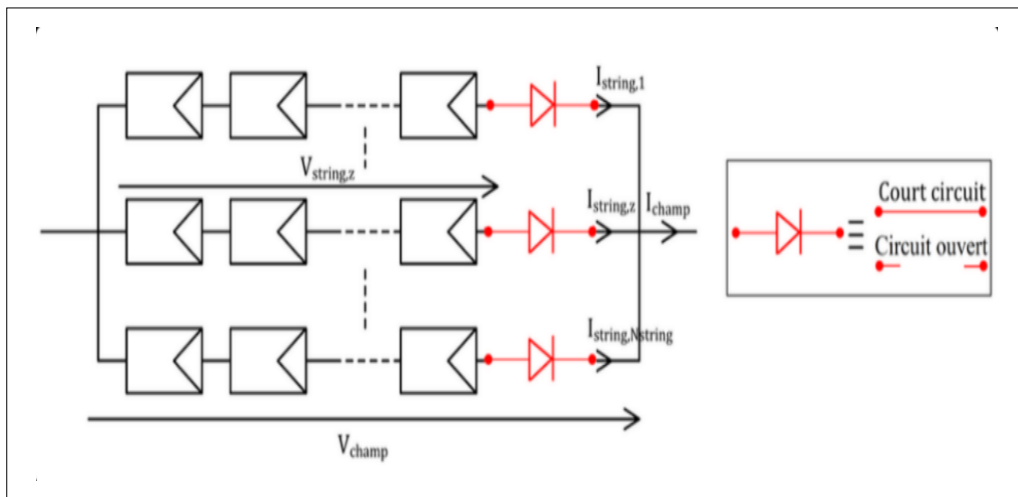


Figure II.26: Module Fault Configuration.

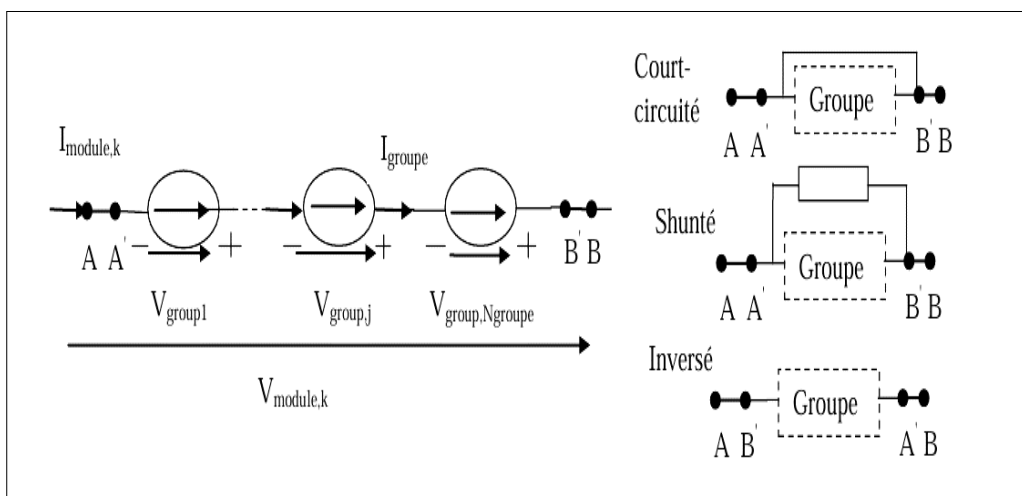
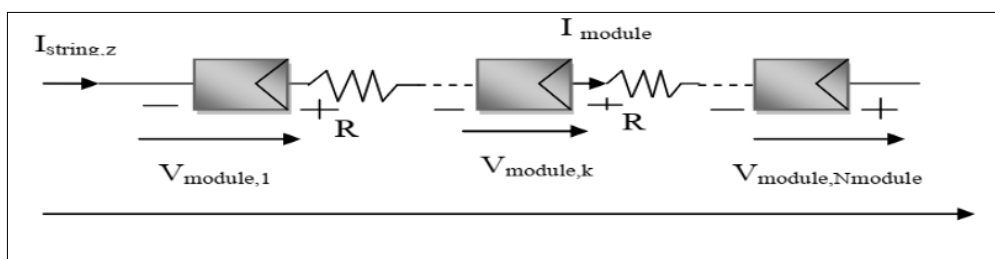


Figure II.27: Installation of a PV field with a faulty reverse diode.**II.3.2.3. Bypass diode connection Fault:**

This has to do with the problem of higher connection resistance between two PV modules. This connection resistance is nearly nonexistent in a typical state. However, in a few unusual circumstances, such corrosion of the connector or a loose screw, its value can be raised. In severe situations, a disconnected module from the PV string may be represented by an infinite resistance. The figure below (figure II.28) describe the bypass diode dis-connected fault. [49][50]

**Figure II.28:** Bypass diode dis-connected.**II.3.3. Decrease in shunt resistance (Rsh) :**

A decrease in shunt resistance (R_{sh}) in photovoltaic (PV) modules can lead to significant power losses, particularly in low light conditions. This is because a low shunt resistance provides an alternate current path for the light-generated current, reducing the amount of current flowing through the solar cell junction and reducing the voltage from the solar cell. The effect of a low shunt resistance is particularly severe at low light levels, as there will be less light-generated current, and at lower voltages, where the effective resistance of the solar cell is high. [32]

II.3.4. Increase in series resistance (Rs) :

An increase in series resistance in a solar cell can lead to a decrease in the fill factor (FF) and, in extreme cases, a reduction in the short-circuit current (I_{sc}). [21] The main impact of series resistance is to reduce the fill factor, although excessively high values may also reduce the short-circuit current. The series resistance in a solar cell has three causes: the movement of current through the emitter and base of the solar cell, the contact resistance between the metal contact and the silicon, and the resistance of the top and rear metal contacts.

The formula for the effect of series resistance on the IV curve is an implicit function, which requires numerical methods to solve, and the voltage across the diode is varied to generate the plot, avoiding the need to solve an implicit equation. [41] As it shown in the figure below (figure II.29).



Figure II.29: Increasing series resistance fault .

Conclusion:

In this chapter, we discussed and explained some possible faults and their causes in the solar panel, in addition to how to diagnose faults and the various diagnostic methods and principles. We also delved into modeling the DC-DC converter, then explored various types of MPPT control and their modeling, detailing the P&O type used in this study, as well as mentioning and diagnosing the faults that will be simulated in the next chapter.

CHAPTER III

III. Introduction:

For industrial photovoltaic (PV) systems, it is crucial to have a monitoring system that can detect, isolate, and identify any failures that may occur. Consequently, the diagnosis of PV systems is an essential area of research to enhance production and enable predictive or fast corrective maintenance after each breakdown. [7]

This ensures improved utilization of the installation and fewer service interruptions. There are various faults that can affect the performance of PV panels, [8] with environmental conditions and panel degradation being major contributing factors. These faults include diode bypass issues, [7] increased series resistance, and shading over the panel, all of which can impact the power output of the PV panel. This chapter aims to design a model in MATLAB/Simulink that allows the detection, classification, and localization of eight types of faults occurring in PV cells, series resistance, shunt resistance, and bypass diodes. [10] The model will simulate both normal (healthy) and faulty conditions of the PV panel. The proposed techniques for PV panel diagnosis are based on the analysis of several characteristic quantities, such as power, voltage, and current. [51]

III.1. Modeling and simulation:

Photovoltaic module modeling is a critical aspect of designing and analyzing solar energy systems. The process involves creating mathematical models of PV modules that can predict the performance of the module under various conditions. The models can be developed using various software tools, including Matlab/Simulink, [52] and involve defining the fundamental components of a PV module and modeling their behavior using mathematical equations. The models can be used to investigate the solar PV array operation from different physical parameters and working conditions, optimizing the design of solar energy systems. [53]

III.1.1. Photovoltaic module modeling:

To optimally utilize photovoltaic (PV) modules, it's essential to employ dependable modeling techniques that forecast the behavior of PV systems under conditions distinct from those detailed in the manufacturer's datasheets. Accurate models can facilitate:

- The study of solar cell behavior.
- Monitoring the performance of PV systems.
- The analysis of losses in solar PV systems.
- The forecasting of produced PV output power.
- The development and testing of maximum power point tracking algorithms.
- The fault diagnosis of PV systems.

These models help to ensure the optimal performance of PV systems under various conditions, such as different weather patterns, temperature fluctuations, and aging effects. [54]

III.1.2. Solar cell modeling:

The most commonly used equivalent circuit for solar cells is the single diode model, also known as the five parameters model (R_{Sh} , R_S , a , I_{Ph} and I_0), as depicted in Figure bellow [14]. The circuit shown in Figure bellow can be described by the following equation:

$$I = I_{Ph} - I_0 \left[\exp^{\frac{q(V+IR_S)}{BTc}} - 1 \right] - \frac{V - IR_S}{R_{Sh}} \quad (3.1)$$

where:

I_{Ph} : the light-generated current, i.e., the short-circuit current neglecting the parasitic resistances.

I_0 : the dark saturation current due to recombination.

q : the electron charge. $e=1.6*10^{-19}C$.

R_S : a series resistance.

B : the Boltzmann's constant. ($1.3854*10^{-23}JK^{-1}$).

Tc : the solar cell temperature (in K).

R_{Sh} :a shunt resistance.

a : an ideality factor. The light-generated current is directly proportional to the solar irradiance.

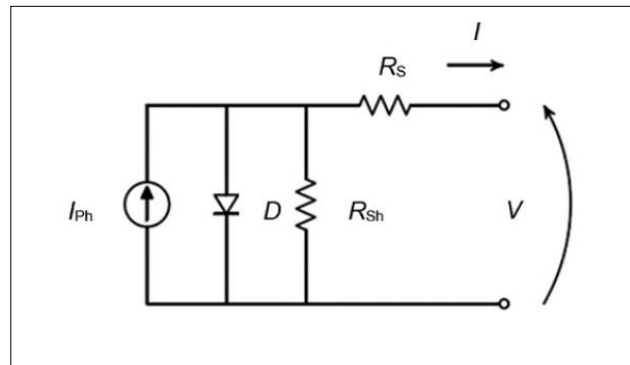


Figure III.1: Solar cell equivalent circuit-five-parameters model.

The figure below displays a standard I-V curve of a solar cell. Every solar cell is defined by its peak power output (P_{mp}), fill factor (FF), and efficiency (η). So

$$FF = \frac{I_{mp} \times V_{mp}}{I_{sc} \times V_{oc}} \text{ " and " } \eta = \frac{I_{mp} \times V_{mp}}{S \times G} \quad (3.2)$$

Where :

I_{mp} : maximum current.

V_{mp} : maximum voltage.

S : the effective surface of the solar cell.

G : the incident solar irradiance.

I_{sc} : short circuit current.

V_{sc} : open circuit voltage.

III.1.3. PV module characteristics :

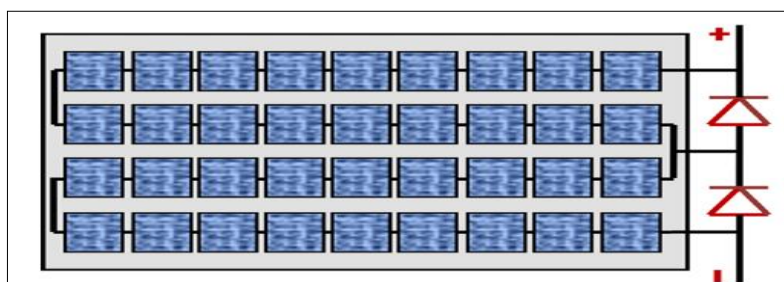
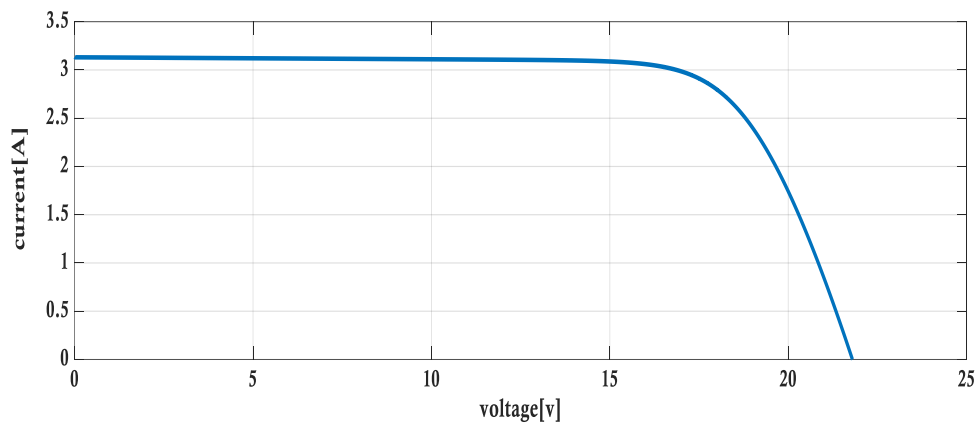
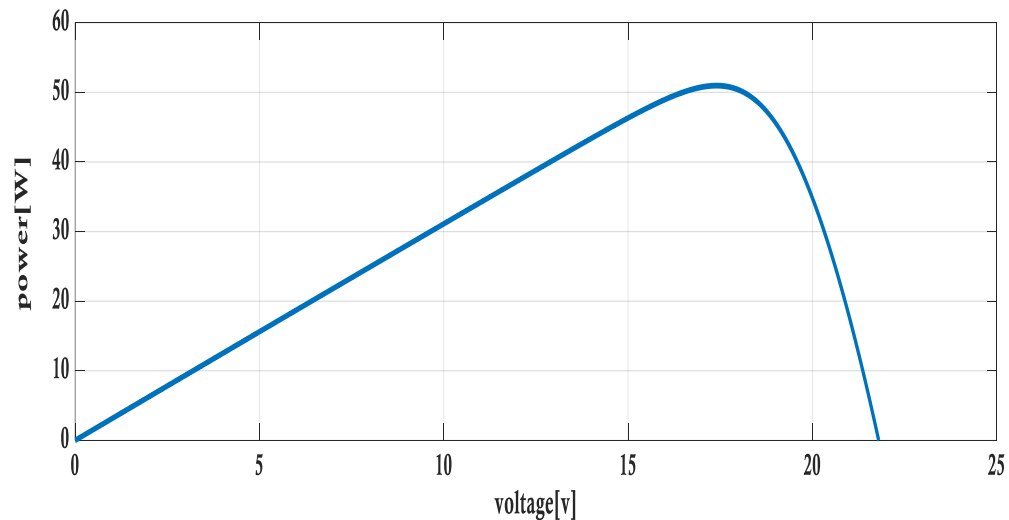


Figure III.2: Schema of photovoltaic module.

Table III.1: Electrical characteristics of the JARRETT PV module.

Pmax : Maximum power.	50 W
Vmp : Voltage at Maximum power.	17.4 V
Imp : Current at Maximum power.	2.93 A
Voc : Open Circuit Voltage.	21.8 V
Isc : Short Circuit Current .	3.14 A
The total number of cells connected in series.	36
Number of bypass-diodes.	2

**Figure III.3:** I-V Characteristic of a PV module under STC (25 Cand1000W/m²).**Figure III.4:** P-V Characteristic of a PV module under STC (25 Cand1000W/m²).

III.2. PV module faults :

While maintaining consistent solar radiation over the panel with each cell operating at its Maximum Power Point (MPP) is ideal. In actuality, PV panels frequently encounter a number of anomalous circumstances that have a detrimental impact on both their efficiency and overall output power. Eight PV module defects are selected for this investigation and are mentioned in Table III.2.

Table III.2: Different type of faults chosen for the diagnosis.

Symbol	Fault type
F1	By-pass diode disconnected.
F2	By-pass diode short circuited.
F3	Shading of a cell of the submodule 1 and another of the submodule 2 of the panel at 50%
F4	Shading of one cell in submodule of the panel at 50%.
F5	Shading of one cell in submodule of the panel at 100%.
F6	Shading of a cell of the submodule 1 and another of the submodule 2 of the panel at 100%.
F7	Decrease the shunt resistors ($R_{sh} = 5 \Omega$) module.
F8	Increase the serie resistors ($R_s = 0.9 \Omega$) module.

III.3. Fault Diagnosis PV System :

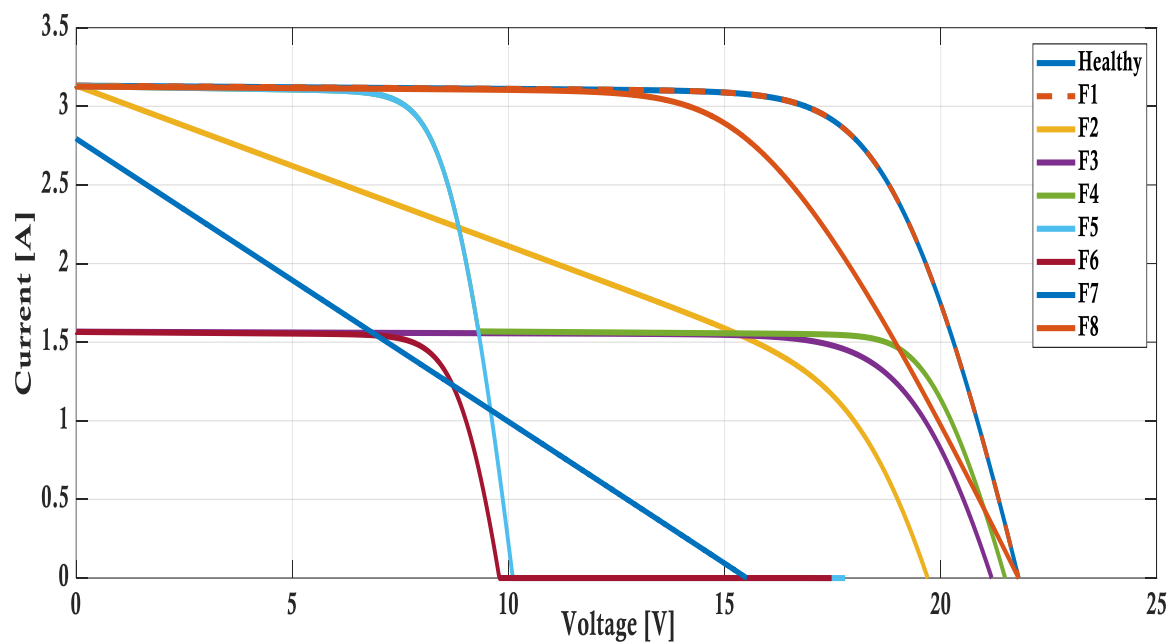


Figure III.5: I-V Curves of different type of faults.

III.3.1. Interpretation of results :

Under standard test conditions (STC) (25°C and 1000 W/m^2), the PV panel utilized in this study is a JARRETT module. This panel consists of 36 PV cells and two bypass diodes, as depicted in Figure III.2. It has a power rating of 50 W and is made of polycrystalline silicon. The electrical characteristics are detailed in Table III.1. The I(V) and P(V) curves demonstrating the panel's electrical performance are shown in Figures III.3 and III.4 using Simulink/Matlab.

The figure III.5 illustrates the various faults studied in this thesis, where the healthy model is compared with the other models. We observe the changes in current and voltage for each fault

Results are taken from the simulation and compared to the health status curve (healthy), then apply each fault separately and note the difference and changes that occur to the IV curves in each fault as its illustrates above.

The I-V curve may show an unusual flattening, with the current dropping off sharply at lower voltages than expected.

The short-circuited diode allows current to bypass entire sections of the array, resulting in lower voltage and reduced current through the operational cells (F2).

The I-V curves indicate that the array is experiencing partial shading (F3, F4: irradiation decrease 50%, F5, F6: irradiation decrease 100%),

The hot spots confirm that specific cells within panels are shaded, causing those cells to dissipate energy as heat..

Lower shunt resistance (F7) allows more leakage current to bypass the load, reducing the net current available for power generation, thus decreasing the overall power output.

The I-V curve shows a less steep slope (F8) near the short-circuit current (I_{sc}) and a significant voltage drop as current increases. The knee of the curve becomes less sharp and more rounded.

The increased series resistance causes a larger voltage drop within the cell as current flows, reducing the overall voltage available at higher currents.

III.4. DC-DC boost Simulation :

The simulation of DC-DC boost converters with solar panels is essential for optimizing the performance of solar PV systems, ensuring efficient energy conversion, and maximizing power output under varying climatic conditions

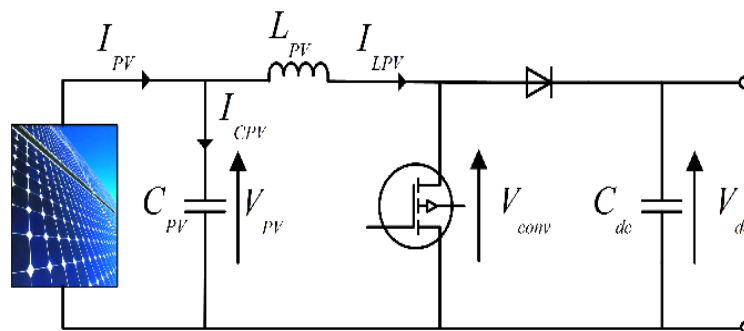


Figure III.6: Diagram of a Boost Chopper Powered by a Photovoltaic Generator.

III.4.1. Dimensioning and Calculation of the Components Constituting the Boost Chopper Used :

We shall dimension the values of the components that make up the boost chopper for two distinct duty cycles, with a power of $P=50W$ and an input voltage of $V_e = 12V$.

Calculation of Components :

To obtain an output voltage $V_s=145V$ at the output of the boost chopper that powers a resistive load R_{ch} : We have:

-Input voltage $V_e = 21.8V$.

-Output power $P = 50W$.

-Duty cycle α :

$$\alpha=1-(V_e/V_s) \quad (3.3)$$

$-\alpha=1-(12/80)$; $\alpha= 0.85$;

1. Calculate the output current:

$$I_{out} = P / V_s \quad (3.4)$$

- $I_{out} = 50W / 80V = 0.625 A$

$$I_{Lmax} = (V_s/V_e)*2*I_{out}, \quad (3.5)$$

- $I_{Lmax} = 8.33A$

2. Calculate the inductor value:

$$L = (V_e/I_{Lmax}) * \alpha * 1/f_s \quad (3.6)$$

- Assuming a switching frequency $f_s = 5 \text{ kHz}$ and a maximum inductor ripple current of 30% of the average inductor current, we can calculate the minimum inductor value
- $L = 100\mu H$

3. Calculate the capacitor value:

$$C = (V_s * \alpha) / (8 * L * f_s^2 * \Delta V_s) \quad (3.7)$$

- $C = 470\mu F$;

In summary, to obtain an output voltage of 80V from a 12V input with a 50W resistive load, the key component values are:

- Inductor $L = 100mH$

- Capacitor C = 470 μ F

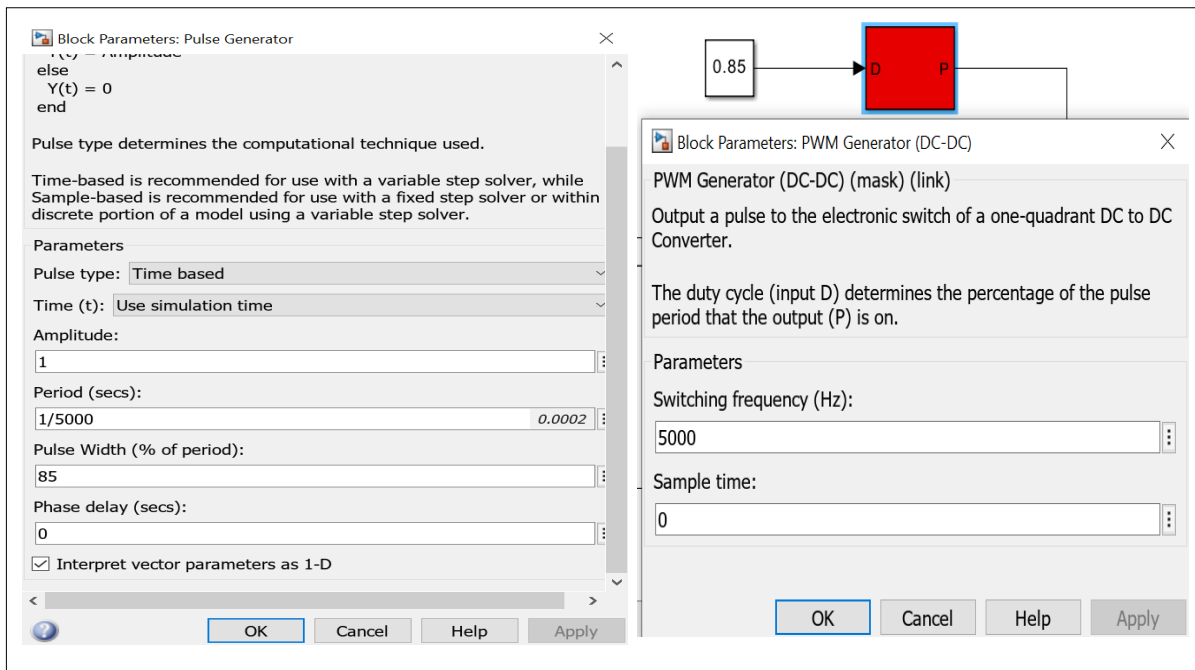


Figure III.7: Generation of the Control Signal for $\alpha=0.85$ and $f_s=5000$. Matlab, Simulink.

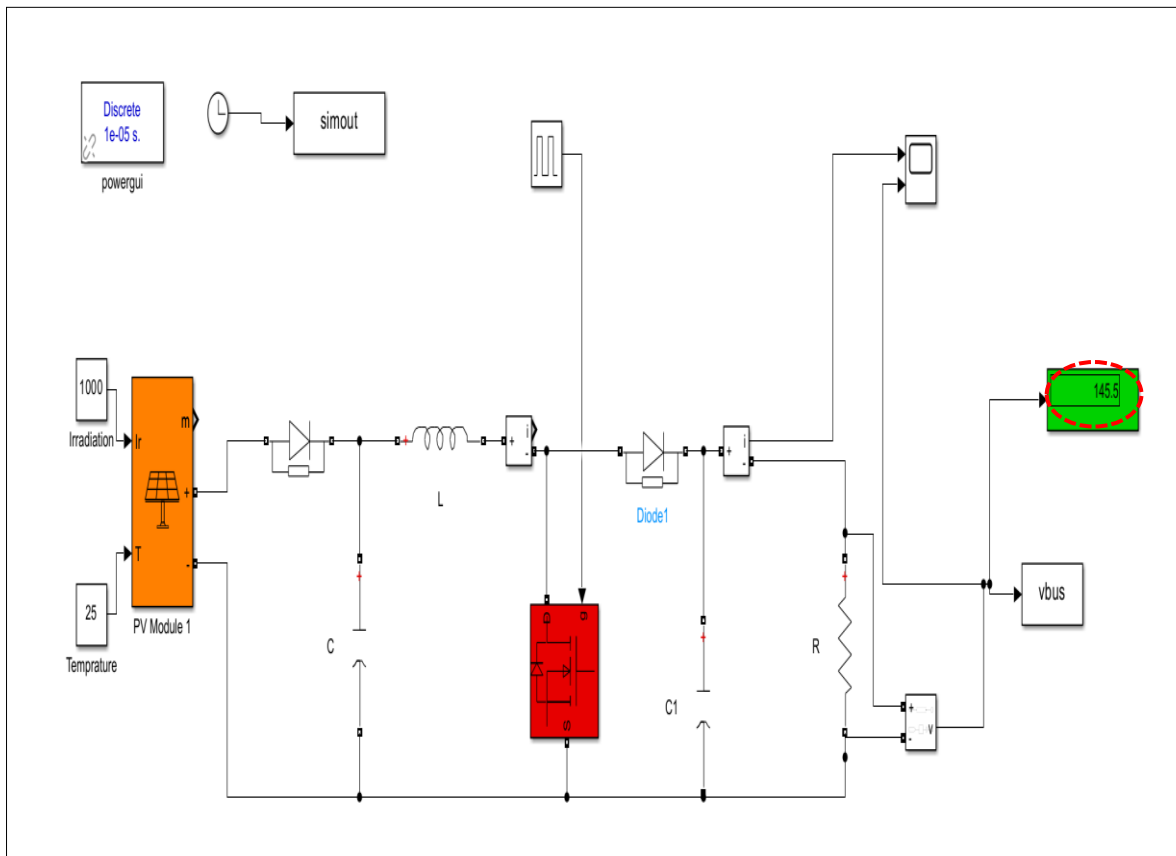


Figure III.8: Block Diagram of the Boost Chopper for $\alpha=0.85$, Matlab/Simulink.

To obtain an output voltage $V_s=365$ V at the output of the boost chopper that powers a resistive load R_{ch} : We have:

-Input voltage $V_e = 21.8$ V.

-Output power $P = 50$ W.

-Duty cycle α :

$$\alpha=1-(V_e/V_s)$$

- $\alpha=1-(12/180)$; $\alpha= 0.94$;

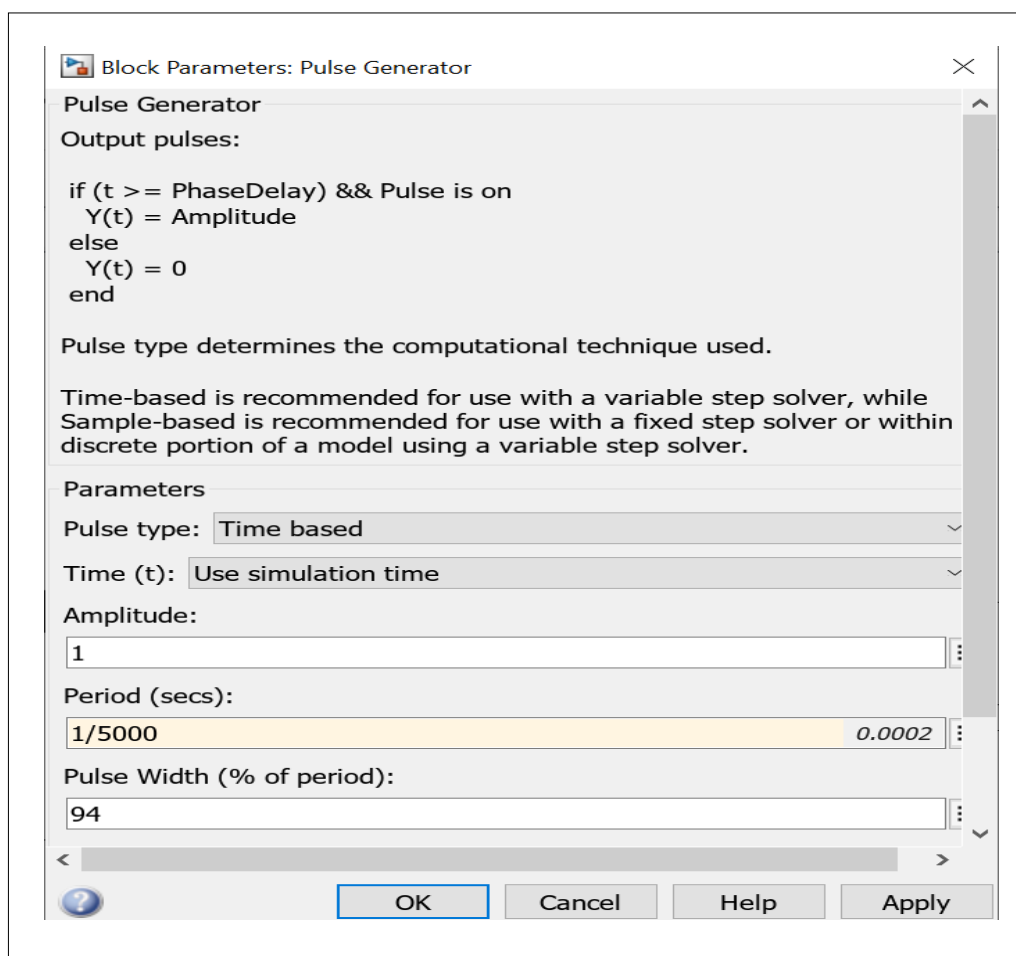


Figure III.9: Generation of the Control Signal for $\alpha=0.94$ and $f_s=5000$.Matlab,Simulink.

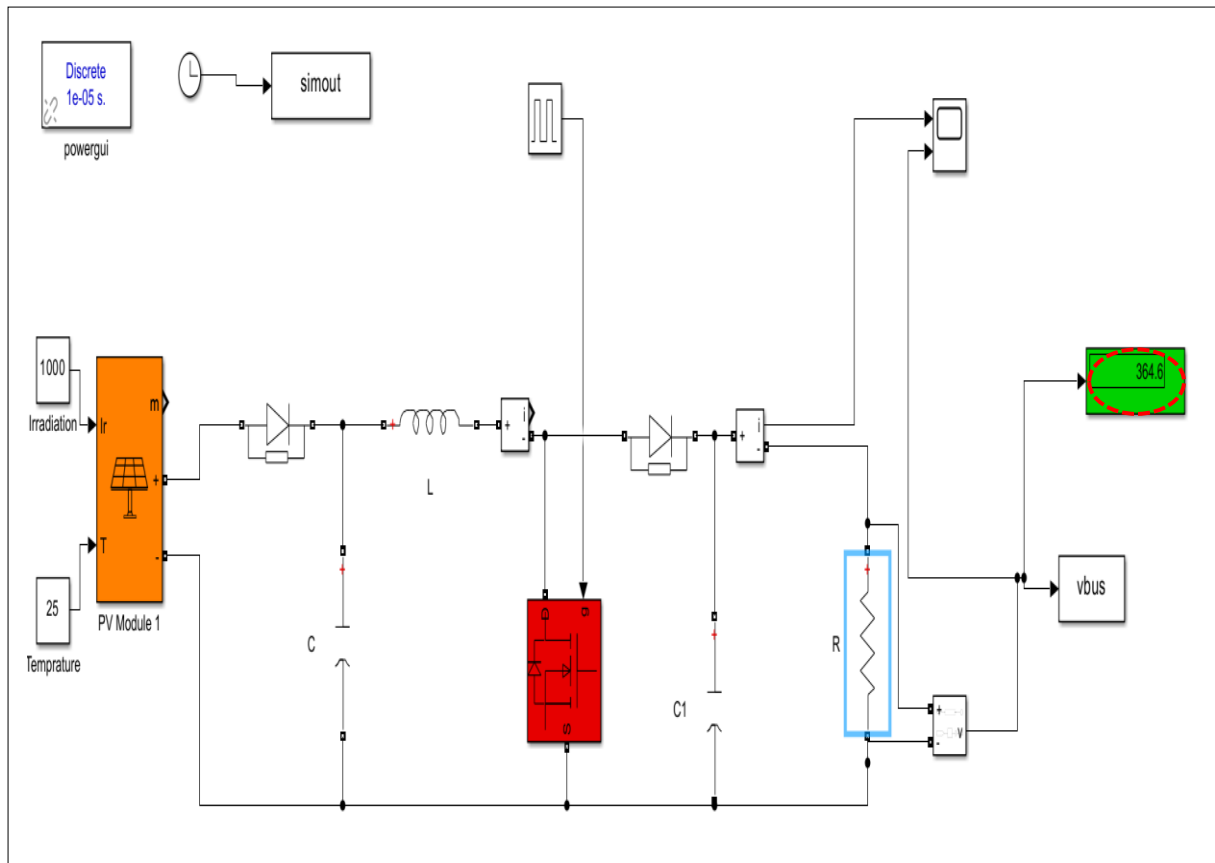


Figure III.10: Block Diagram of the Boost Chopper for $\alpha=0.94$, Matlab/Simulink.

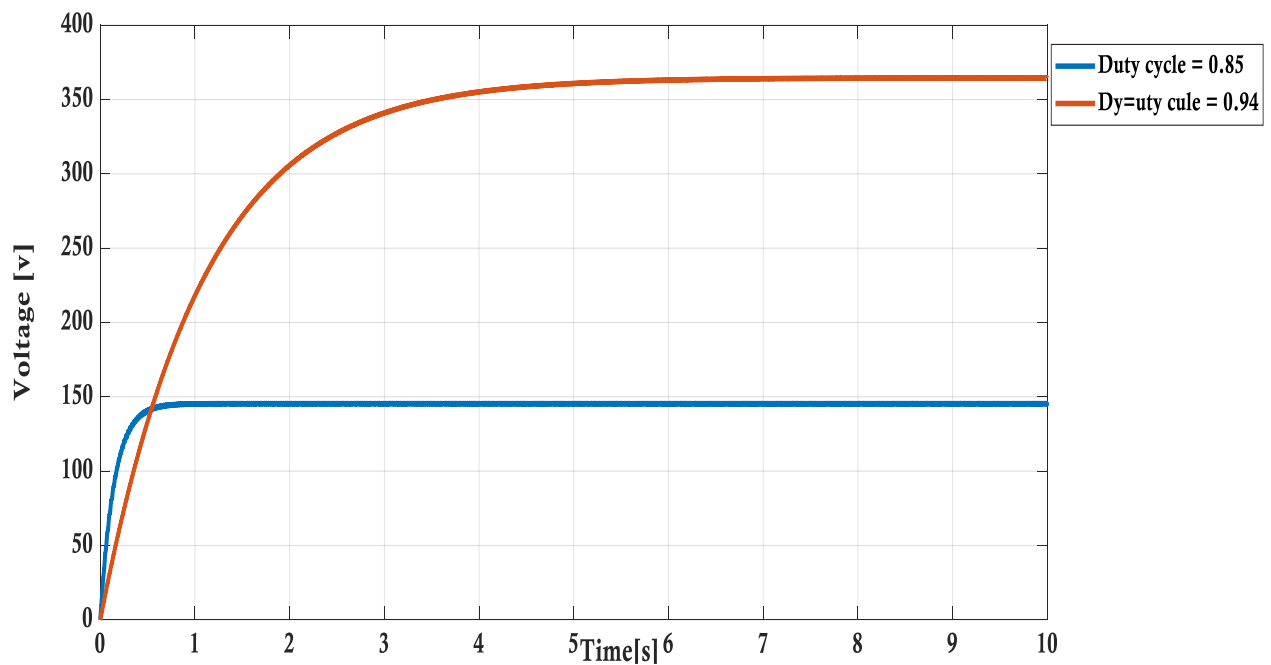


Figure III.11: Voltage Curve DC-DC boost .

III.5. Fault of PV System with MPPT control:

III.5.1 PV System with MPPT control healthy model:

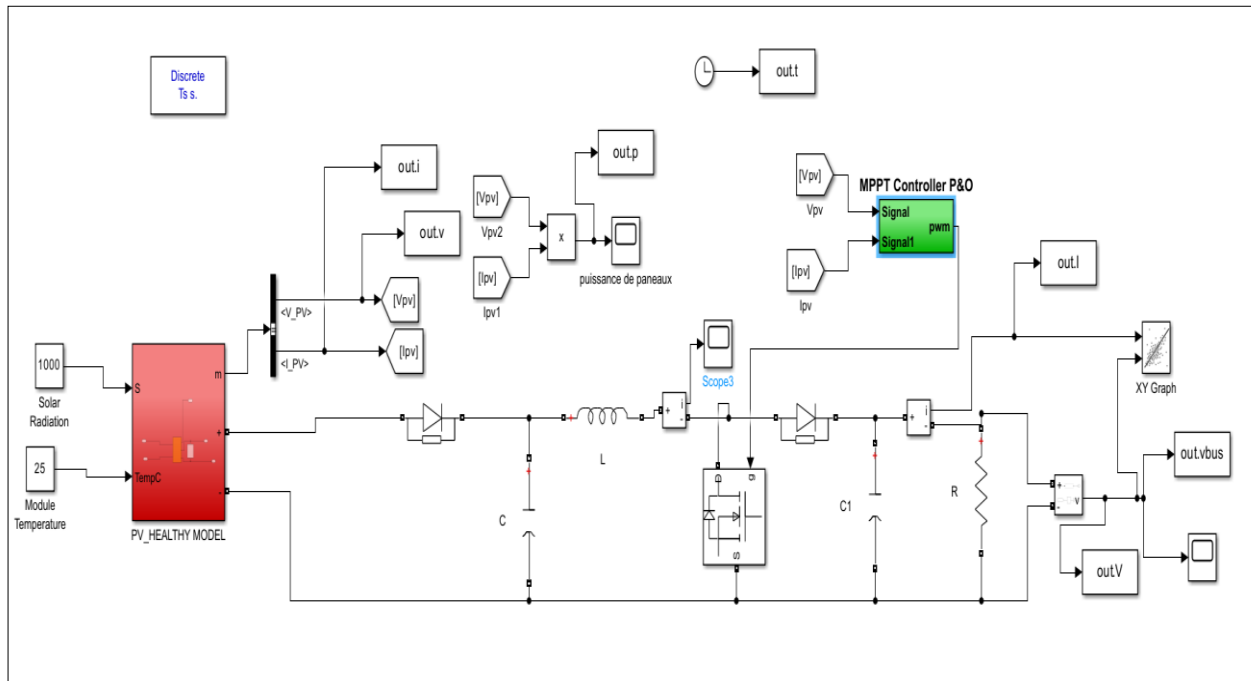


Figure III.12: Diagnosis PV system. Healthy model with MPPT controller. Matlab, Simulink.

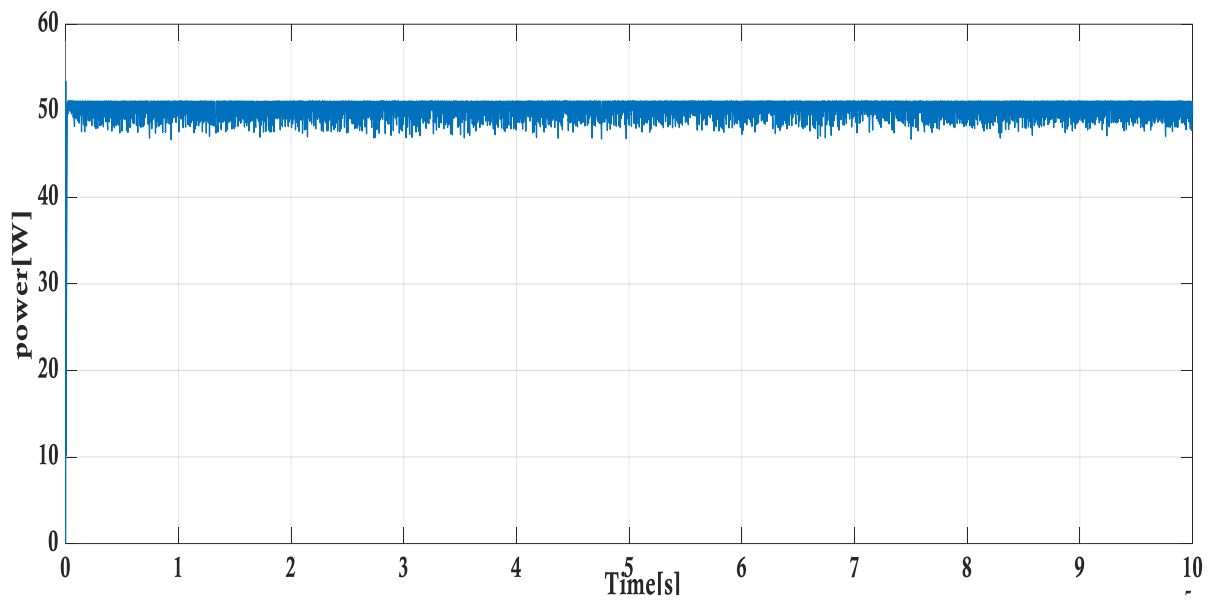


Figure III.13: The Power of PV Healthy model with MPPT controller. Matlab, Simulink.

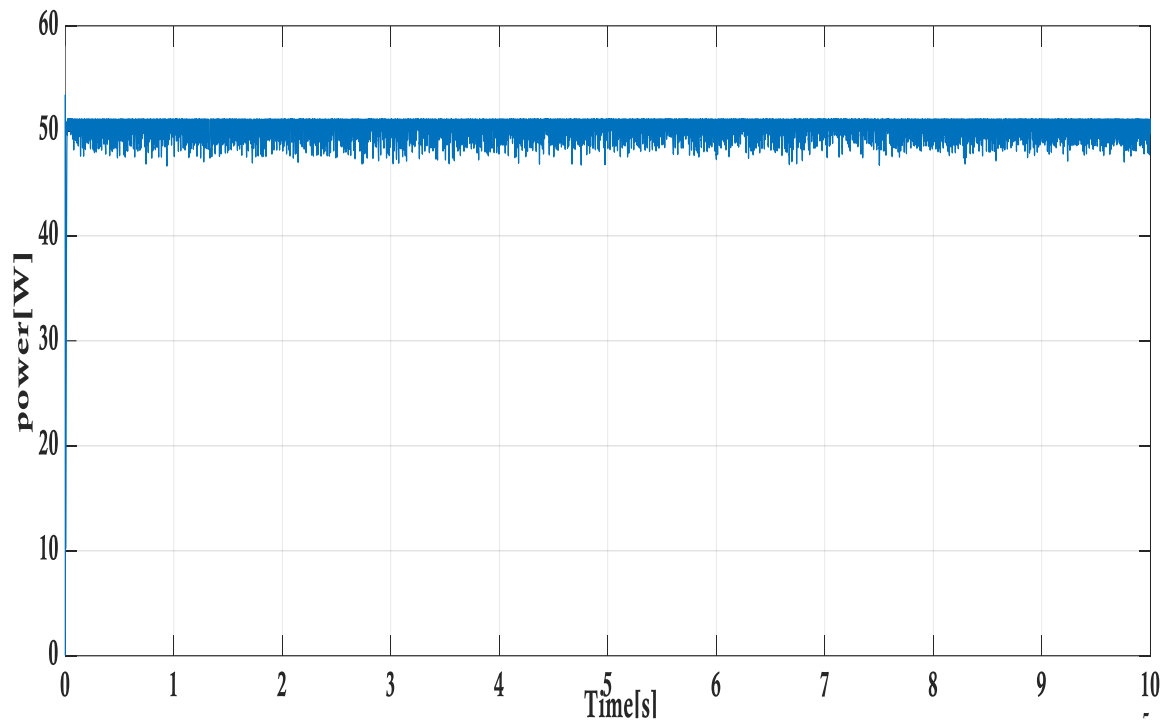
III.5.2 PV System with MPPT control faulty model diode by-pass disconnected:

Figure III.14: The Power of PV faulty model with MPPT controller F1. Matlab, Simulink.

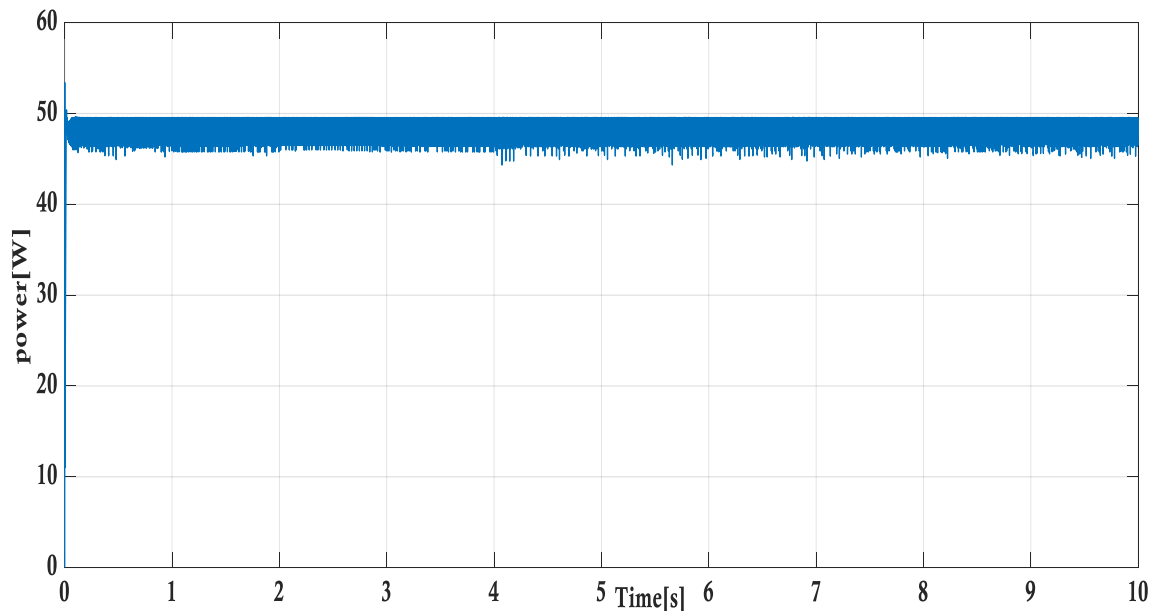
III.5.3. PV System with MPPT control faulty model diode by-pass short-circuited:

Figure III.15: The Power of PV faulty model with MPPT controller F2. Matlab, Simulink.

III.5.4. PV System with MPPT control faulty model Shading of a cell of the submodule 1 and another of the submodule 2 of the panel at 50%:

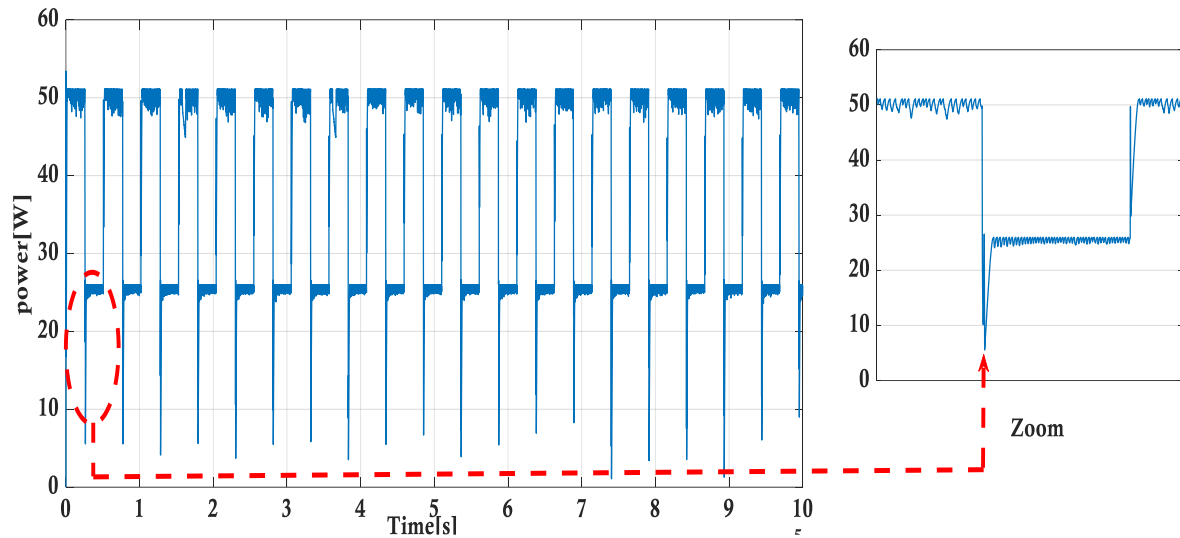


Figure III.16: The Power of PV faulty model with MPPT controller F3. Matlab, Simulink.

-The “Zoom” represent the occur moment of the shading fault.

III.5.5. PV System with MPPT control faulty model Shading of one cell in in submodule of the panel at 50%:

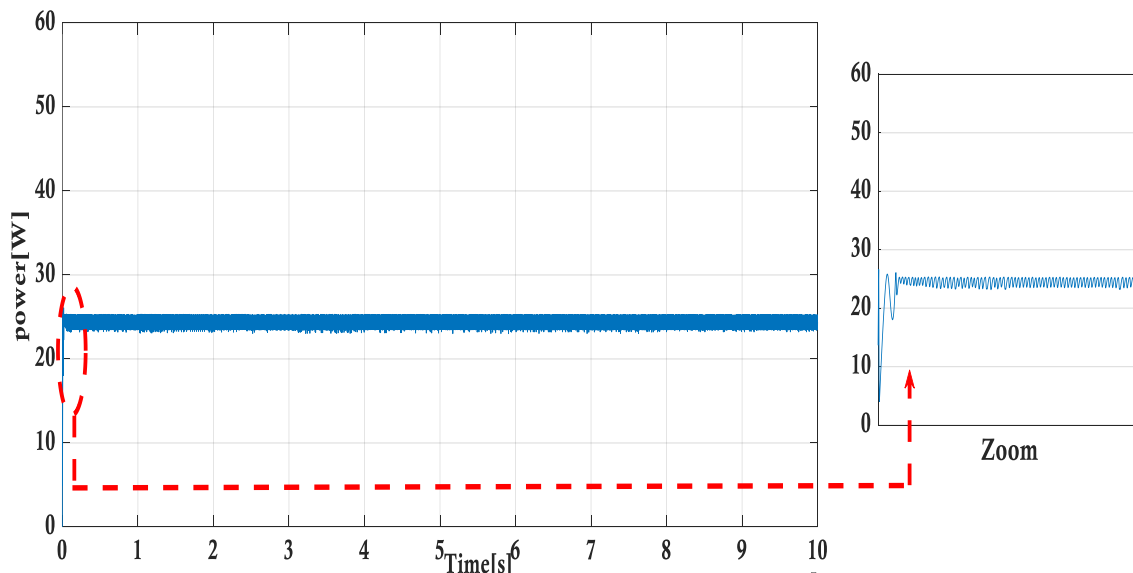


Figure III.17: The Power of PV faulty model with MPPT controller F4. Matlab, Simulink.

-The “Zoom“ represent the decreasing the power to 25[w].

III.5.6. PV System with MPPT control faulty model Shading of one cell in submodule of the panel at 100%:

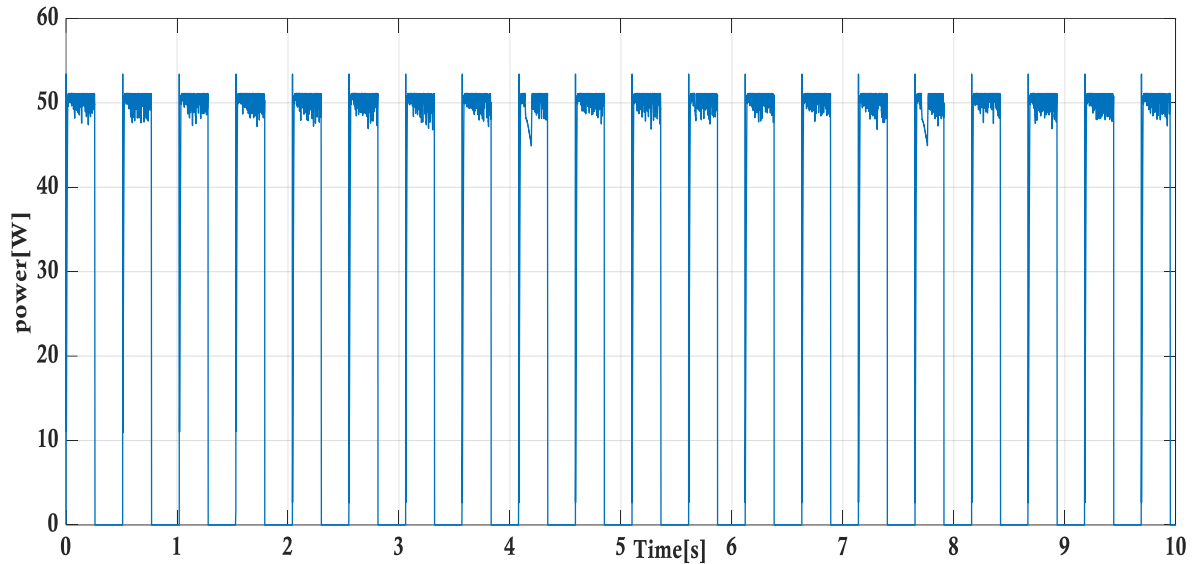


Figure III.18: The Power of PV faulty model with MPPT controller F5. Matlab, Simulink.

III.5.7. PV System with MPPT control faulty model shading of a cell of the submodule 1 and another of the submodule 2 of the panel at 100%:

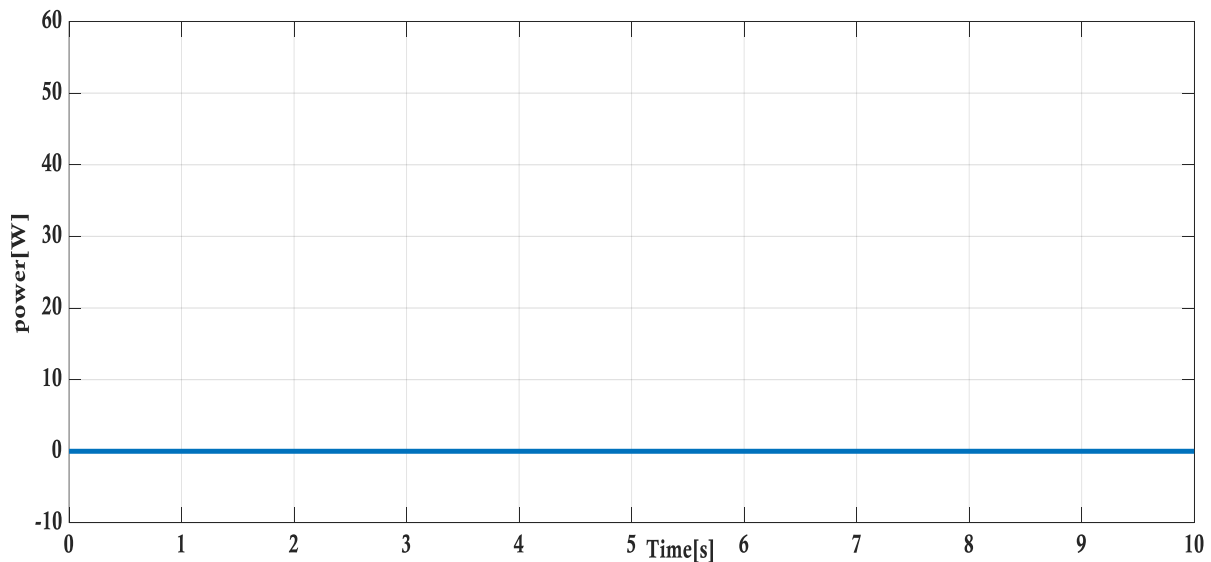


Figure III.19: The Power of PV faulty model with MPPT controller F6. Matlab, Simulink.

III.5.8. PV System with MPPT control faulty model Decrease the shunt resistors ($R_{sh} = 5 \Omega$) module:

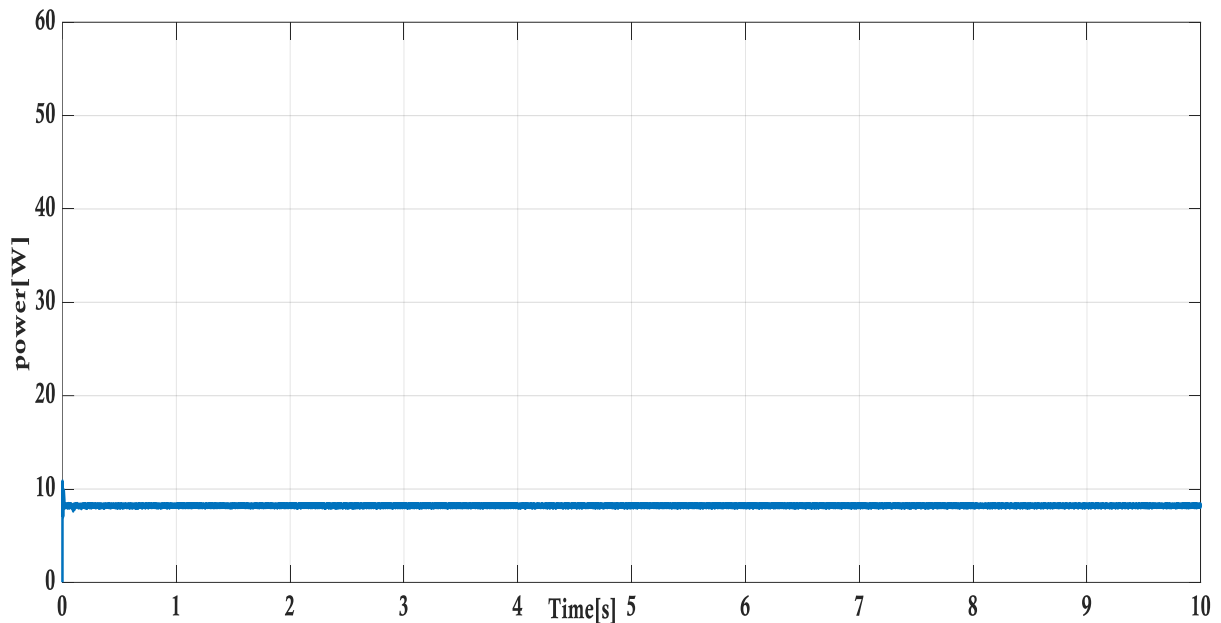


Figure III.20: The Power of PV faulty model with MPPT controller F7. Matlab, Simulink.

III.5.9. PV System with MPPT control faulty model Increase the serie resistors ($R_s = 0.9 \Omega$) module:

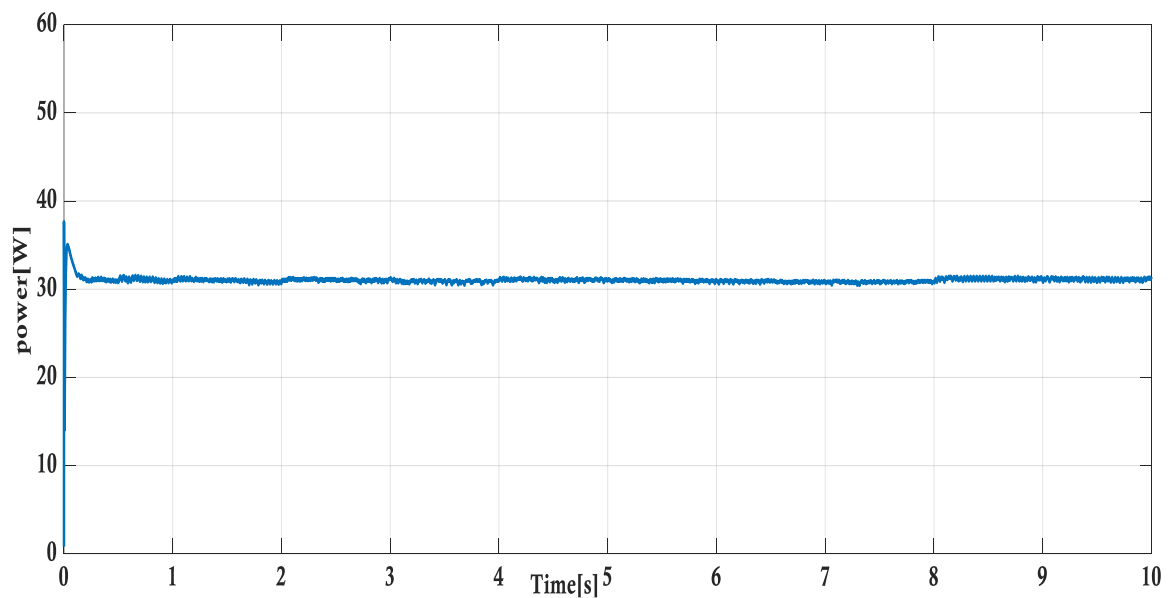


Figure III.21: The Power of PV faulty model with MPPT controller F8. Matlab, Simulink.

III.5.10. Interpretation of results:

a-DC-DC boost :

the figure III.11 illustrates the voltage curve DC-DC boost of two different states which is when duty cycle $\alpha=0.85$ and $\alpha=0.94$ and $V_{in} = 21.8V$.

A boost converter is a kind of DC-DC converter that uses an inductor as an energy storage device to step up the input voltage to a higher output voltage. By storing energy in the magnetic field of the inductor and transferring it to the load via a switching circuit, the boost converter works.

The results of the simulation and the calculations are nearly exact. The simulation indicates that by adjusting the duty cycle, the chopper's output voltage may be adjusted from 21.8V to any desired value. The passive components fluctuate in value as the output voltage rises, thus choosing the right values for the capacitance and inductance requires accuracy and care. As it shown in $\alpha=0.85$ the output voltage $V_{out}=145V$ and in $\alpha=0.94$ the output voltage $V_{out}=365V$.

Although a boost converter's theoretical output voltage is linearly proportional to the duty cycle, non-idealities and losses can cause actual converters to display variations from this relationship. To achieve efficient power conversion, one should take into account a boost converter's efficiency, which is often above 80%.

b-MPPT control of healthy model:

By comparing the measured power produced by the PV panel with MPPT ($P_m=50\%$) to the maximum power produced without MPPT (P_{mpp}), the efficiency of MPPT controllers is assessed.

The photovoltaic (PV) system's operational conditions are being successfully adjusted by the MPPT algorithm to track the maximum power point (MPP) with great accuracy, as seen by the system's high duty cycle of 0.85. In order to maximize power generation, the MPPT system effectively converts the input voltage (V_e) of 21.8 V to the output voltage (V_s) of 145 V. The system can be precisely and quickly adjusted to maintain the MPP, which guarantees smooth operation and improved control over the power conversion process.

This is made possible by the switching frequency (f_s) of 5 kHz. The MPPT system is more stable and efficient when the switching frequency is high. The notable rise in voltage from 21.8V (V_e) to 145V (V_s) indicates how well the MPPT algorithm works to maximize the PV system's power output. The system is able to retain high power conversion efficiency while achieving a significant voltage boost through effective duty cycle adjustment and MPP operation.

A high duty cycle, the right switching frequency, and the voltage change from V_e to V_s together show that the MPPT system is working as efficiently as possible to take the maximum amount of power from the sun's rays. The PV system's overall performance is improved by this effective power conversion process, which guarantees that the system can provide its maximum power output in a variety of environmental circumstances.

c-MPPT control of faulty model:

-Diode by-pass disconnected:

In a flawed MPPT model with partial shade, a duty cycle of 0.85, a switching frequency of 5 kHz, and certain voltage values (V_e and V_s) could lead to less than ideal performance. The MPPT algorithm's performance under partial shade conditions may be affected by the characteristics $P=50$, which could have an impact on how well the algorithm adjusts the operational parameters.

-Paratial shading fault:

The efficiency of MPPT algorithms can be considerably impacted by partial shading, making it difficult to track the maximum power point (MPP) precisely in a variety of irradiance situations. Partial shade can cause variations in the photovoltaic (PV) system's output power, (50% , $P_{mp}=5W$; 100% , $P_{mp}=0W$) ;which can affect how well the MPPT algorithm maintains optimal power generation.

-Resistance fault:

-Shunt Resistance:

When there are shunt and series resistance faults present, the MPPT system may operate less well if certain voltage values (V_e and V_s), a high duty cycle (0.85), and an adequate switching frequency (5 kHz) are used. Inaccurate tracking of the maximum power point by the

MPPT algorithm may result in decreased power generation and PV system efficiency. In our research it drops to 8W

-Series Resistance:

The MPPT system's capacity to precisely adjust the operating parameters can be hampered by the presence of a series resistance defect, which can interfere with regular system performance.

The defect could cause variations in the power output, decreased efficiency, and difficulties in keeping the system operating at the MPP in a variety of environmental circumstances.

Conclusion:

This chapter revolves about simulation study, thresholding techniques were employed to detect and diagnose eight types of faults in a photovoltaic panel. The comparison involved evaluating various characteristics (such as power, voltage, and current) of both the normal and faulty I-V curves of the PV panel. Additionally, the simulation work included an explanation of MPPT control, its operation, and the outcomes. [55] Upon reviewing the simulation findings, it became evident that the threshold method was unable to differentiate all faults effectively, prompting the need for a more efficient classification approach.

CHAPTER IV

IV. Introduction :

Throughout the earlier chapters, we have formulated the essential measures to accomplish our objective and enable the deployment of our electronic gadget, a "solar regulator based on a microcontroller for maximum power control and output voltage regulation." The size and technical specifications of the components that are available in the laboratory of Eloued's Faculty of Science and Applied Sciences serve as the basis for the system implementation. We will examine two experimental configurations of a full PV system in this chapter: (Detection Device + PV array + load)

IV.1. Tools Employed:

IV.1.1. Chopper components:

a-Transistor:

The transistor must be sized to support the maximum current delivered to the load. We choose two MOSFETs «50T65FSC-LB43106GE» and «SFA66UP30DN-T11A19G001 »

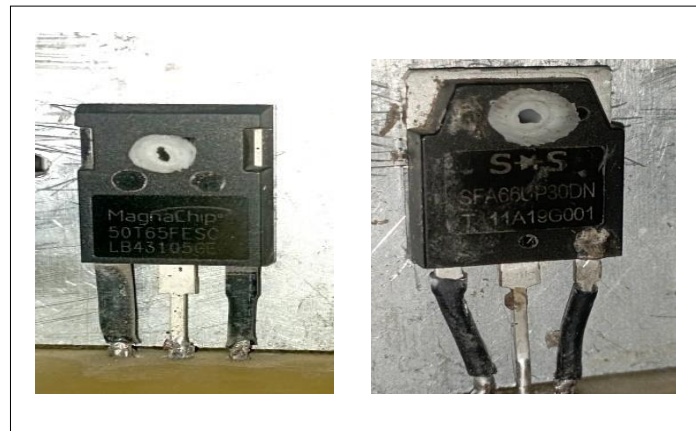


Figure IV.1 : for the «50T65FSC-LB43106GE» and «SFA66UP30DN-T11A19G001 » mosfets.

b-Coil :

This element is the most delicate to determine. Indeed, an inductance that is too low does not allow the power card to function, while an inductance that is too high would cause significant power losses due to Joule effect. We choose coil of "100mh"

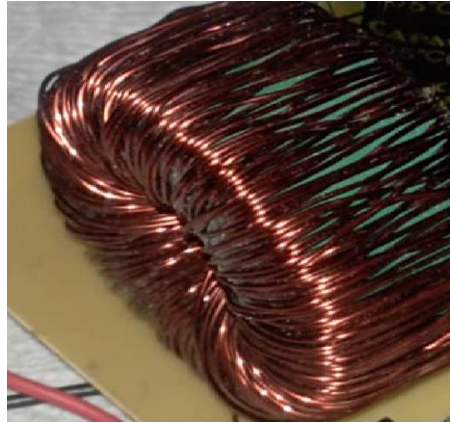


Figure IV.2: 100mH Coil.

c-Capacitor:

The concept of a "chopper boost capacitor" relates to the use of capacitors in boost chopper circuits. In these circuits, capacitors play a vital role in storing and releasing electrical energy to achieve voltage boosting. The capacitor in a boost chopper circuit helps stabilize the voltage across the load, smooth out the output voltage, and reduce voltage ripples. It is an essential component that ensures a constant and reliable output voltage for the load. By selecting capacitors with appropriate characteristics, such as low equivalent series resistance (ESR), losses can be minimized, leading to improved efficiency and performance of the boost chopper circuit. In our project we used «470 μ F-400V »Capacitor.



Figure IV.3: «470 μ F-400V »Capacitor.

d-Diode:

The diode used must be fast and able to withstand the maximum current supplied to the load. We have chosen a Schottky SBT80-10LS diode.

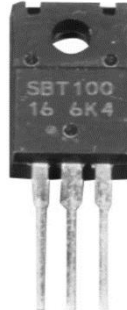


Figure IV.4 : « Schottky SBT80-10LS » diode.

e-Driver:

Gate drivers are essential components in power electronics systems as they provide the necessary voltage and current to switch power devices on and off effectively. These drivers play a crucial role in ensuring the proper operation, efficiency, and reliability of power electronics systems by accurately driving the gates of semiconductor devices. Gate drivers are designed to optimize the performance of power switches in various applications like converters, inverters, motor drives, and more, making them a key interface between control circuits and high-power electronics components . we used «EVISUN B0515S-1W 2048» driver.

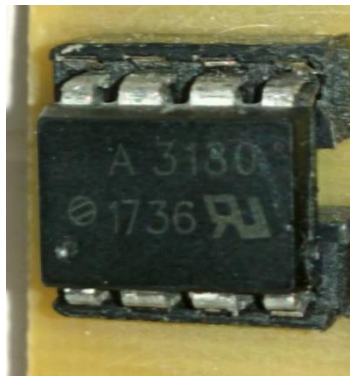


Figure IV.5:«A3130-1736» driver.

f-Relay driver:

To drive a relay in a boost chopper circuit, you typically need a relay driver that can handle the voltage and current requirements of the relay coil. This driver would receive the

control signals from the chopper circuit and provide the necessary power to activate the relay at the appropriate times in the circuit operation. It's essential to choose a relay driver that can handle the voltage spikes and current demands inherent in chopper circuits to ensure reliable operation.



Figure IV.6: «EVISUN B0515S-1W 2048» Relay driver.

g-Resistor:

In a boost converter, the load resistor (R) represents the electrical load connected to the converter, and it is crucial for determining the necessary voltage and current provided by the converter to the load. Additionally, resistors can be used in feedback networks to regulate the output voltage or current of the boost converter.



Figure IV.7: Resistor.

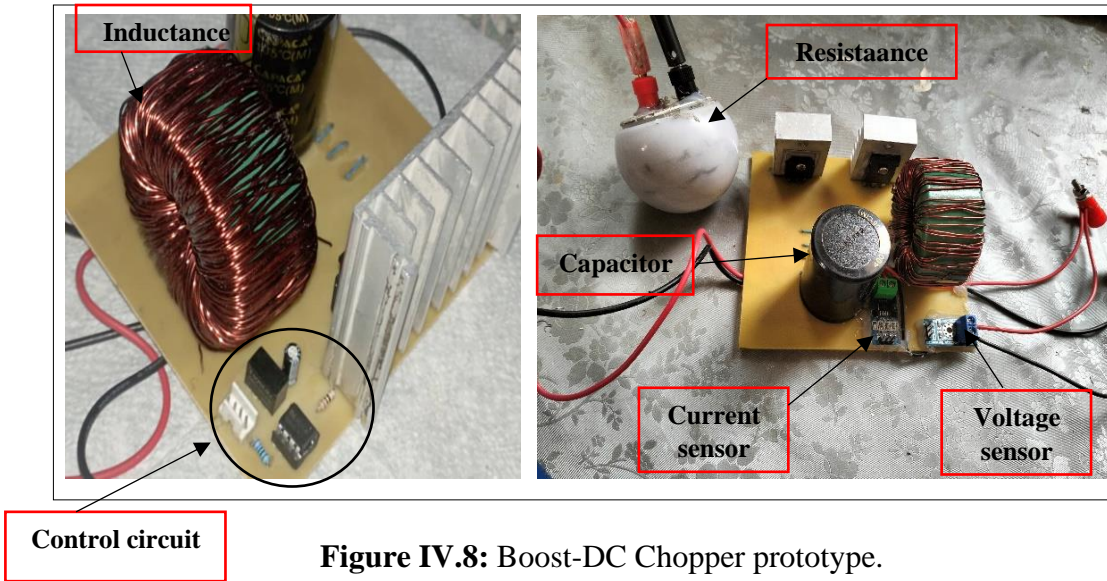


Figure IV.8: Boost-DC Chopper prototype.

IV.2. The solar panel:

We made use of the 7.4V, 54W lab bench solar panel that is shown in Figure (IV.9).

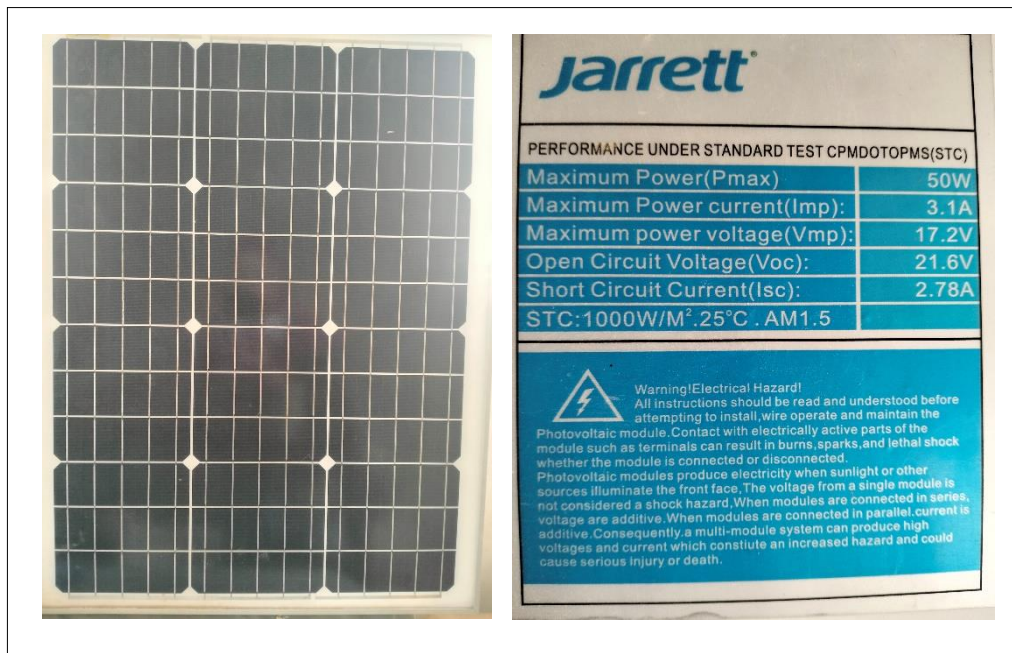


Figure IV.9: Characteristics the PV array.

IV.3. Current Sensor:

To precisely detect AC or DC current signals, the ACS712s sensor relies on the Hall effect. It can handle up to 5 amps of maximum current. Through an analog interface, the current signal can be read.

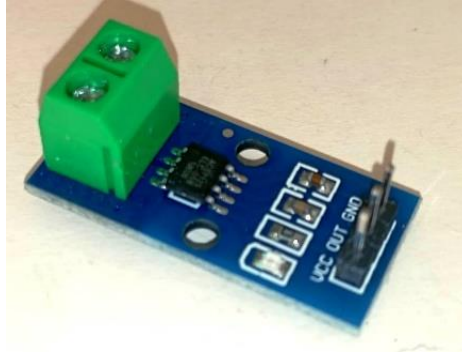


Figure IV.10: ACS712s current sensor.

IV.4. Voltage Sensor:

a three-pin voltage sensor (VCC, GND, SIGNAL). Up to 25V can be handled by it. This module may reduce the input power voltage from the red terminal by five times and operates on the resistance point pressure principle.



Figure IV.11: Voltage sensor.

IV.5. Photoresistor:

A photoresistor, also referred to as a photocell or light-dependent resistor (LDR), is a passive electronic element that alters its resistance according to the intensity of light it is exposed to. When in darkness, a photoresistor exhibits high resistance, whereas in light, its resistance diminishes notably. These devices find widespread use in applications like light-sensitive detector circuits, light-triggered switches, and dark-triggered switches.

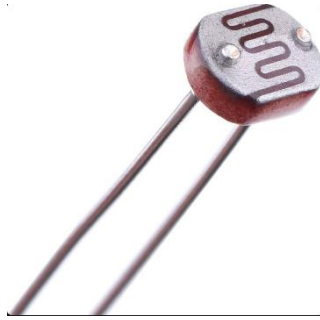


Figure IV.12: Photoresistor.

IV.6. The Microcontroller (ARDUINOBOARD):

IV.6.1. Definition:

Arduino NodeMCU (LoLin) refers to the integration of the Arduino platform with the NodeMCU development board, specifically the LoLin version. The NodeMCU LoLin V3 is a development board based on the ESP8266 microcontroller chip, offering WiFi connectivity and enhanced capabilities for IoT projects. It can be programmed using Arduino IDE, allowing users to leverage the strengths of both platforms for projects requiring wireless communication, IoT functionalities, and more advanced applications beyond what a standard Arduino board can provide. The NodeMCU LoLin V3 features GPIO pins, a micro USB port, a status LED, and a USB to UART converter, making it suitable for interactive and programmable projects at a low cost. It supports Lua scripting and can also be programmed using C++ with the Arduino IDE, providing flexibility in development approaches. The NodeMCU LoLin V3 is open-source and offers a cost-effective solution for projects requiring WiFi connectivity and IoT capabilities.

IV.6.2. Characteristics :

The Arduino NodeMCU (LoLin) is a development board that combines the Arduino platform with the NodeMCU module, specifically the LoLin version. Here are the characteristics of the NodeMCU (LoLin) based on the provided sources:

- Microcontroller: Espressif ESP8266 (ESP-12F).
- Processor: Tensilica Xtensa 32-bit LX106.
- Compatible with Arduino IDE for easy programming.
- GPIO pins for connecting sensors, actuators, and other peripherals.

- USB interface for power and programming.
- Integrated voltage regulator for stable operation.
- Support for Lua scripting in addition to Arduino programming.
- Compact size and lightweight design for prototyping IoT projects.

IV.6.3. Why Arduino NodeMCU (LoLin) :

- Integrated Wi-Fi module for easy wireless connectivity.
- Arduino IDE compatibility for simple programming.
- GPIO pins for versatile project development.
- Lua scripting support for additional programming flexibility.
- Compact design ideal for prototyping IoT projects.
- Cost-effective solution for IoT applications.
- Community support and resources available for guidance and troubleshooting.

IV.6.4. Arduino software interfaces :

. Arduino IDE (Integrated Development Environment): This is the official software used to write code for Arduino boards. It includes a text editor for writing code, a message area, a text console, a toolbar with buttons for common functions, and a series of menus.

. Web-based Arduino Create: An alternative to the Arduino IDE, Arduino Create is a platform that allows you to write code, access libraries, and upload sketches to your Arduino board directly from a web browser.

. Third-party IDEs: Some developers prefer using third-party Integrated Development Environments like Visual Studio Code or PlatformIO for a more feature-rich coding experience when working with Arduino boards.

These interfaces provide the necessary tools for writing, compiling, and uploading code to Arduino boards, making it easier for users to create projects and develop applications.



Figure IV.13: Arduino Uno Board .

IV.7. Results:

IV.7.1. Chopper Results :

IV.7.1.1. Steps of Work:

In our experimental validation work we followed the following steps to achieve the results required .

1. Designing the Circuit

a. Define Specifications:

- Input voltage (V_{in}) Ascertain the input voltage's range.
- Output voltage (V_{out}) Ascertain the output voltage's range.
- Load current (I_{out}): Find out how much current the load can draw at its maximum.

b. Calculate Duty Cycle (D):

c. Select Switching Frequency (f_s):

$$f_s = 25 \text{ kHz}$$

d. Inductor Selection (L) :

- The inductor value using: $L = 100\text{H}$

2. Selecting Components**a. Inductor**

- Choose an inductor with the calculated inductance and a current rating higher than the peak inductor current.

b. Capacitors

- Choose capacitors with low ESR (Equivalent Series Resistance) and suitable voltage ratings.
 $C = 470\ \mu\text{f}$.

c. Switching Device (MOSFET)

- Select a MOSFET that can handle the input voltage, output current, and has a low on-resistance $R_{DS(on)}$.

d. Diode

- Use a fast recovery diode or a Schottky diode with a current rating higher than I_{out} and a reverse voltage rating higher than V_{out} .

3. Building the Circuit:**a. Schematic Design:**

- Draw the circuit schematic, including all components.

b. PCB Layout

- Design the PCB layout or use a breadboard for initial testing.
- Ensure proper placement of components to minimize noise and losses (short and wide traces for high-current paths).

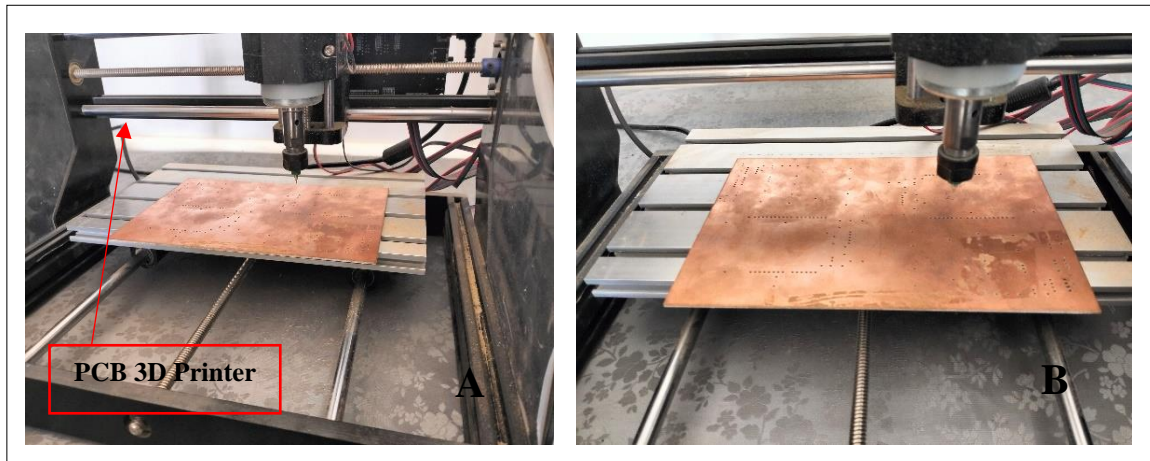


Figure IV.14: A, B: During the printing and drilling.

c. Assembly

- Assemble the circuit on a PCB or breadboard.
- Solder components carefully, ensuring no short circuits.

4. Testing the Circuit:

a. Initial Power-Up:

- Use a bench power supply with current limiting set to a safe level, In our case we tried $V = 12V$.
- Gradually increase the input voltage while monitoring the output voltage and current.our test in the figures (figure IV.20, figure IV.21) shown below.

b. Load Testing

- Connect different loads (resistive load or electronic load) to ensure the converter can handle various conditions.

In our project we made a resistor ourselves $R = 57\Omega$.

- d. Thermal Performance :** - Check the temperature of the components during operation to ensure they are within safe limits.

5. Troubleshooting and Optimization

a. Check Waveforms

- Use an oscilloscope to check the switch node voltage, inductor current, and other key signals.

b. Adjust Components

- If the performance is not as expected, consider adjusting the inductor, capacitors, or switching frequency.

c. Stability Analysis

- Ensure the converter is stable under all operating conditions. Add compensation networks if necessary.

6. Final Implementation

- Once the circuit operates correctly and reliably, finalize the design.

- If on a breadboard, consider designing a robust PCB for long-term use.

The use of integrated circuits requires a regulated and stabilized power supply. They need a 5V power supply and another power supply of 12V, $I=0.04$.



Figure IV.15: power supply of 12.6 V, $I=0.04$.

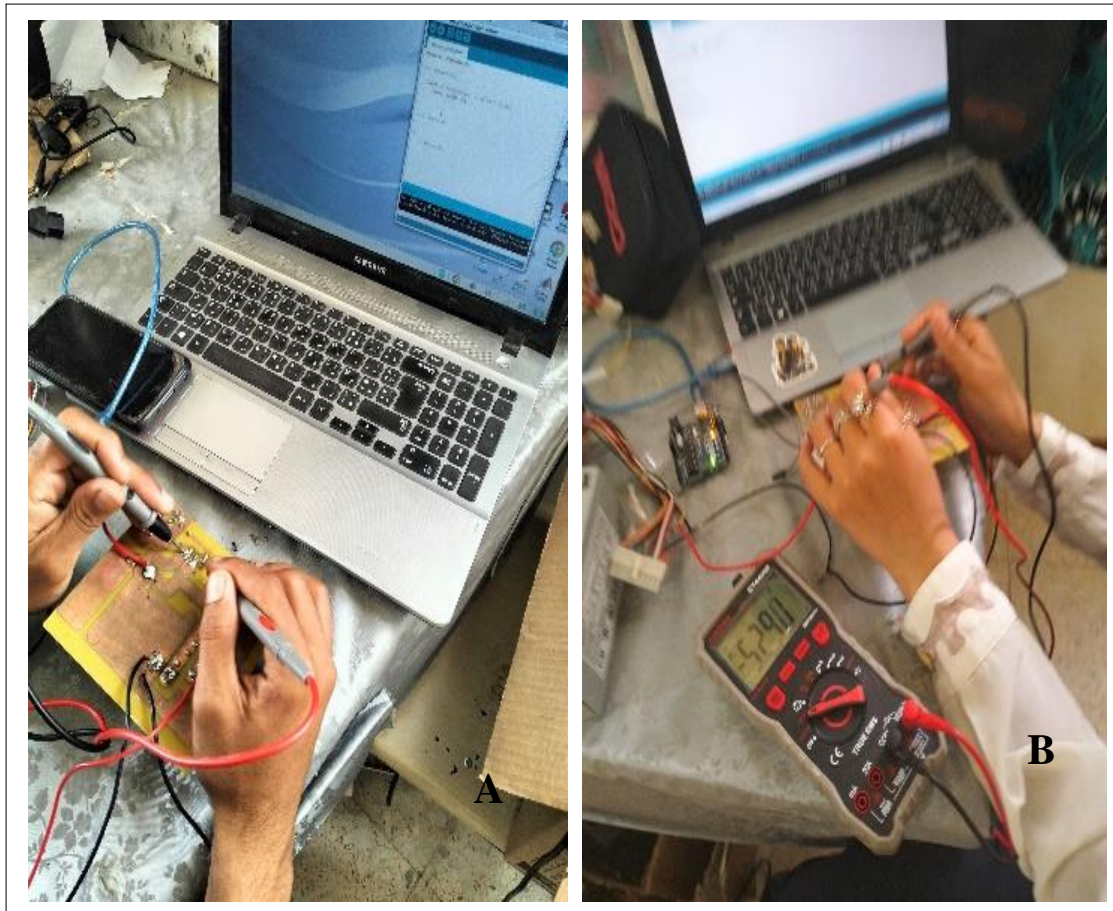


Figure IV.16: (A,B)Testing of DC-boost converter.

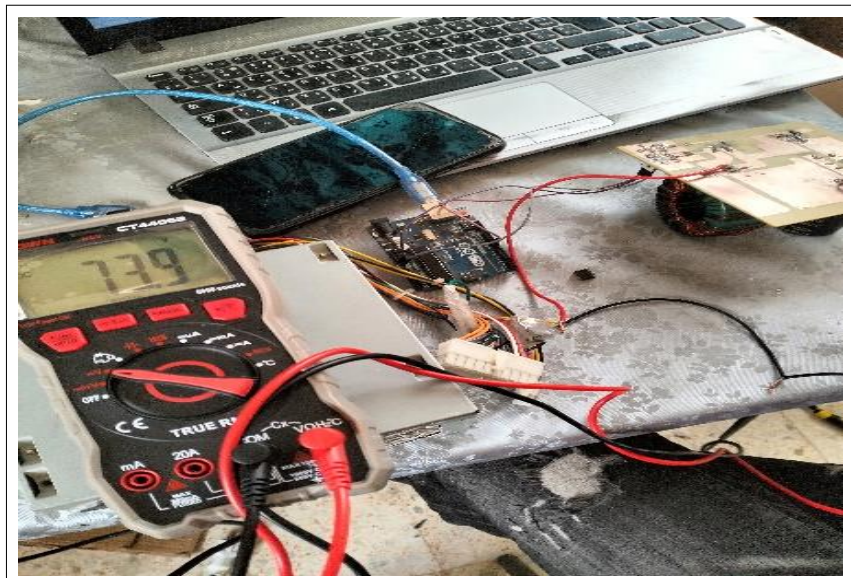


Figure IV.17:Vout



Figure IV.18: Vout while duty cycle variation.

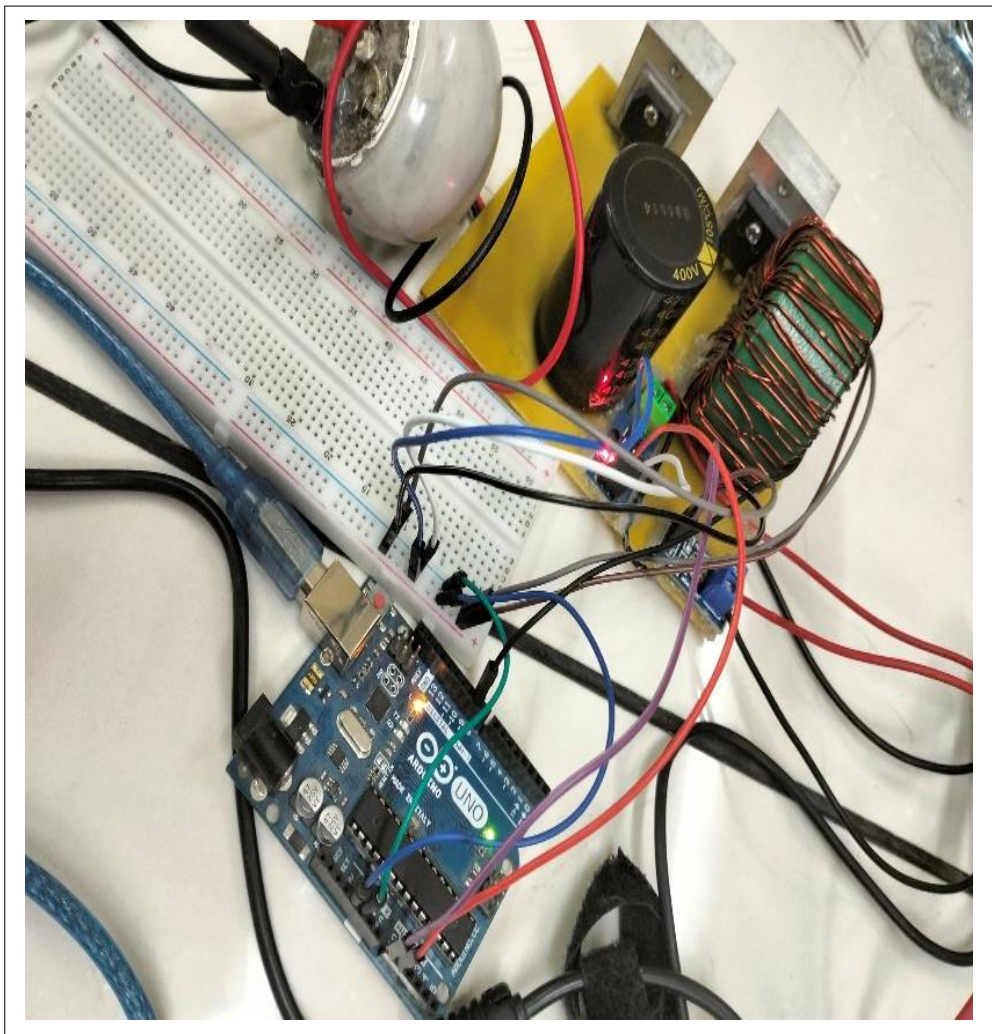


Figure IV.19: Validation of results.

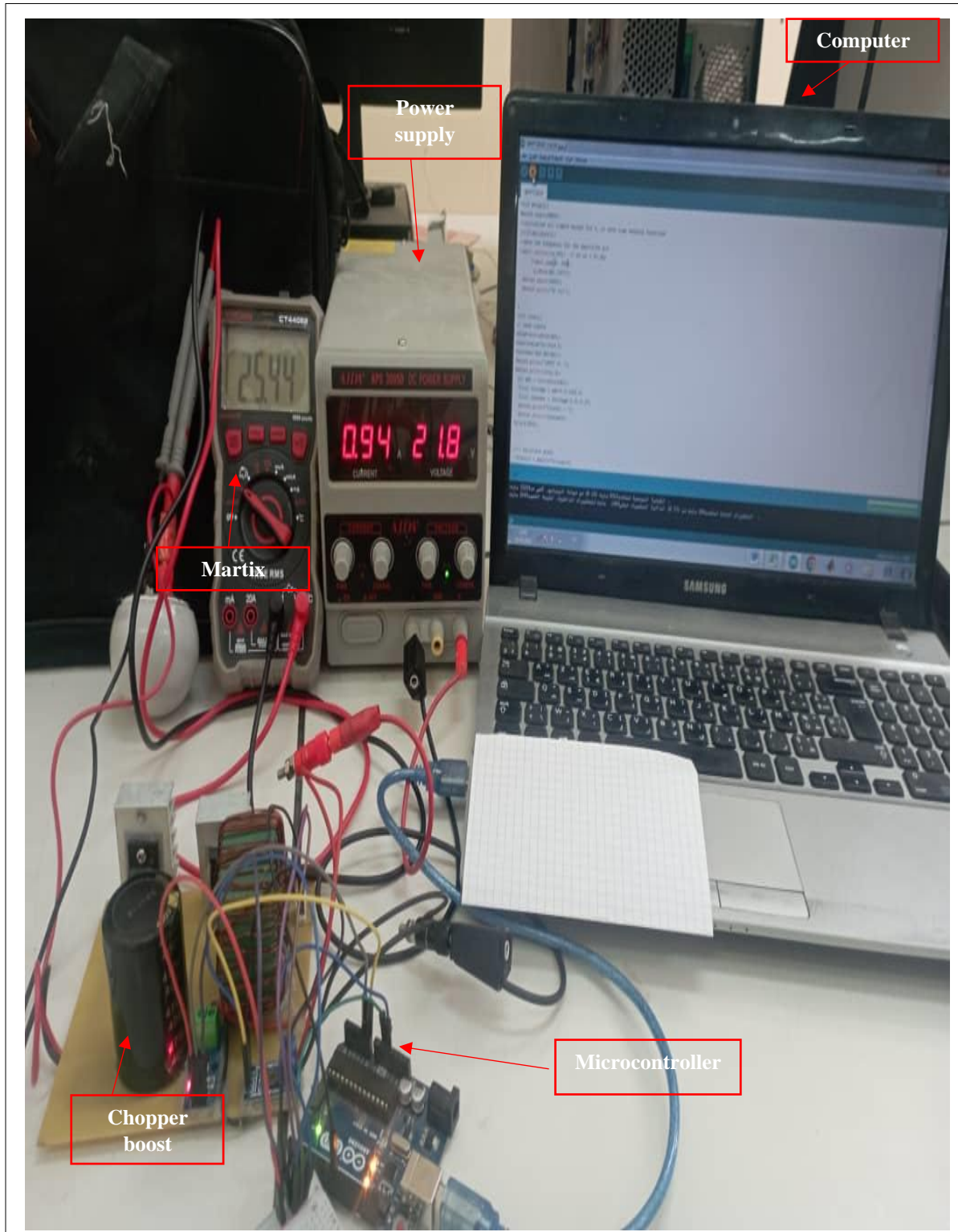


Figure IV.20: Validation of results.

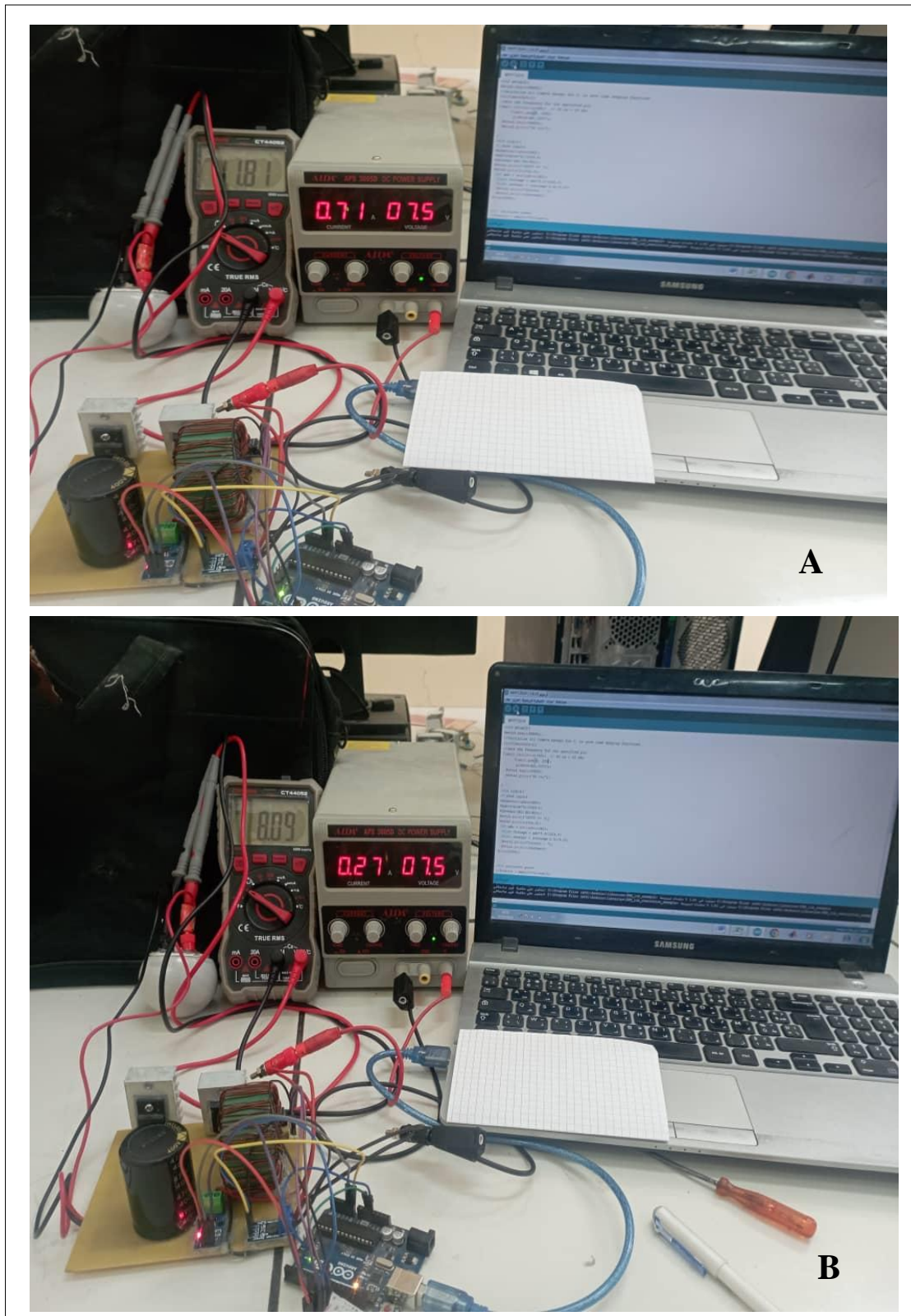


Figure IV.21:The results with input voltage = 7.5V, A:duty cycle 10%, B:duty cycle 20%.

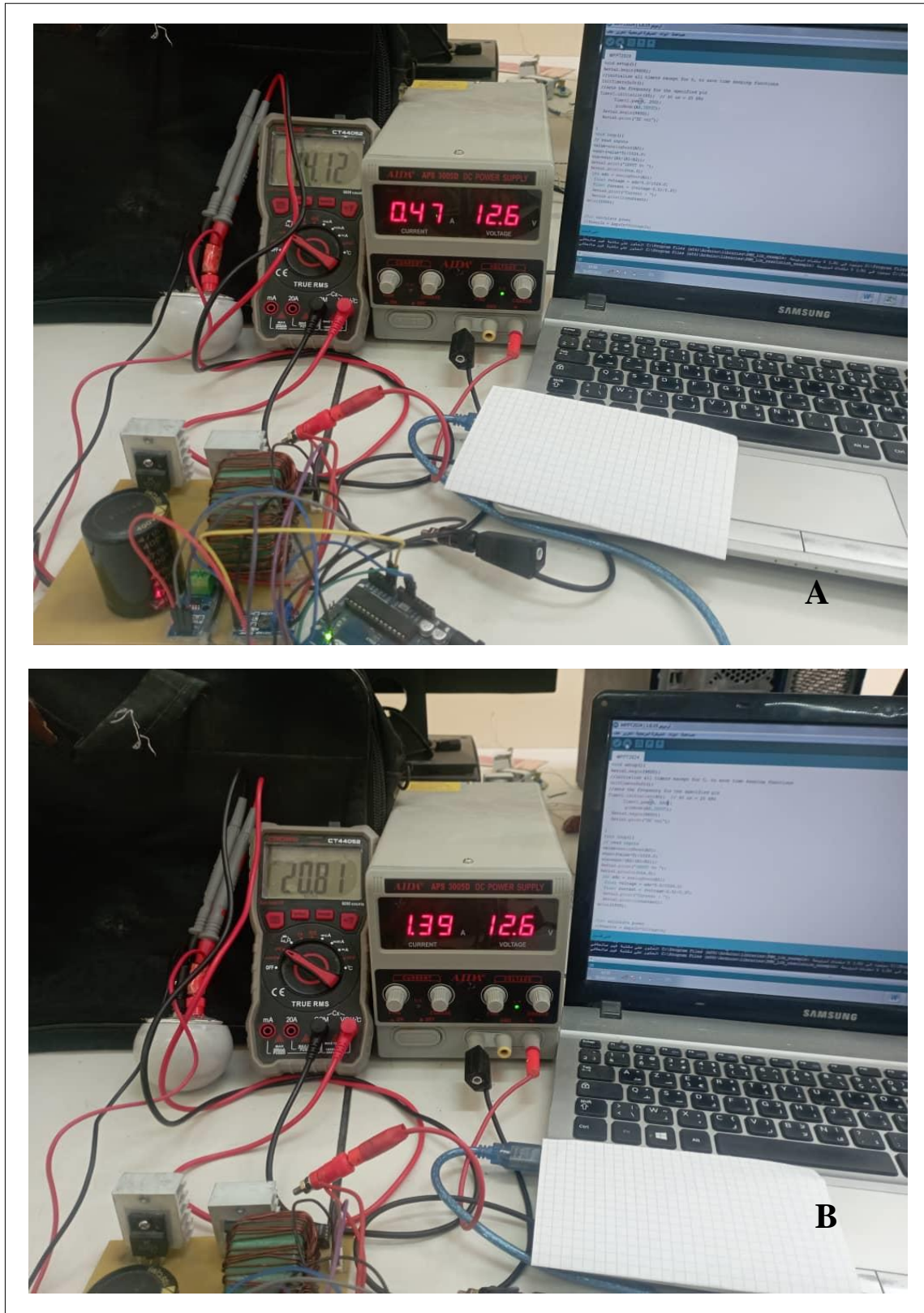


Figure IV.22:The results with input voltage = 12.5V, A:duty cycle 10%, B:duty cycle 20%.

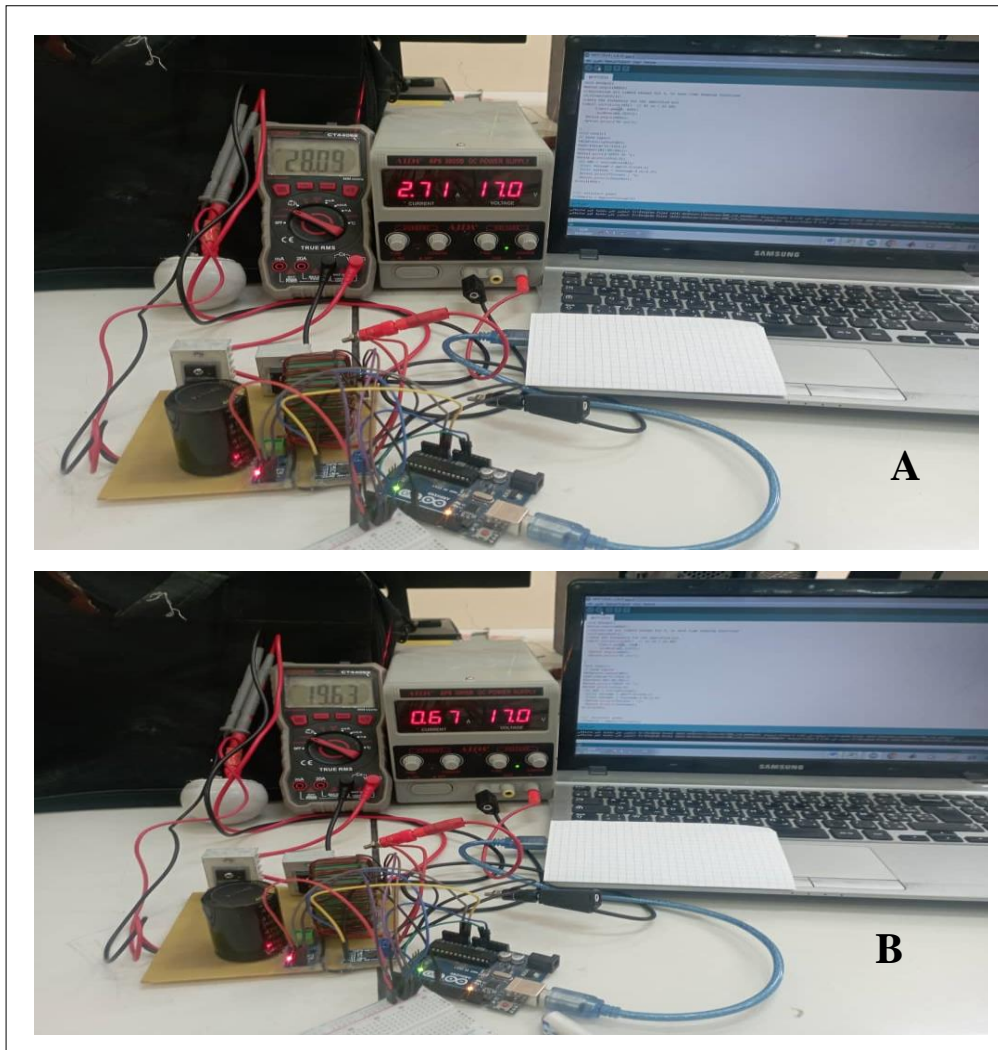


Figure IV.23:The results with input voltage = 17V, A:duty cycle 10%, B:duty cycle 20%.

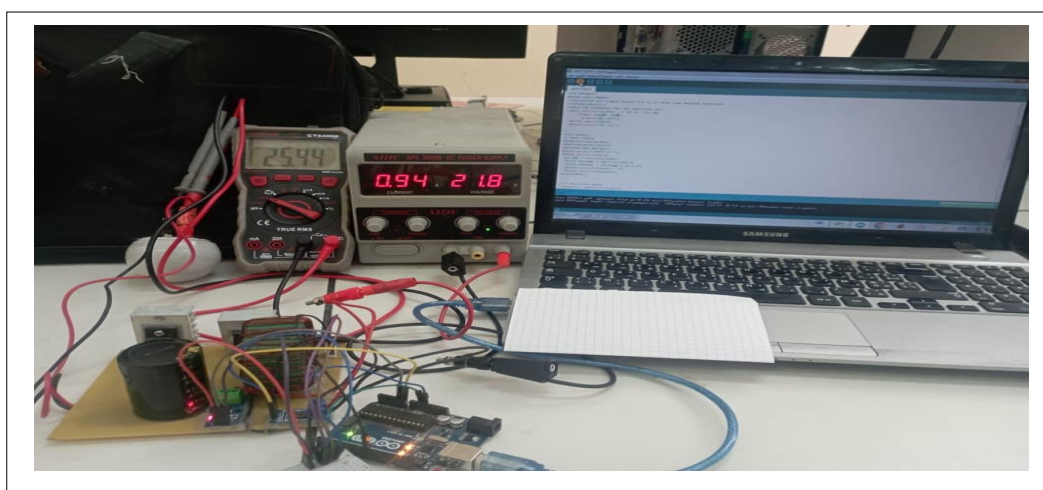


Figure IV.24:The results with input voltage = 21.8V.

Table IV.1: The variations in Current and Voltage with changes in duty cycle when $V_{out}=7.5V$.

Duty cycle	Input voltage[V]	Output voltage [V]	Output current [A]
dc10%	7.5	7.61	0.17
dc20%	7.5	8.48	0.21
dc30%	7.5	9.56	0.27
dc40%	7.5	10.99	0.36
dc50%	7.5	12.84	0.5
dc60%	7.5	15.42	0.74
dc70%	7.5	19.19	1.22
dc80%	7.5	24.95	2.35

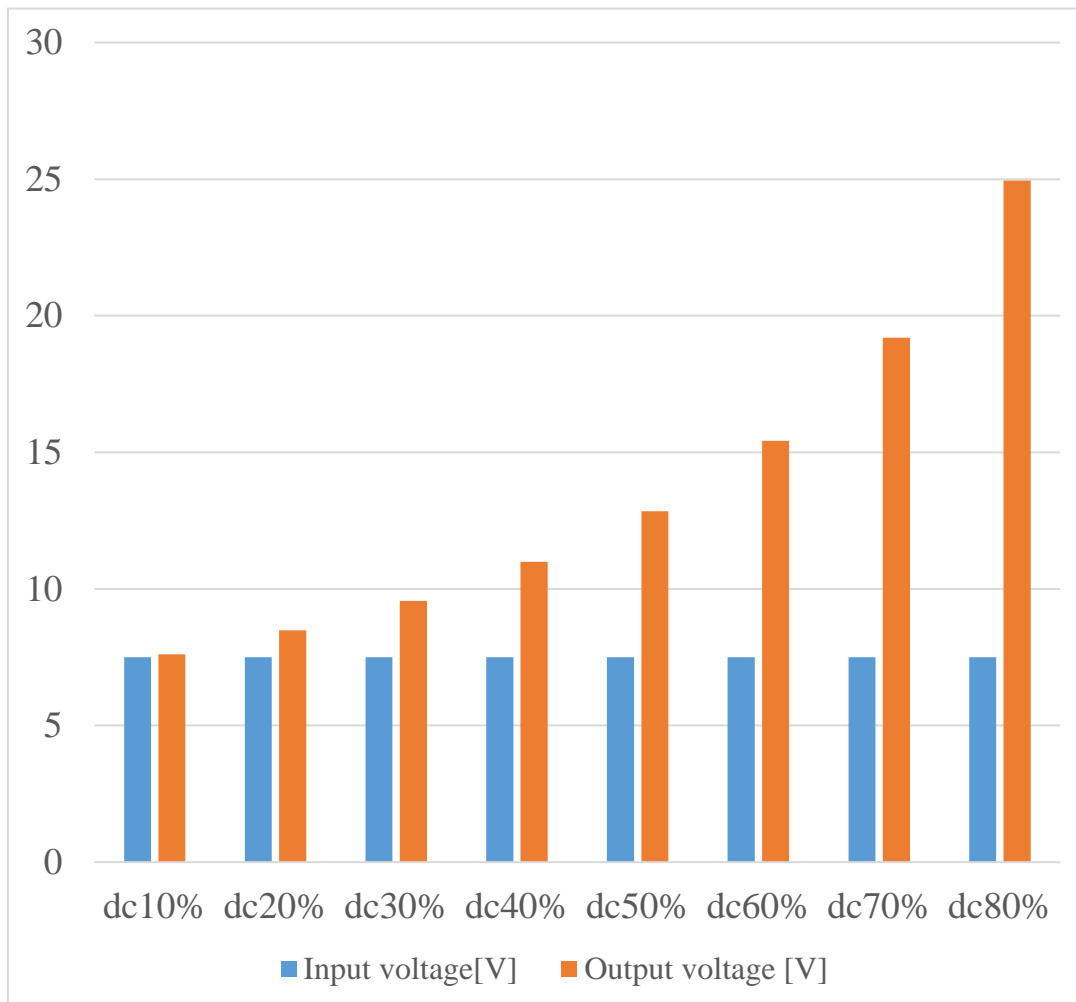


Figure IV.25: The increasing of output Voltage with the variation of duty cycle, where input voltage = 7.5V.

Table IV.2: The variations in Current and Voltage with changes in duty cycle when $V_{out}=12.5V$.

Duty cycle	Input voltage[V]	Output voltage [V]	Output current [A]
dc10%	12.5	13.12	0.29
dc20%	12.5	14.62	0.36
dc30%	12.5	16.51	0.47
dc40%	12.5	19.04	0.63
dc50%	12.5	22.36	0.88
dc60%	12.5	27	1.32
dc70%	12.5	33.72	2.17
dc80%	12.5	43.76	4.2

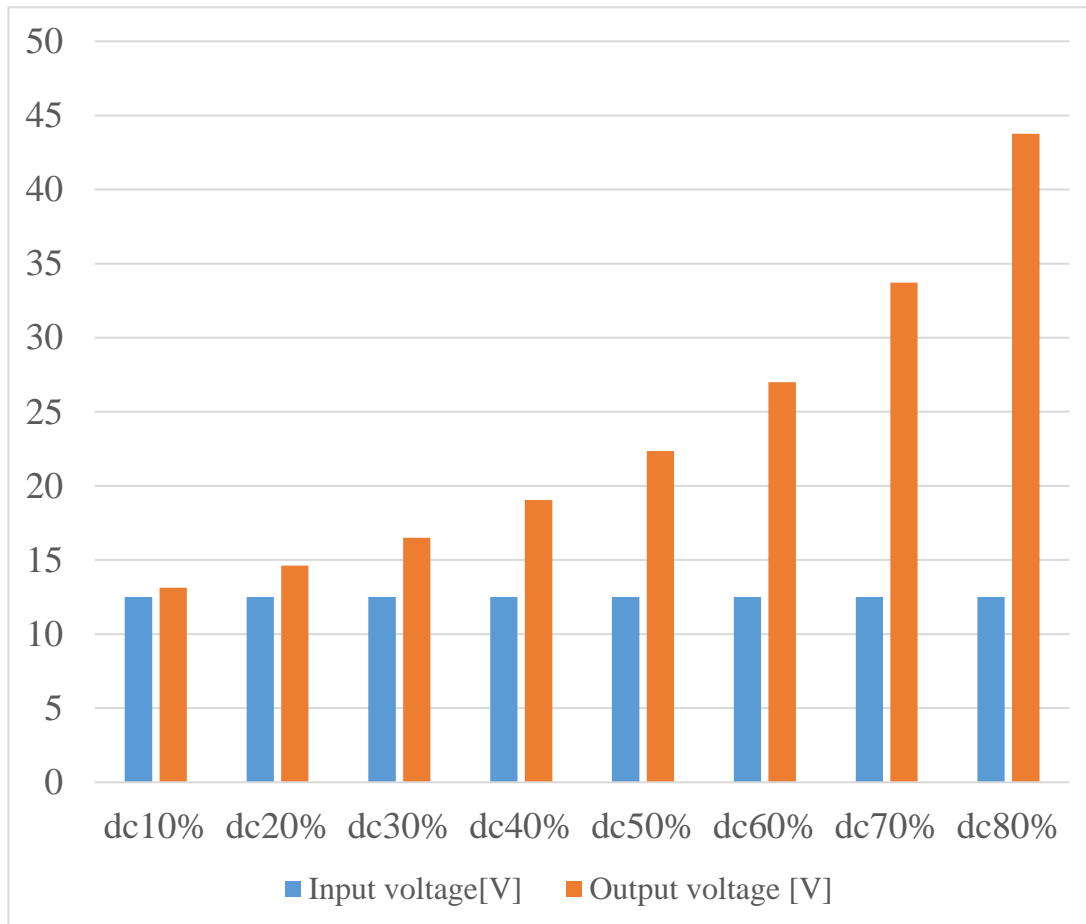


Figure IV.26: The increasing of output Voltage with the variation of duty cycle, where input voltage = 12.5V.

Table IV.3: The variations in Current and Voltage with changes in duty cycle when $V_{out}=17V$.

Duty cycle	Input voltage[V]	Output voltage[V]	Output current [A]
dc10%	17	18.11	0.4
dc20%	17	20.18	0.5
dc30%	17	22.78	0.64
dc40%	17	26.3	0.82
dc50%	17	30.75	1.2
dc60%	17	35.83	1.7
dc70%	17	46.6	3.03
dc80%	17	52.5	5

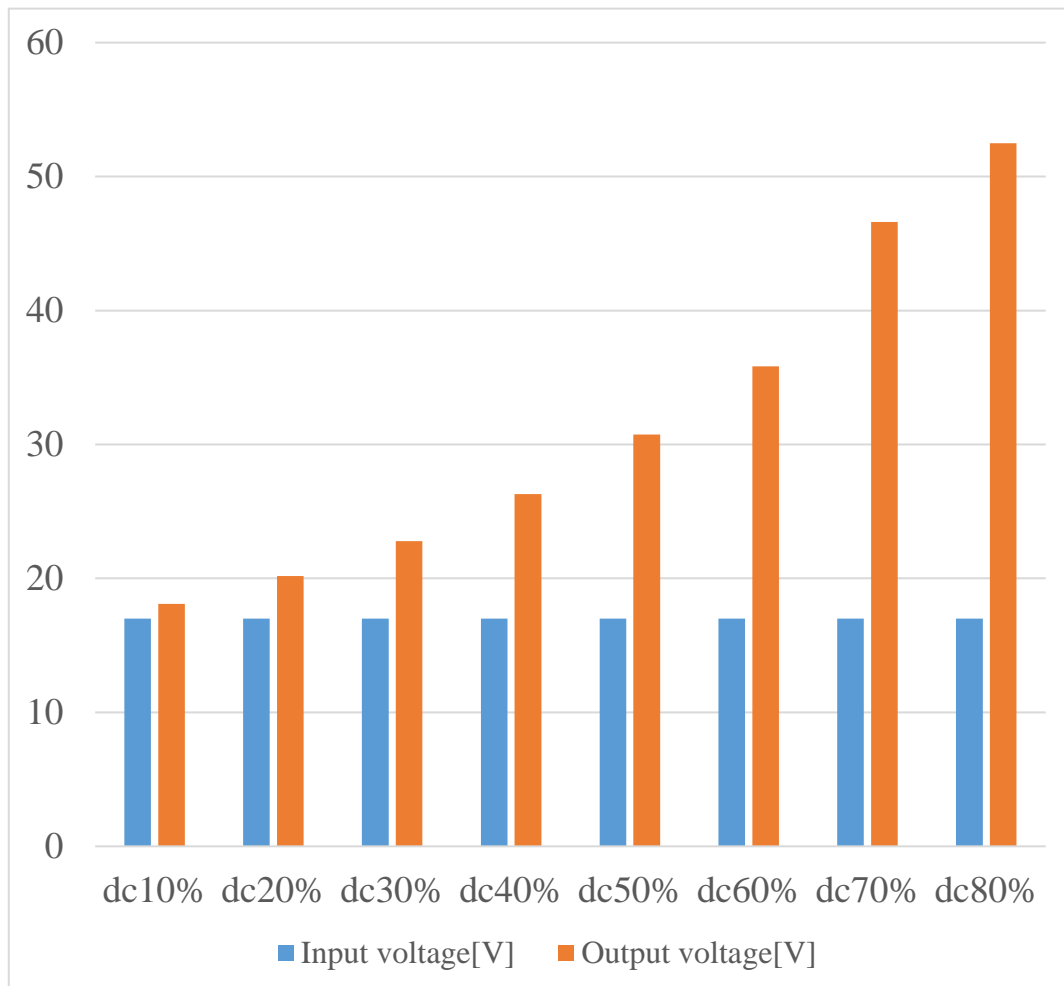


Figure IV.27: The increasing of output Voltage with the variation of duty cycle, where input voltage = 17V.

Table IV.4: The variations in Current and Voltage with changes in duty cycle when $V_{out}=21.8V$.

Duty cycle	Input voltage[V]	Output voltage[V]	Output current [A]
dc10%	21.8	22.9	0.5
dc20%	21.8	26.08	0.55
dc30%	21.8	29.52	0.83
dc40%	21.8	34.13	1.12
dc50%	21.8	40.15	1.58
dc60%	21.8	48.58	2.39
dc70%	21.8	60.57	3.94
dc80%	21.8	70.42	5

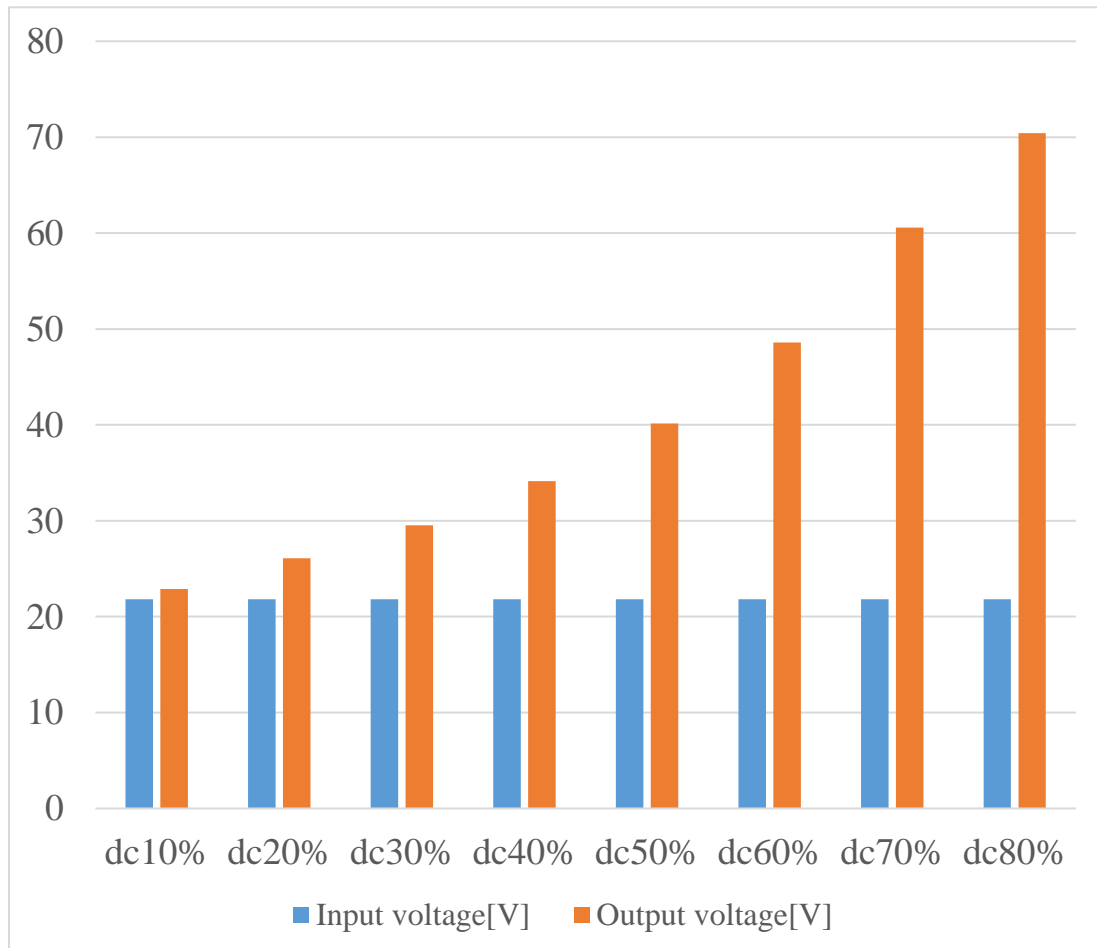


Figure IV.28: The increasing of output Voltage with the variation of duty cycle, where input voltage = 21.8V.

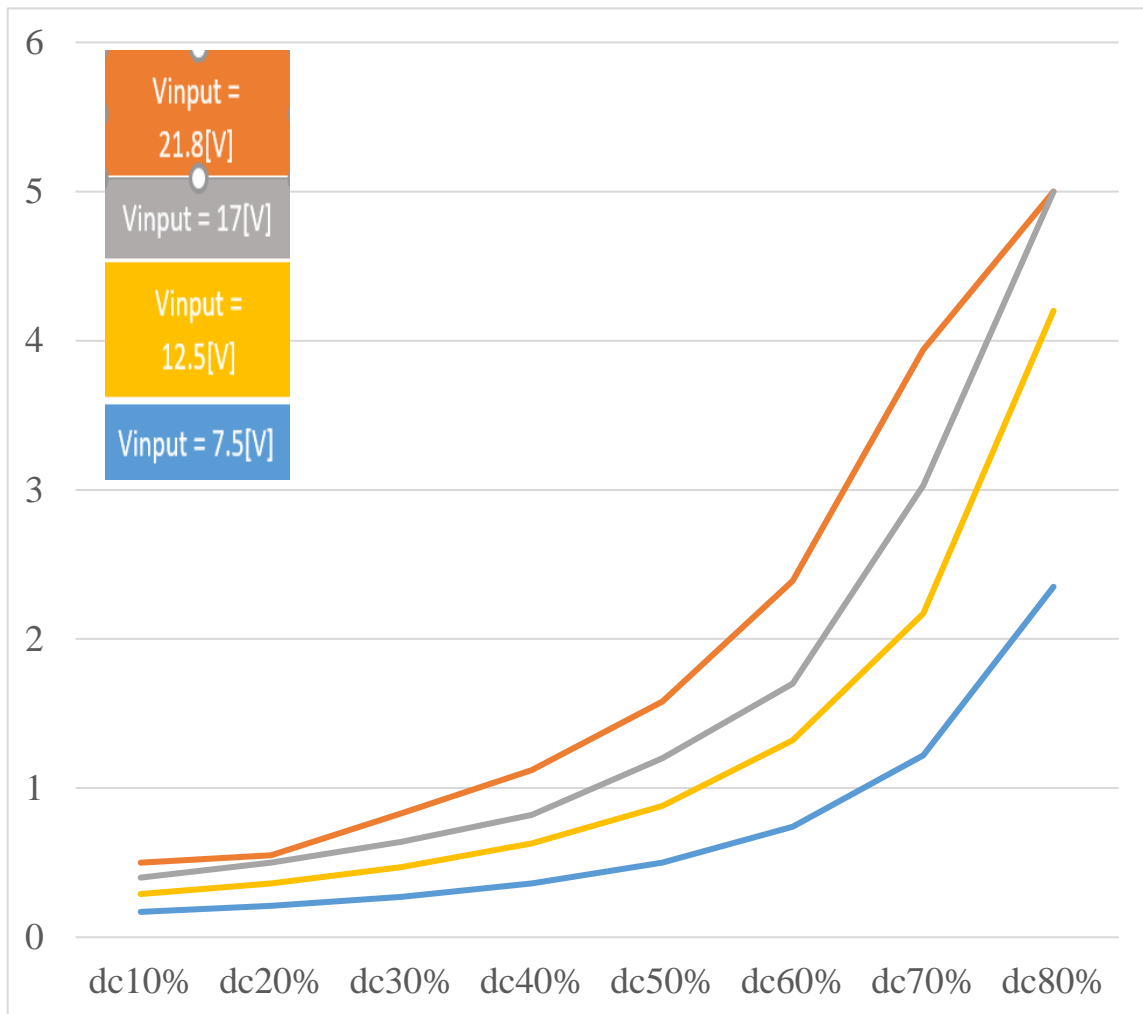


Figure IV.29: Current results with duty cycle variation.

IV.7.1.2. Interpretation of Results :

- Efficiency: As the duty cycle increases, the output voltage increases, but so does the potential for losses due to increased current through the components, leading to higher conduction losses and potential efficiency drops.
- Ripple Voltage: The ripple voltage on the output can increase with higher duty cycles, especially if the converter is not properly designed to handle high currents at these duty cycles.
- Component Stress: Higher duty cycles mean higher currents through the inductor and switch, which can lead to increased stress on these components, potentially reducing their lifespan if not properly rated.

IV.7.2. MPPT control:

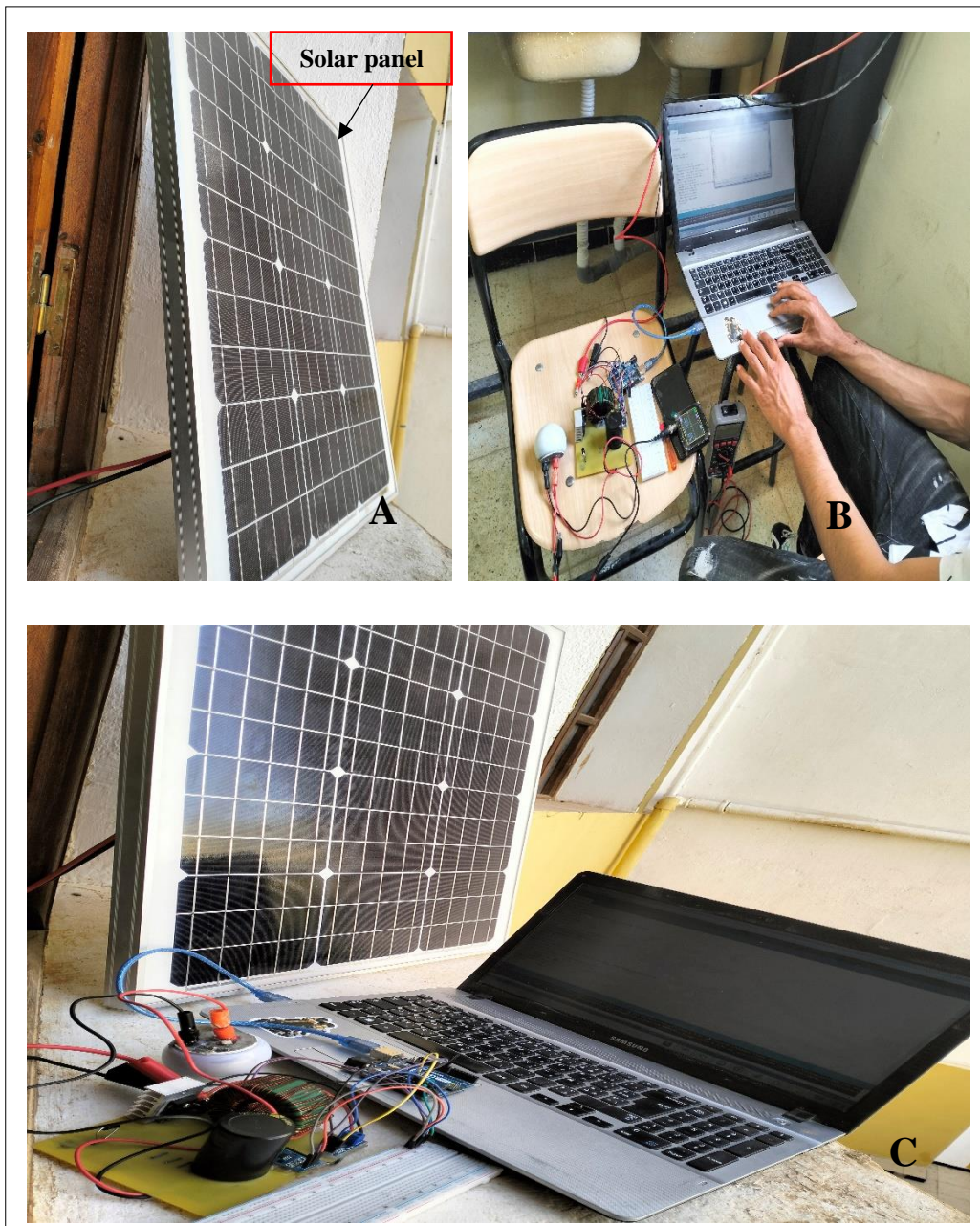


Figure IV.30:Global experimental test healthy model.

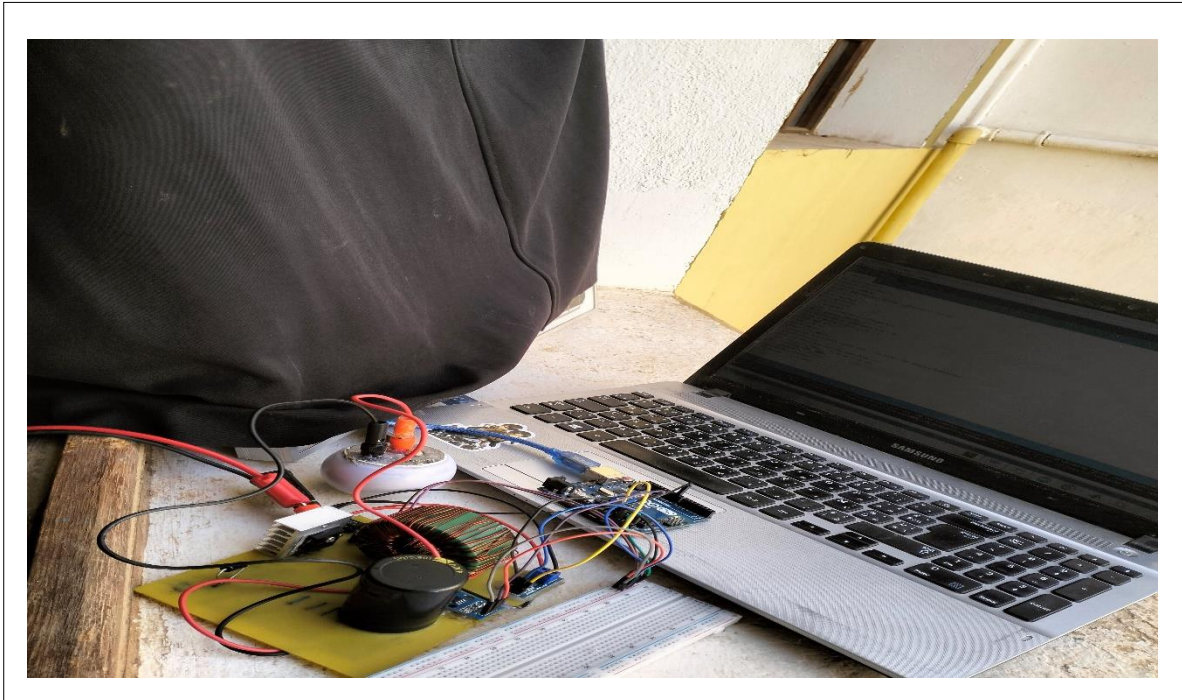


Figure IV.31:Global experimental test faulty model “full-shading”.

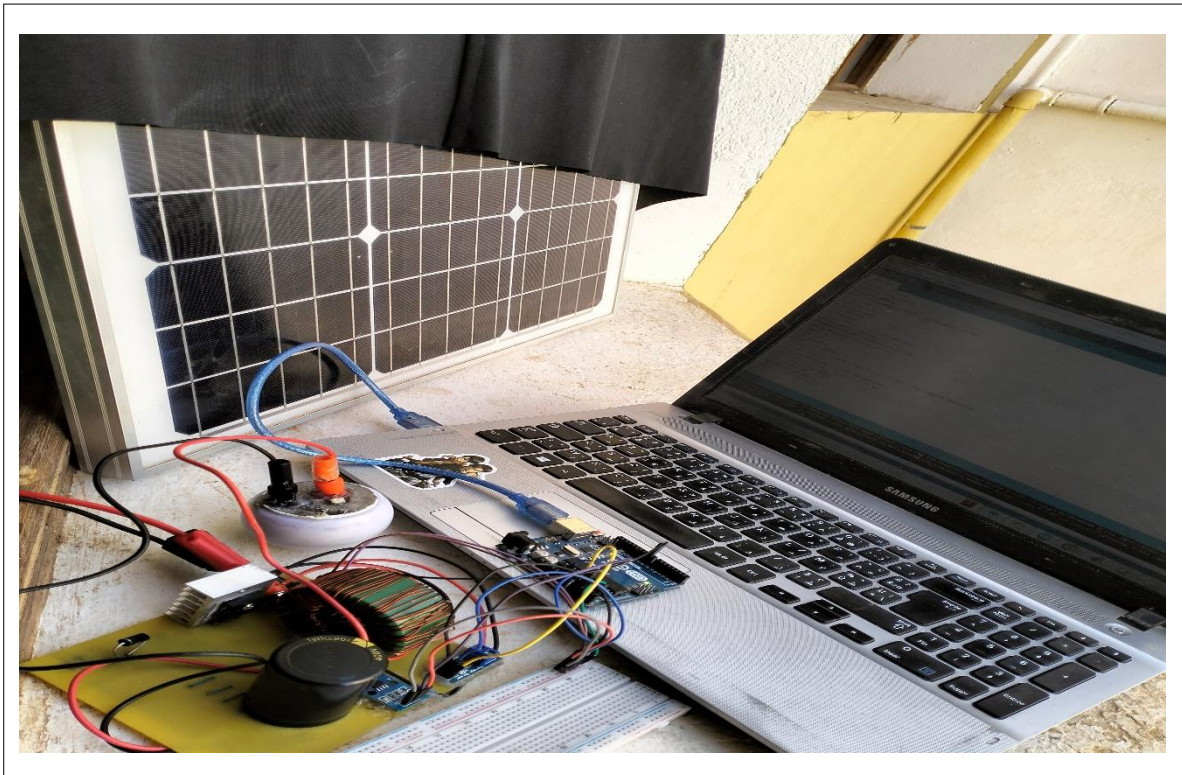


Figure IV.32: Global experimental test faulty model “paratial-shading”.

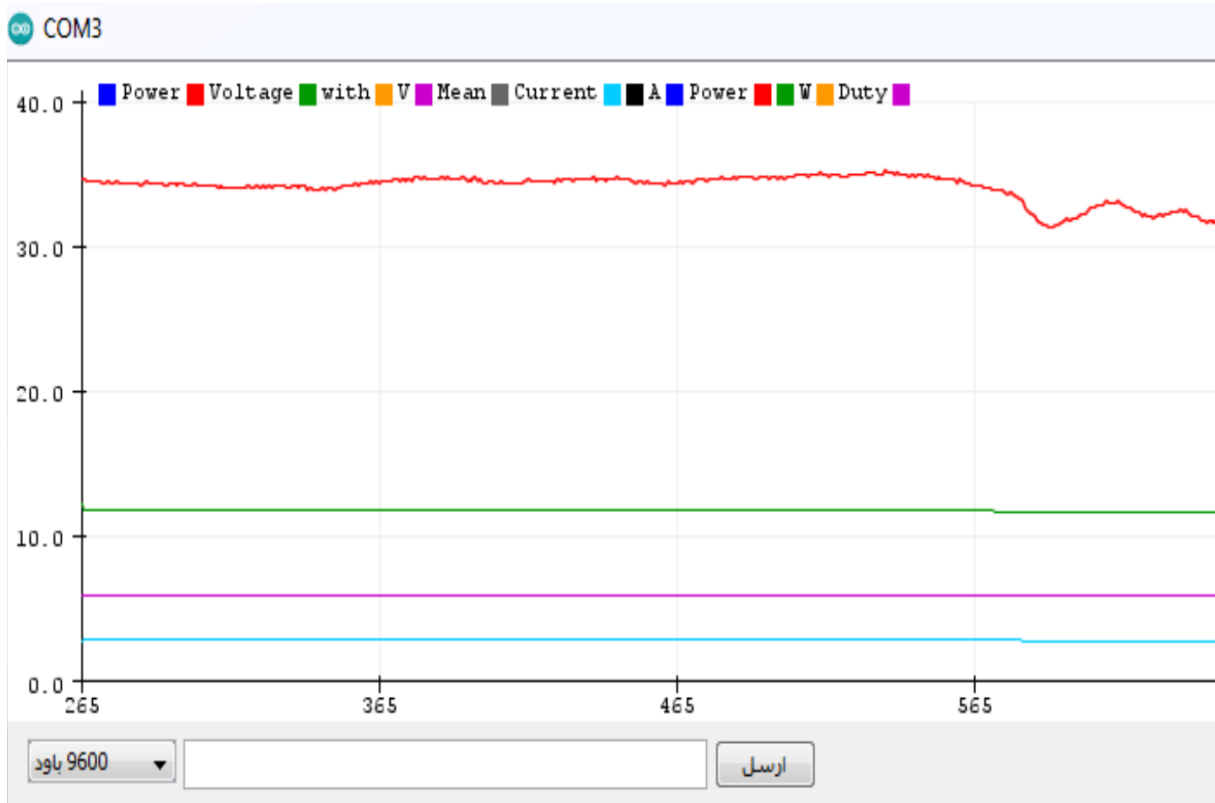


Figure IV.33: Serial curves results of MPPT control healthy model.

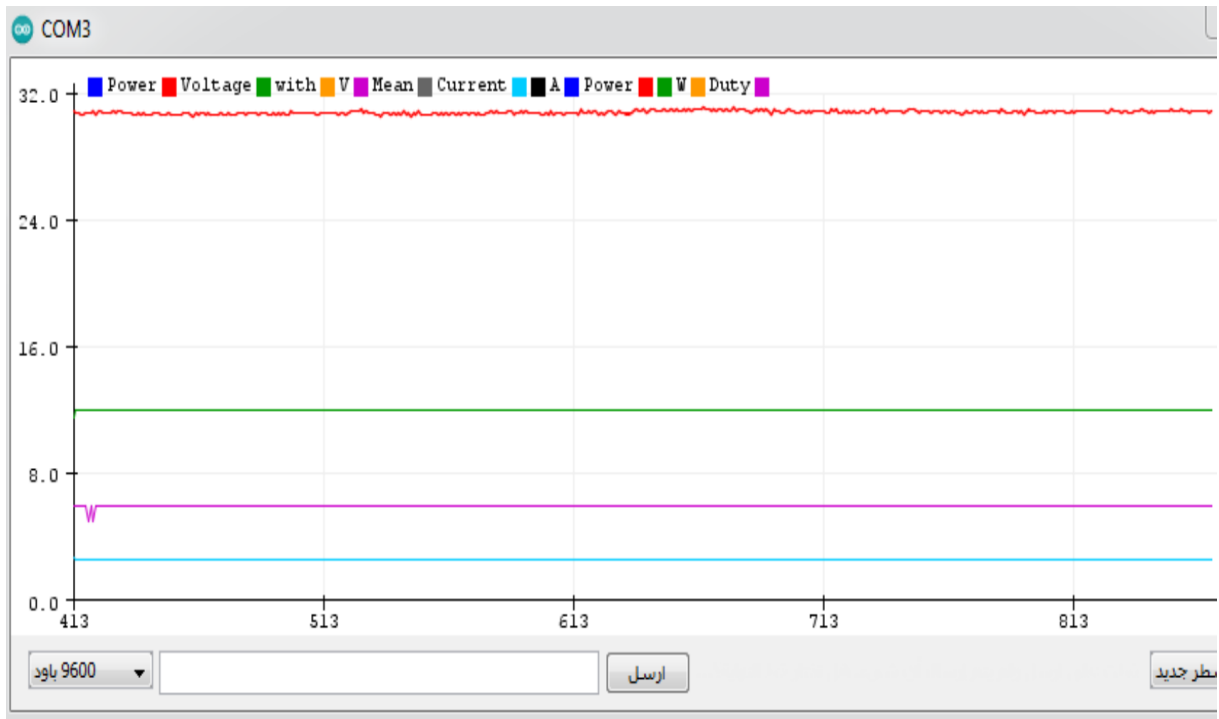


Figure IV.34: Serial curves results of MPPT control healthy model without LCD.

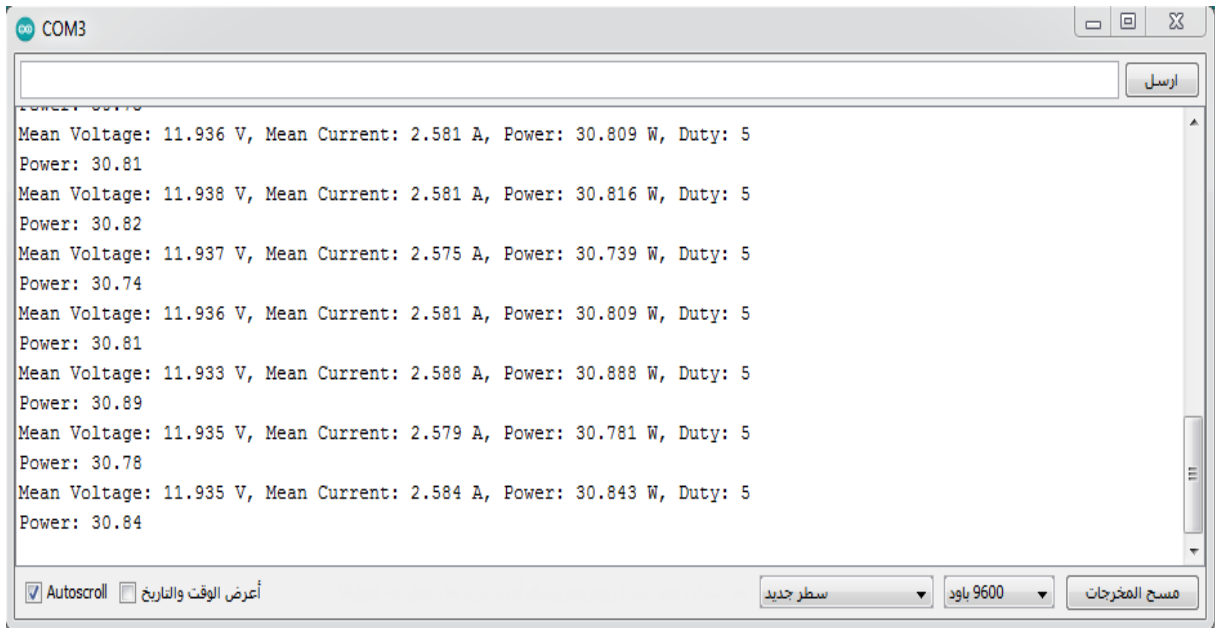


Figure IV.35: Serial results of MPPT control healthy model without LCD.

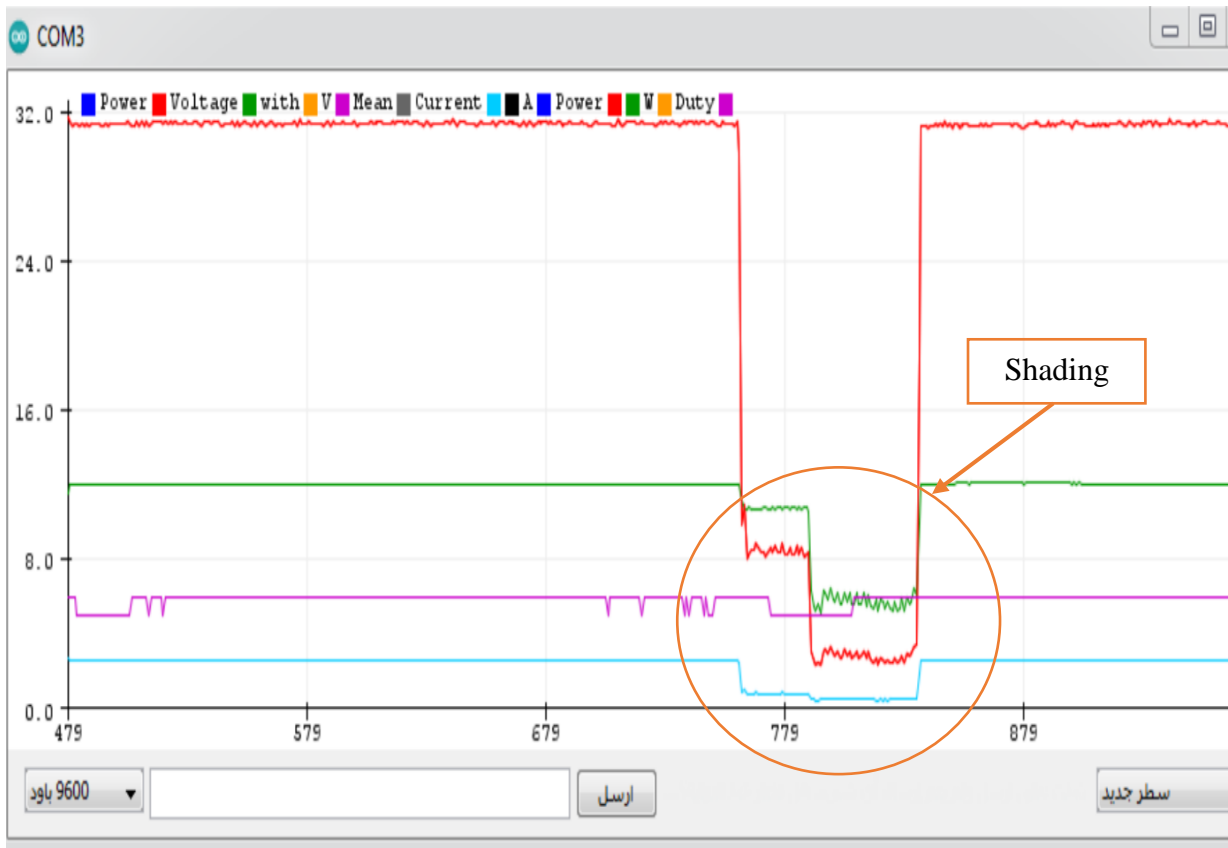


Figure IV.36: Serial curves results of MPPT control faulty model shading fault.

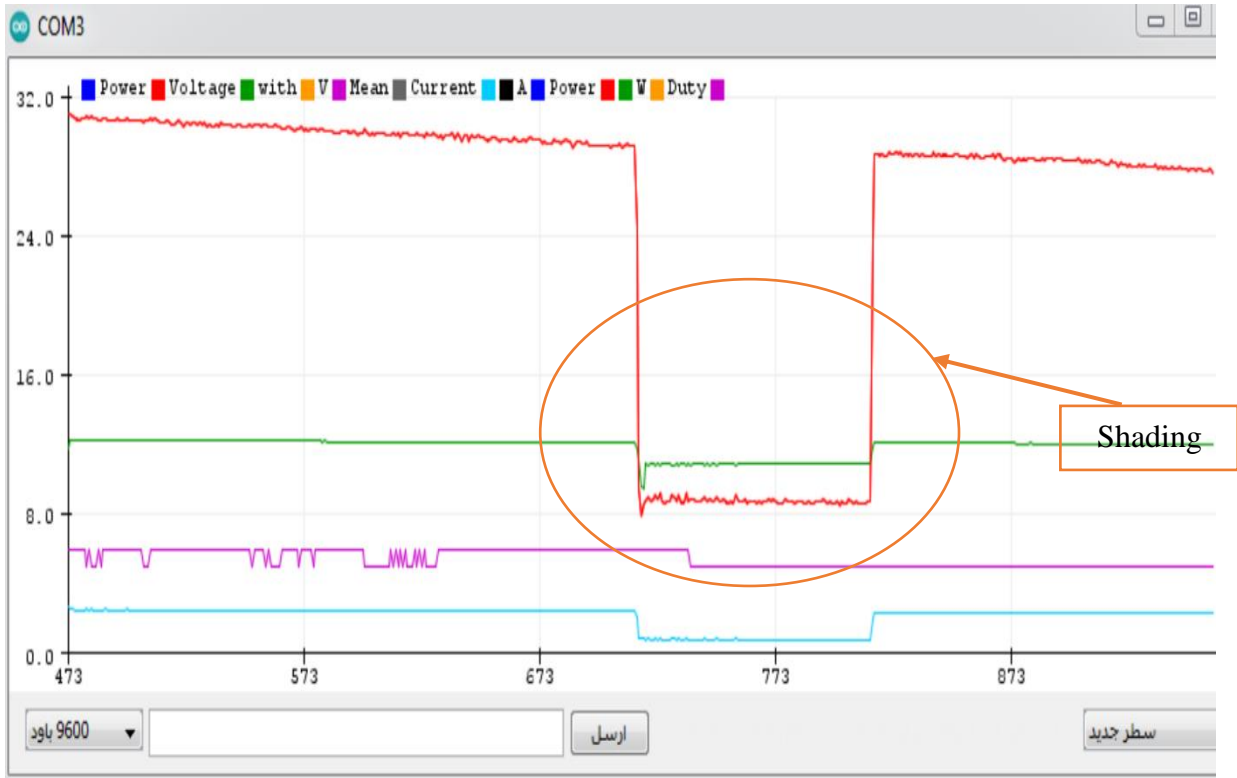


Figure IV.37: Serial curves results of MPPT control faulty model shading fault.

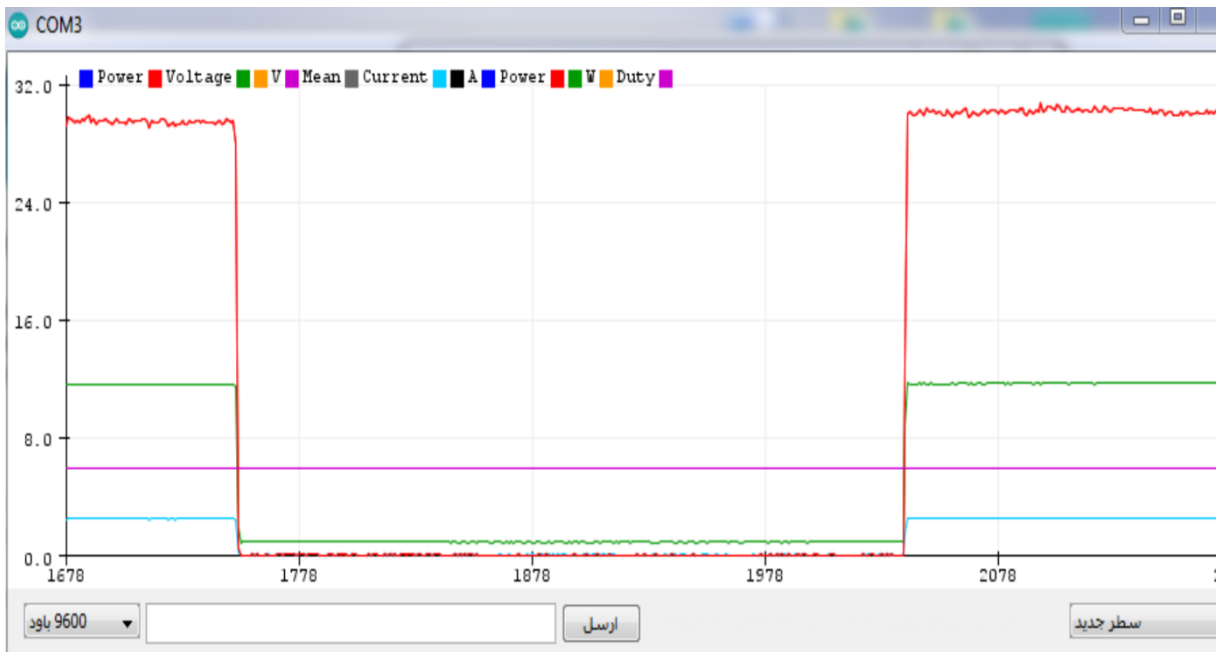


Figure IV.38: Serial curves results of MPPT control faulty model shading fault with LCD.



Figure IV.39: Final prototype.

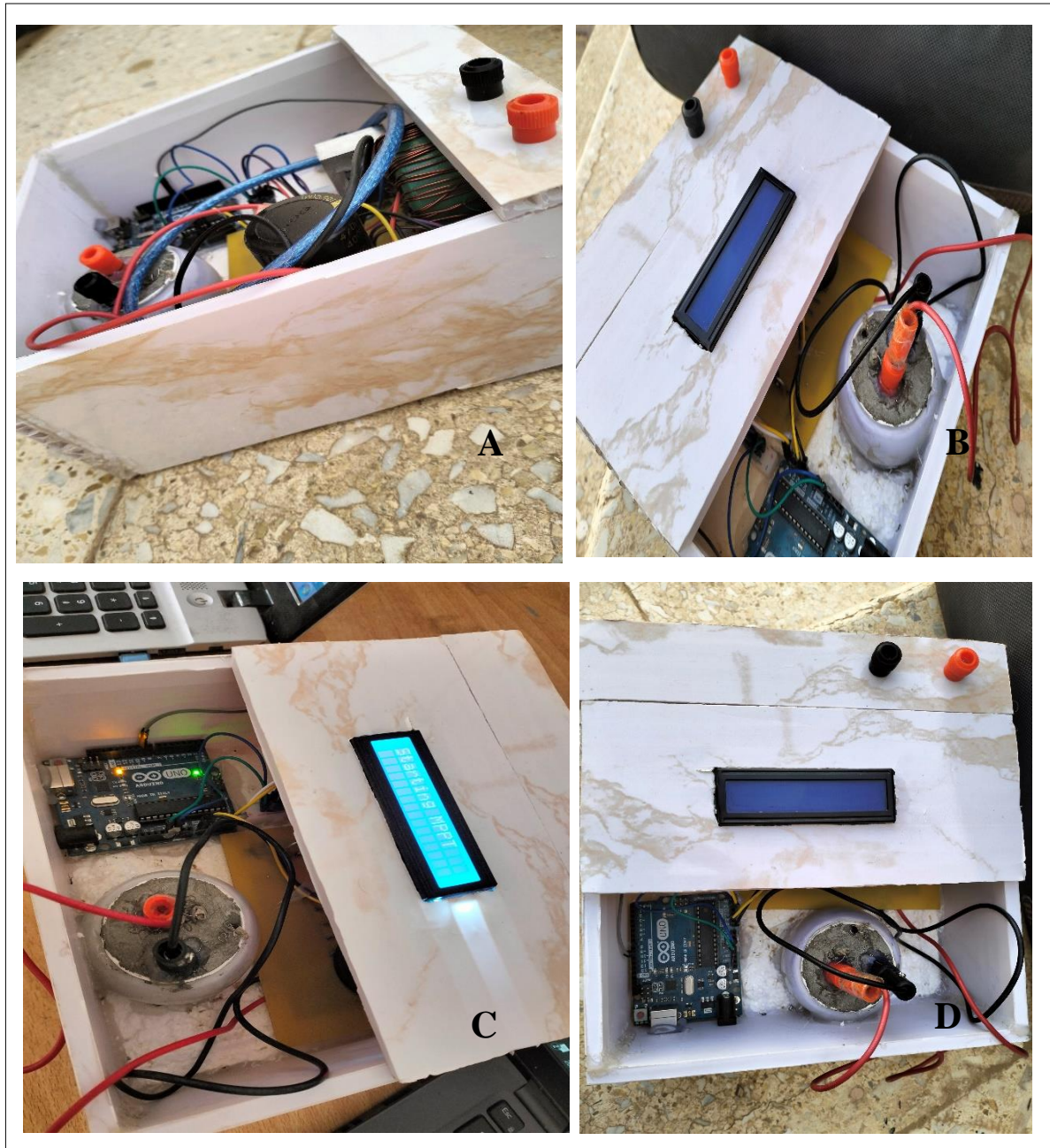


Figure IV.40: A, B, C and D, Final prototype.

Conclusion :

In this chapter, we performed an experimental validation of the fault detection method for solar panels. A model of the CHOPPER BOOST was developed, and its results were verified and discussed. It was then connected to the solar panel and the necessary sensors to obtain the required results for this study, confirming the effectiveness of the proposed methodology in identifying faults quickly and accurately.

GENERAL CONCLUSION

The experimental validation of fault detection in photovoltaic (PV) systems has significantly advanced the field by enhancing both efficiency and sustainability of solar energy technologies. Rigorous experimental trials and the formulation of fault detection models have unequivocally demonstrated the efficacy of the proposed methodology in swiftly and accurately pinpointing faults. This capability not only minimizes downtime but also optimizes overall system performance.

The findings from the experiments highlight that smart systems leveraging artificial intelligence and data analytics techniques offer effective resolutions to maintenance and operational complexities within solar energy frameworks. Moreover, the study underscores the criticality of utilizing authentic field data to ensure the reliability and practical applicability of developed solutions.

Moving forward, the study advocates for expanded research endeavors aimed at broadening the scope of fault detection models and validating them across diverse environmental and operational contexts. It further recommends fostering collaborative efforts between researchers and industry stakeholders to integrate fault detection technologies seamlessly with smart energy management systems.

In conclusion, this study emphasizes the imperative of continual innovation and progress within the renewable energy sector. Enhanced fault detection methodologies are pivotal in realizing enduring environmental and economic sustainability objectives.

References :

- [1] IEA, Snapshot of global photovoltaic markets, Report IEA-PVPS T1-39, 2021 (Accessed April 2021).
- [2] International Renewable Energy Agency (IRENA), Renewable Energy Statistics 2020, 2020, Available at: https://www.irena.org/-/media/Files/IRENA/Agency/Publication/2020/Jul/IRENA_Renewable_Energy.
- [3] IEA, Sunspot of global PBV markets, 2020. Report IEA-PVPS T1-37:2020 (Accessed April 2020).
- [4] IEA, Trend in photovoltaic applications, 2019. IEA PVPS T1-36: 2019.
- [5] C.A. Gueymard, D.R. Myers, Solar radiation measurement: progress in radiometry for improved modeling, in: *Modeling Solar Radiation at the Earth's Surface*, Springer, Berlin, Heidelberg, 2008, pp. 1–27
- [6] V. Badescu, *Modeling Solar Radiation at the Earth's Surface*, vol. 1, Springer, Berlin, Heidelberg, 2014.
- [7] J.S. Stein, W.F. Holmgren, J. Forbess, C.W. Hansen, PVLIB: open source photovoltaic performance modeling functions for Matlab and Python, in: *43rd Photovoltaic Specialists Conference*, 2016.
- [8] J. Meydbray, K. Emery, S. Kurtz, Pyranometers and reference cells, what's the difference? (No. NREL/JA-5200-54498), National Renewable Energy Lab. (NREL), Golden, CO, United States, 2012.
- [9] P. Gevorkian, *Large-Scale Solar Power System Design: An Engineering Guide for GridConnected Solar Power Generation*, McGraw-Hill Education, 2011.
- [10] M.E. Becquerel, Memoire sur les effets electriques produits sous l'influence des rayons solaires, in: *Comptes rendus hebdomadaires des seances de l'Academie des Sciences*, vol. 9, 1839, pp. 561–567.
- [11] M.H. Shubbak, Advances in solar photovoltaics: technology review and patent trends, (U.S. Energy Information Administration states) *Renew. Sust. Energ. Rev.* 115 (2019) 109383.
- [12] S. Philipps, W. Warmuth, Photovoltaics report fraunhofer institute for solar energy systems, in: *ISE With Support of PSE GmbH November 14th*, 2019.
- [13] V. Benda, L. Cerna, PV cells and modules—state of the art, limits and trends, *Heliyon* 6

(12) (2020) e05666.

[14] S.A. Kalogirou, *Solar Energy Engineering: Processes and Systems*, second ed., Academic Press, 2014.

[15] S. Hochreiter, J. Schmidhuber, Long short-term memory, *Neural Comput.* 9 (1997) 1735–1780.

[16] Adel-Mellit-Soteris-Kalogirou-Handbook-of-Artificial-Intelligence-Techniques-in-Photovoltaic-Systems_-Modeling-Control-Optimization-Forecasting-and-Fault-Diagnosis-Academic-Press-2022

[17] A. Labouret and M. Villoz, *Energie solaire photovoltaïque*, vol. 3. Dunod Paris, 2006

[18] A. Sharma and S. K. Kar, *Energy Sustainability Through Green Energy*. 2015. doi: 10.1007/978-81-322-2337-5.

[19] Hybrid PV Systems for the use of Total Solar Energy" by S. Sutikno / Overview of the hybrid solar system" by ResearchGate, which summarizes hybrid solar cells with PV systems / Solar Photovoltaic Technology Basics" by the U.S. Department of Energy, which covers the basics of how PV technology works / Types of photovoltaic systems: characteristics and advantages" by BIBLUS, which lists the characteristics and advantages of various PV systems

[20] K. J. Aström, P. Albertos, M. Blanke, A. Isidori, W. Schaufelberger, and R. Sanz, *Control of complex systems*. Springer Science & Business Media, 2011.

[21] R. Isermann, "On the applicability of model-based fault detection for technical processes," *Control Eng. Pract.*, vol. 2, no. 3, pp. 439–450, 1994.

[22] V. Venkatasubramanian, R. Rengaswamy, K. Yin, and S. N. Kavuri, "A review of process fault detection and diagnosis: Part I: Quantitative model based methods," *Comput. Chem. Eng.*, vol. 27, no. 3, pp. 293–311, 2003.

[23] G. Zwingelstein, "failures diagnosis. Theory and practice for industrial systems," 1995.

[24] A. e. M. A.GUELLAL, «La Commande MPPT Basée sur les Algorithmes Intelligents Destinée aux Applications Photovoltaïques : Etude comparative et implémentation sur FPGA, Le 4ème Séminaire International sur les Energies Nouvelles et renouvelable,» 2016.

- [25] C.CABAL, «Optimisation énergétique de l'étage d'adaptation électronique dédié à la conversion photovoltaïque.», Thèse Doctorat, UNIVERSITE DETOULOUSE, 2008..
- [26] [En ligne]. Available: <http://energie28.blogspot.com/2016/11/definition-et-explications-sur-le-mppt.html>.
- [27] F.BENADEL, Etude Et Simulation D'une Commande MPPT Pour Système PV,mémoire de Master Académique, M'SILLA: département de génie électrique: université de Mohamed Boudiaf - M'SILLA, 2016.
- [28] A.Talha, Développement d'une Méthode MPPT pour un Système Photovoltaïque, Premier Séminaire International sur les Energies Nouvelles.
- [29] H. K. A. M. A.Hanen, "Etude comparative de cinq algorithmes de commande MPPT pour un système photovoltaïque", Tunisie: Conférence Internationale des Energies Renouvelables (CIER'13) , 2013.
- [30] [En ligne]. Available: http://ipco-co.com/CEEE_Journal/CIER'13-CEEE/ID_003.pdf.
- [31] M. A. K. M. G. Amar, «La Commande MPPT Basée sur les Algorithmes Intelligents Destinée aux Applications Photovoltaïques», 25 octobre 2016: Etude comparative et implémentation sur FPGA, 2016.
- [32] A. B. H. S. B. B. H. M. A. B. Z. Ayache, Commande MPPT et Contrôle d'un Système Photovoltaïque par la Logique Floue, Commande MPPT et Contrôle d'un Systèmen Photovoltaïque par la Logique Floue.
- [33] A.A. Djalab, M.M. Rezaoui, L. Mazouz, A. Teta, N. Sabri, Robust Method for Diagnosis and Detection of Faults in Photovoltaic Systems Using Artificial Neural Networks, Periodica Polytechnica Electrical Eng. Comput. Sci. 64 (3) (2020) 291–302.
- [34] W. Chine, A. Mellit, V. Lughi, A. Malek, G. Sulligoi, A. Massi Pavan, A novel fault diagnosis technique for photovoltaic systems based on artificial neural networks, Renewable Energy 90 (2016) 501–512.
- [35] A. Belaout, F. Krim, A. Mellit, Neuro-fuzzy classifier for fault detection andclassification in photovoltaic module, in: 8th International Conference onModelling, Identification and Control (ICMIC), IEEE, 2016, pp. 144–149.

- [36] R.G. Vieira, M. Dhimish, F.M. de Araújo, M.I. Guerra, PV Module Fault Detection Using Combined Artificial Neural Network and Sugeno Fuzzy Logic, *Electronics* 9 (12) (2020) 2150.
- [37] S. Samara, E. Natsheh, Intelligent PV panels fault diagnosis method based on NARX network and linguistic fuzzy rule-based systems, *Sustainability* 12 (5) (2020) 2011.
- [38] International Electrotechnical Commission, Photovoltaic System Performance Monitoring—Guidelines for Measurement, Data Exchange and Analysis, IEC61724 (1998).
- [39] F. GUESSOUMI and A. SAADI, “Commande de panneau solaire à l’aide d’une carte à pic.” 2010. [10] A. Borni and A. Bouzid, “Etude et régulation d’un circuit d’extraction de la puissance maximale d’un panneau solaire,” 2017.
- [40] B. F.-D. Delagnes and B. Flèche, “Energie solaire photovoltaïque. doc,” juin 2007, 2007.
- [41] B. Yaacoub, “Modélisation et simulation d’un système photovoltaïque adapté par une commande MPPT,” 2013.
- [42] U. Raccordes and A. U. Reseau, “L ’ ENERGIE SOLAIRE PHOTOVOLTAÏQUE”.
- [43] H. Merakchi and B. Goumeidane, “Optimisation d’un système solaire de pompage d’eau,” 2010. [15] C. énergies Des, “Solaire-Photovoltaïque @ Www.Connaissancedesenergies.Org.” 2015. [Online]. Available: <http://www.connaissancedesenergies.org/fiche-pedagogique/solaire-photovoltaïque>.
- [44] “index @ www.explorateurs-energie.ch.” [Online]. Available: <https://www.explorateurs-energie.ch/>.
- [45] J. Gertler, (1991) "Analytical Redundancy Methods in Failure Detection and Isolation". SAFEPROCESS 91, Baden-Baden (Germany), pp. 9–21.
- [46] O. Hachana, G. M. Tina, and K. E. Hemsas, (2016) “PV array fault diagnostic technique for BIPV systems,” *Energy and Buildings*, vol. 126, pp. 263–274, Aug. 2016, doi: 10.1016/j.enbuild.2016.05.031.
- [47] N. Femia, G. Petrone, G. Spagnuolo and M. Vitelli, (2005) "Optimization of perturb and observe maximum power point tracking method," *Power Electronics, IEEE Transactions on*, vol. 20, pp. 963-973.

- [48] P. M. Frank., (1996) "Analytical and Qualitative Model-based Fault Diagnosis - A Survey and Some New Results", *European Journal of Control*, 2(1), pp. 6–28.
- [49] F. Sreedhar, B. Fernandez . & Masada G. Y. (1993) "Robust Fault Detection in Nonlinear Systems Using Sliding Mode Observers", *IEEE Conference on Control Applications*, September 13-16, Vancouver, Canada.
- [50] H. E. Suryanto, S. R. Wenham , and M. A. Green, (1986.) "Shadow tolerance of modules incorporating integral bypass diode solar cells," *Solar Cells*, vol. 19, pp. 109-122.
- [51] S. Chikha, «Optimisation de la puissance dans les systèmes photovoltaïques», *Mémoire de Magistère, université de OEB*, 2011/2012.
- [52] H. Abbes, H. Abid, K. Loukil, A. Toumi, M. Abid, « Etude comparative de cinq algorithmes de commande MPPT pour un système photovoltaïque », université de Sfax, Tunisie, 2013. [21]. M.S. Amamra « Optimisation de la production d'un générateur Photovoltaïque », thèse master université de Ouargla 2015.
- [53] P. Prouvost« Instrumentation et régulation», 2eme édition, Dunod, Paris 2010/2015.
- [54] Woyte A. et al., *Analytical Monitoring of Grid-connected Photovoltaic Systems : Good Practices for Monitoring and Performance Analysis*, IEA International Energy Agency, IEA PVPS Task 13, Subtask 2 Report IEA-PVPS T13-03: 2014; 2014.
- [55] Chao KH, Ho SH, Wang MH. Modeling and fault diagnosis of a photovoltaic system. *Electr Power Syst Res* 2008;78:97–105.
- [56] Guash D, Silvestre S, Calatayud R. Automatic failure detection in photovoltaic systems, in *Proceedings of the 3rd world conference on photovoltaic energy conversion*, Osaka, Japan; 2003.
- [57] B. Brooks, "The Bakersfield fire— A lesson in ground-fault protection", *SolarPro Mag.*, pp.62-70, Feb./Mar. 2011.
- [58] Sreelakshmy. J, Pradeepkumar. B, Saravana Ilango. G and Nagamani. C, "Identification of Faults in PV Array using Maximal Overlap Discrete Wavelet Transform", *IEEE Xplore*, 2018.
- [59] Performance Analysis of a Solar-Fed Induction Motor Drive under Various PV Array Fault Conditions Karthickraja J*, Senthamizh Selvan S†, Venkadesan A‡ Department of

Electrical and Electronics Engineering National Institute of Technology Puducherry Karaikal, India

[60] B. A. Alsayid, S. Y. Alsadi, J. S. Jallad, and M. H. Dradi. Partial shading of pv system simulation with experimental results. *Smart Grid & Renewable Energy*, 4(6):429–435, 2013.

[61] S. K. Firth, K. J. Lomas, and S. J. Rees. A simple model of pv system performance and its use in fault detection. *Solar Energy*, 84(4):624–635, 2010.

[62] S. Stettler, P. Toggweiler, E. Wiemken, W. Heydenreich, A. de Keizer, W. van Sark, S. Feige, M. Schneider, G. Heilscher, E. Lorenz, et al. Failure detection routine for grid-connected pv systems as part of the pvsat-2 project. In *Proceedings of the 20th European Photovoltaic Solar Energy Conference & Exhibition, Barcelona, Spain*, pages 2490–2493, 2005.

[63] B. Brooks, “The Bakersfield fire– A lesson in ground-fault protection”, *SolarPro Mag.*, pp.62-70, Feb./Mar. 2011.

[64] I. Khalil et al., “Comparative Analysis of Photovoltaic Faults and Performance Evaluation of its Detection Techniques”, *IEEE Access*, vol. 8, pp. 26676-26700, 2020.

[65] Sreelakshmy. J, Pradeepkumar. B, Saravana Ilango. G and Nagamani. C, “Identification of Faults in PV Array using Maximal Overlap Discrete Wavelet Transform”, *IEEE Xplore*, 2018.

[66] M. E. D. K. M. SEBHI, *Etude et réalisation d’une commande MPPT pour systèmes photovoltaïques*, Mémoire de master, Université Djillali Liabes, Sidi-Bel-Abbès, 2013.